

See discussions, stats, and author profiles for this publication at: <https://www.researchgate.net/publication/23196158>

# ChemInform Abstract: Controlled/Living Radical Polymerization in Dispersed Systems

ARTICLE *in* CHEMICAL REVIEWS · OCTOBER 2008

Impact Factor: 46.57 · DOI: 10.1021/cr800242x · Source: PubMed

---

CITATIONS

326

---

READS

116

3 AUTHORS, INCLUDING:



**Per Zetterlund**

University of New South Wales

158 PUBLICATIONS 3,218 CITATIONS

SEE PROFILE



**Masayoshi Okubo**

Kobe University

327 PUBLICATIONS 7,051 CITATIONS

SEE PROFILE

# Controlled/Living Radical Polymerization in Dispersed Systems

Per B. Zetterlund,\* Yasuyuki Kagawa, and Masayoshi Okubo\*

Department of Chemical Science and Engineering, Graduate School of Engineering, Kobe University, Kobe 657-8501, Japan

Received October 31, 2007

## Contents

1. Introduction	3747	2.6.4. Microemulsion RAFT Polymerization	3779
1.1. Scope and Previous Reviews	3747	2.6.5. ITP in Microemulsion	3779
1.2. Background	3748	2.7. Dispersion and Precipitation Polymerizations	3779
1.3. Mechanisms of CLRP—General Considerations	3749	2.7.1. General Considerations	3779
1.3.1. CLRP Based on the Persistent Radical Effect (PRE)	3750	2.7.2. NMP	3780
1.3.2. CLRP Based on Degenerative Transfer	3750	2.7.3. ATRP	3781
1.4. Experimental Evaluation of Control/Livingness	3750	2.7.4. RAFT	3782
1.5. Importance of CLRP	3751	2.7.5. Dispersion ITP	3782
1.6. Dispersed Systems	3752	3. Cross-linking CLRP in Dispersed Systems	3783
2. CLRP in Dispersed Systems	3752	3.1. General Considerations	3783
2.1. Colloidal Stability	3752	3.2. Cross-linking NMP	3783
2.1.1. Ostwald Ripening	3752	3.3. Cross-linking ATRP	3784
2.1.2. Superswelling	3752	3.4. Cross-Linking RAFT Polymerization	3784
2.1.3. Entry/Exit Considerations	3753	3.5. Cross-Linking ITP	3784
2.2. Theoretical Aspects of CLRP in Dispersed Systems	3754	4. Particle Morphology	3785
2.2.1. General Considerations	3754	4.1. General Considerations	3785
2.2.2. CLRP Based on the Persistent Radical Effect (PRE)	3754	4.2. Core—Shell Particles	3785
2.2.3. CLRP Based on Degenerative Transfer	3757	4.3. Hollow Particles	3785
2.3. Miniemulsion Polymerization (Incl. Suspension Polymerization)	3759	4.4. Multilayered Particles	3786
2.3.1. Nitroxide-Mediated Radical Polymerization (NMP)	3759	5. Conclusions and Outlook	3787
2.3.2. Atom Transfer Radical Polymerization (ATRP)	3762	6. List of Abbreviations	3788
2.3.3. RAFT Polymerization	3765	7. Acknowledgments	3789
2.4. Emulsion Polymerization	3768	8. References	3789
2.4.1. Nitroxide-Mediated Radical Polymerization (NMP)	3768		
2.4.2. Atom Transfer Radical Polymerization (ATRP)	3771		
2.4.3. RAFT Emulsion Polymerization	3773		
2.5. Miscellaneous Miniemulsion and Emulsion CLRP	3776		
2.5.1. Iodine Transfer Polymerization (ITP)	3776		
2.5.2. Organotellurium-Mediated Radical Polymerization (TERP)	3777		
2.5.3. Cobalt-Mediated Radical Polymerization (CMRP)	3777		
2.6. Microemulsion Polymerization	3778		
2.6.1. General Considerations	3778		
2.6.2. Microemulsion NMP	3778		
2.6.3. Microemulsion ATRP	3778		

## 1. Introduction

### 1.1. Scope and Previous Reviews

This is a comprehensive review of the field of controlled/living radical polymerization (CLRP) in dispersed systems, aiming at covering the literature up to and including 2007, with selected references from early 2008. Surface initiated CLRP (initiation from dispersed particle surfaces, etc.) goes beyond the scope of the present review.

CLRP in dispersed systems has previously been reviewed by Cunningham in 2002<sup>1</sup> and 2007,<sup>2</sup> by Qiu, Charleux, and Matyjaszewski in 2001,<sup>3</sup> and by Save, Guilleaume, and Gilbert in 2006.<sup>4</sup> A review covering nitroxide-mediated radical polymerization (NMP), atom transfer radical polymerization (ATRP), and reversible addition—fragmentation chain transfer (RAFT) in emulsion and miniemulsion was published in 2005 by Monteiro and Charleux.<sup>5</sup> NMP in miniemulsion was reviewed by Cunningham in 2003,<sup>6</sup> and McLeary and Klumperman reviewed RAFT polymerization in dispersed systems in 2006.<sup>7</sup> CLRP in miniemulsion was reviewed by Asua in 2002<sup>8</sup> and by Schork and co-workers in 2005.<sup>9</sup>

A comprehensive review of CLRP in bulk/solution was published by Braunecker and Matyjaszewski in 2007,<sup>10</sup> and kinetic aspects of CLRP were reviewed by Goto and Fukuda in 2004.<sup>11</sup> Advances in CLRP over the years have also been

\* Corresponding authors. Telephone and Fax: +81-(0)78-803-6161. E-mail: pbzttd@cx6.scitec.kobe-u.ac.jp (P.B.Z.) and okubo@kobe-u.ac.jp.



Per B. Zetterlund was born in Karlskoga, Sweden, in 1968. He graduated from The Royal Institute of Technology in Stockholm (Sweden) in 1994 with a M.Sc. in Chemical Engineering, and he obtained his Ph.D. in the School of Chemistry at Leeds University (U.K.) in 1998 under the supervision of Prof. A. F. Johnson in radical cross-linking polymerizations. He carried out postdoctoral research at Griffith University (Brisbane, Australia) with Ass. Prof. W. K. Busfield and Prof. I. D. Jenkins in nitroxide-mediated polymerization (NMP) and the use of nitroxides as radical traps. In 1999, he became Assistant Professor at Osaka City University (Osaka, Japan) in the group headed by Prof. B. Yamada, and he worked on the kinetics/mechanism of high conversion radical polymerization, synthesis/polymerization of macromonomers, and NMP. In 2003, he moved to Kobe University (Kobe, Japan), where he was promoted to Associate Professor in 2006. His current research focuses on NMP and atom transfer radical polymerization (ATRP) in aqueous and supercritical carbon dioxide based dispersed systems, as well as the kinetics/mechanism of radical polymerization in general. He has published 72 peer-reviewed papers and two book chapters, and he is a member of the IUPAC Macromolecular Division (IV) Subcommittee on Modeling of Polymerization Kinetics and Processes, The International Polymer and Colloid Group, The American Chemical Society, and The Society of Polymer Science, Japan.



Yasuyuki Kagawa was born in Nishinomiya, Japan, in 1979. He received a B.Sc. from the Department of Chemical Science and Engineering at Kobe University, Japan, in 2002 (Emulsifier-free emulsion polymerization), an M.Sc. from the Graduate School of Science and Technology (Kobe University) in 2004 (ATRP in aqueous dispersed systems), and a Ph.D. from the same institution in 2007 (Controlled/living radical polymerization in dispersed systems) under the supervision of Prof. M. Okubo. He became a Research Fellow of the Japan Society for the Promotion of Science in 2006, and he remained in the same research group as a postdoctoral researcher until March 2008 working on CLRP in dispersed systems, including morphological aspects and the use of supercritical CO<sub>2</sub>. He is currently employed by Mitsui Chemicals Incorporation (Tokyo). He is a member of The Society of Polymer Science, Japan.

compiled in a series of books edited by Matyjaszewski.<sup>12–15</sup> In addition, there exist several reviews covering specific CLRP techniques in bulk/solution, e.g. NMP,<sup>16</sup> ATRP,<sup>17,18</sup> and RAFT.<sup>19–22</sup>

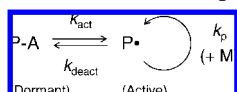


Masayoshi Okubo graduated from Kobe University (Kobe, Japan) in 1969 and obtained the master's degree in 1971. He began his research career as a research associate in the polymer chemistry group of Prof. Tsunetaka Matsumoto at Kobe University, and he subsequently received the doctor's degree of engineering from Kyoto University (Japan) in 1976. His doctoral thesis focused on the preparation of functional polymer particles. He carried out postdoctoral research on the measurement of surface tension of polymer solutions at Fritz-Haber-Institut der Max-Planck-Gesellschaft in Berlin in 1976–1977 with the late Prof. Kurt Ueberreiter. He was promoted to Associate Professor in 1985 and Professor in 1995 at Kobe University. He was director of The Instilment Center at Kobe University in 2000–2002. His research is in the field of polymer colloids chemistry, with special focus on the development of novel functional polymer particles (capsules) by (emulsifier-free) emulsion polymerization, miniemulsion polymerization, dispersion polymerization, microSuspension polymerization, and various seeded polymerizations. He is recently also working on implementation of controlled/living radical polymerization in dispersed systems using environmentally friendly media, e.g. water and supercritical carbon dioxide. He has coauthored over 300 original papers and 80 patents. He has developed synthetic routes to various novel polymer particles with unique shapes, morphologies, and hollow structures, and he formed a venture company, "Smart Spheres Work Shop, Inc.", in July 2006. He has served as vice president of The Adhesion Society of Japan and is the current chairman of The Kansai Regional Chapter of The Society of Polymer Science, Japan. He is the recipient of The Award of the Adhesion Society of Japan in 2003 and The Science Award of Hyogo Prefecture in 2005.

## 1.2. Background

Radical polymerization is of enormous industrial importance; approximately 50% of all commercial polymers are produced by radical polymerization.<sup>23</sup> The process is tolerant to impurities, compatible with water, relatively easy to implement in an industrial plant, and very versatile with respect to compatibility with functional monomers. The major drawback is that radical polymerization proceeds with very limited control; it is not possible to prepare block copolymers, polymers of narrow molecular weight distributions (MWDs), and more complex architectures due to the high reactivity of the propagating radicals and their propensity to undergo bimolecular termination, transfer, and other side reactions. The lifetime of a propagating radical (the time that passes between initiation and end-formation for a given chain) is typically of the order of 1 s, and chains are continuously initiated throughout the polymerization.<sup>11</sup> Living anionic polymerization<sup>24</sup> offers high levels of control in terms of well-defined polymers and precise molecular architectures, but the process is much less flexible than radical polymerization, as it is very intolerant to functionality and impurities. Thus, it has been a long-standing goal in the field of polymer chemistry to develop a process that combines the robustness of radical polymerization with the control and precision offered by living anionic polymerization.

## Scheme 1. General Dormant–Active Equilibrium



CLRP today offers levels of control almost as good as those of living anionic polymerization, while maintaining the robustness of a free radical process in terms of tolerance and flexibility. The work of Otsu and co-workers<sup>25,26</sup> in the early 1980s on iniferter systems, which exhibited partial control/livingness, provided an important stepping stone in the development of more successful CLRPs. The three most well-known CLRP techniques are NMP,<sup>16,27,28</sup> ATRP,<sup>17,18,29,30</sup> and RAFT polymerization<sup>19–22,31</sup> (the latter technique includes macromolecular design via the interchange of xanthates (MADIX)<sup>32</sup>). However, a multitude of other CLRP techniques exist, including iodine-transfer polymerization (ITP),<sup>33–36</sup> single electron transfer–degenerative chain transfer mediated living radical polymerization (SET-DTLRP),<sup>37,38</sup> single electron transfer–living radical polymerization (SET-LRP)<sup>39,40</sup> (the mechanisms of SET-LRP and SET-DTLRP are under debate<sup>41</sup>), organotellurium-mediated polymerization (TERP),<sup>42–46</sup> organostibine-mediated polymerization (SBRP),<sup>47,48</sup> cobalt-mediated polymerization (CMRP),<sup>49–51</sup> reversible chain transfer catalyzed polymerization (RTCP),<sup>52</sup> quinone transfer radical polymerization (QTRP),<sup>53,54</sup> the DPE method (1,1-diphenylethene),<sup>55,56</sup> thioketone-mediated polymerization (TKMP),<sup>57,58</sup> the use of boroxyl-based initiators,<sup>59</sup> the approach based on methacrylic macromonomers,<sup>60,61</sup> as well as verdazyl-mediated polymerization.<sup>62</sup>

### 1.3. Mechanisms of CLRP—General Considerations

CLRP proceeds in such a manner that bimolecular termination of propagating radicals only has a minor influence on the MWD and the average molecular weights (MWs). This is in sharp contrast with conventional radical polymerization, where termination is one of the main kinetic events that shape the MWD. All CLRP systems developed to date operate on the same basic principle of propagating radicals being reversibly deactivated, i.e. alternating between active and dormant states (Scheme 1). In NMP, the dormant state is a polymeric alkoxyamine, in ATRP, it is a polymeric alkyl halide, and in RAFT, it is a polymer chain with a RAFT end-group. The dormant species may also be a stable radical, as exemplified by the DPE method<sup>55,56</sup> and TKMP.<sup>57,58</sup>

The terms control and livingness are often incorrectly used interchangeably in the literature. Livingness refers to the number fraction of polymer chains that are dormant and can be chain extended if monomer is available. Control, on the other hand, refers to  $M_w/M_n$  increasing linearly with conversion and  $M_w/M_n$  decreasing with increasing conversion to approach unity.<sup>63</sup>

It is a widespread misconception that control/livingness is a consequence of the equilibrium between active and dormant species resulting in a low propagating radical concentration ( $[P^*]$ ), which in turn causes a reduction in the termination rate. In fact, *a propagating radical concentration lower than that in a conventional system is not a requirement for control/livingness*.<sup>11</sup> This is clearly illustrated by considering TEMPO-mediated polymerization of styrene at 125 °C relying on thermal (spontaneous) initiation. The spontaneous  $R_p$  of styrene in bulk (no initiator added) is the same as

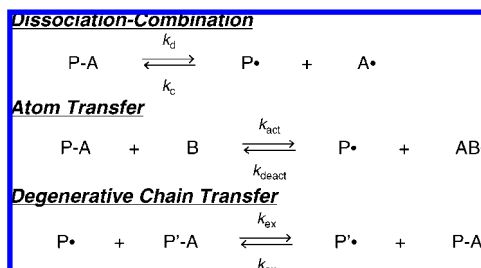
that of styrene in bulk in the presence of a suitable amount of TEMPO after the induction period. If  $R_p$  is the same in both systems, then  $[P^*]$  is also the same ( $R_p = k_p[P^*][M]$ , where  $k_p$  is the propagation rate coefficient and  $[M]$  is the monomer concentration), and consequently the termination rates ( $= 2k_t[P^*]^2$ ) are also the same (neglecting the relatively minor effect of chain-length dependent termination), yet one system is controlled/living and the other is not! There are also examples of RAFT systems without retardation that exhibit good control/livingness.<sup>64</sup> A reduction in  $[P^*]$  does result in a lower termination rate relative to the propagation rate (the propagation rate is proportional to  $[P^*]$  whereas the termination rate is proportional to  $[P^*]^2$ ). However, this is not a fundamental requirement for successful CLRP (although it helps). The key point, often overlooked, is that the number of chains is much greater in CLRP, and thus *the rate of termination per chain is much lower in CLRP* (the rate of chain transfer to monomer per chain is also much lower in CLRP). This illustrates why it is more difficult to maintain control/livingness when high degrees of polymerization (DP) are targeted—under such conditions, the number of chains is lower, and thus the rate of termination per chain increases.<sup>11,65</sup> The higher the targeted DP, the higher is the probability that a termination event or other side reaction will occur for any given chain during its growth. In a conventional system, the lifetime of  $P^*$  is approximately 1 s. Therefore, if the accumulated time in the activated state is 1 s (at the same total  $[P^*]$ ), then the probability of termination will be 100%. In other words, the accumulated time in the activated state should be significantly less than 1 s in order for the termination level to be acceptably low (i.e., 0.1 s would give 10% dead chains). The time in the active state during each activation–deactivation cycle is normally 0.1–10 ms.<sup>11</sup> Notwithstanding the above, it is important to realize that  $[P^*]$  is still an important quantity in CLRP. If a certain relatively high DP cannot be reached with satisfactory control/livingness in a given CLRP process due to excessive termination, then it may be possible to reach that DP by reducing  $[P^*]$ .

A factor that is pivotal in determining the level of control over the MWD (i.e.,  $M_w/M_n$ ) is the rate of exchange between active and dormant states.<sup>66–73</sup> In order to obtain a narrow MWD, the number of activation–deactivation cycles ( $N_{\text{cycles}}$ ) that a given chain experiences as it grows to a given degree of polymerization (DP) must be sufficiently high. If  $N_{\text{cycles}}$  is too low, the MWD is broad, i.e. the control is poor, but this does not preclude a high degree of livingness. There are examples of systems with relatively high livingness but poor control.<sup>74</sup> In an ideal system (a system consisting of only activation, deactivation, and propagation),  $M_w/M_n$  decreases with increasing conversion as  $N_{\text{cycles}}$  per chain increases. In a real system, termination and various side reactions occur, which leads to a higher  $M_w/M_n$  than in an ideal system. Nonetheless, the  $M_w/M_n$  normally decreases with conversion because the effect of the activation–deactivation cycles on  $M_w/M_n$  is greater than that of termination and side reactions (except at very high conversion).

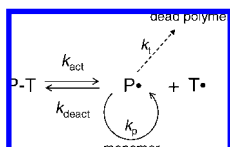
The vast majority of the CLRP systems developed to date proceed via one of two basic mechanisms (both of which involve an equilibrium between active and dormant species): (i) The persistent radical effect (PRE) and (ii) degenerative transfer. In some cases, both (i) and (ii) may be operative simultaneously (e.g., TERP and SET-DTLRP). Systems based on the PRE can be subdivided into dissociation–combination



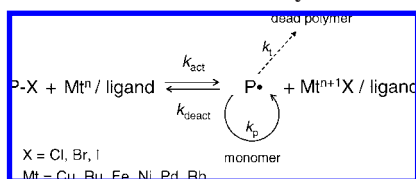
### Scheme 2. The Three Main Mechanisms of Activation–Deactivation in CLRP



### Scheme 3. Nitroxide-Mediated Radical Polymerization (NMP)



### Scheme 4. Atom Transfer Radical Polymerization (ATRP)



(e.g., NMP) and atom transfer (e.g., ATRP). The various mechanisms are illustrated in Scheme 2.

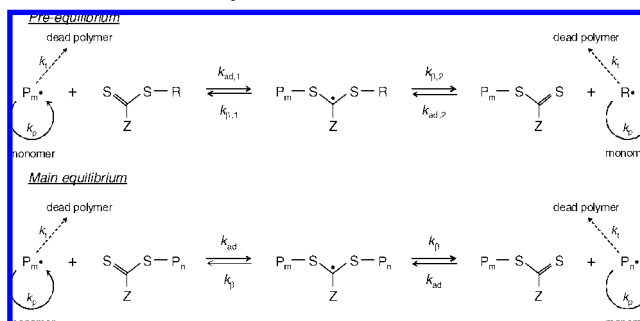
#### 1.3.1. CLRP Based on the Persistent Radical Effect (PRE)

The PRE<sup>68–70,75</sup> has been well-known in organic chemistry for many years but has only recently gained prominence in polymer chemistry with the emergence of CLRP. The PRE will here be explained within the framework of NMP. Activation–deactivation in NMP is depicted in Scheme 3, where  $k_{\text{act}}$  and  $k_{\text{deact}}$  denote the rate coefficients for thermal dissociation of alkoxyamine (activation) and coupling (deactivation), respectively, and PT, P•, and T• denote alkoxyamine, propagating radicals, and nitroxide, respectively. T• does not undergo mutual reaction and is only consumed by reaction with P•, but P• is consumed by reaction with both P• and T•. The net result is that after a very short initial time period when both [P•] and [T•] increase with time in a similar fashion ( $\ll 1$  s), [P•]  $\ll$  [T•], and consequently, the rate of deactivation (P• + T•) is much higher than that of termination (P• + P•). P• is gradually consumed by termination, and a true stationary state is never reached in the absence of an additional source of P• (such as spontaneous (thermal) initiation of styrene). The PRE is also operative in ATRP (Scheme 4) but not in RAFT (Scheme 5), which proceeds via degenerative transfer. Termination plays a crucial role in CLRP systems that operate via the PRE, both as an integral part of the PRE itself and in determining  $R_p$ .<sup>76</sup> CLRP based on the PRE does not require addition of a radical initiator because the activation step itself generates a propagating radical.

#### 1.3.2. CLRP Based on Degenerative Transfer

CLRP systems based on degenerative transfer operate via the interchange of activity (i.e., the radical center) between active and dormant species by a reversible chain transfer

### Scheme 5. Reversible Addition–Fragmentation Chain Transfer (RAFT) Polymerization



mechanism. In contrast with systems based on the PRE, degenerative transfer based systems require the addition of a radical initiator, because the activation–deactivation process is not associated with a change in the number of radicals. As such, in the case of ideal chain transfer (when the kinetic chain length is unaffected), the polymerization kinetics are the same as in the corresponding conventional system, except for chain-length effects such as chain-length dependent termination. Examples of CLRP systems that are based on degenerative transfer include RAFT and ITP.

### 1.4. Experimental Evaluation of Control/Livingness

There are numerous instances when CLRP does not proceed to satisfaction. For example, most CLRP systems are to some degree incompatible with certain monomer types, and the exact experimental conditions can be crucial. It is frequently incorrectly stated in the literature that a linear first-order plot is a criterion for control/livingness. There are many cases when CLRP does not give a linear first-order plot, and moreover, conventional nonliving radical polymerizations often yield linear first-order plots.<sup>11,76</sup> It is straightforward to examine the level of control based on the narrowness of the MWD and whether  $M_n$  increases linearly with conversion. Livingness is more difficult to assess. To date, three separate approaches are in use: (i) chain extensions, (ii) quantitative end group analysis, and (iii) determination of the amount of free deactivator (mainly NMP).

Chain extensions are based on the use of polymer obtained by CLRP as a macroinitiator. Although simple in principle, this approach is associated with several pitfalls and can often yield ambiguous results. MWDs obtained by GPC are plotted as “GPC distributions”, “weight distributions”, or “number distributions”. The  $x$ -axis is normally expressed in  $\log M$  or  $M$ , whereas the  $y$ -axis is defined as follows (where  $M$  and  $n$  denote MW and the number of molecules, respectively):<sup>77,78</sup>

Number distribution:  $y$ -values are proportional to  $n$

Weight distribution:  $y$ -values are proportional to  $nM$

GPC distribution:  $y$ -values are proportional to  $nM^2$

Visual inspection of GPC distributions ( $w(\log M)$  vs  $\log M$ ) of partially successful chain extensions can be misleading. This is illustrated in Figure 1, which shows a GPC distribution and number distribution of such a chain extension. Casual inspection of the GPC distribution may suggest that the vast majority of chains have been extended. However, integration of the number distribution  $P(M)$  (plotted vs  $M$ ) reveals that as much as 20% by number of the chains of the original macroinitiator are dead, assuming that chains of  $M < 17000$  ( $\log M = 4.23$ ) correspond to dead macroinitiator.

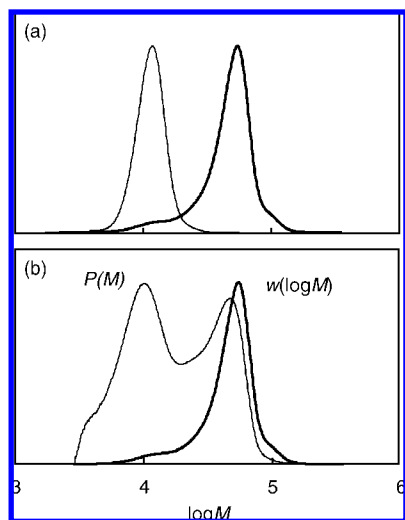


**Figure 1.** Example of chain extension. (a) MWDs displayed as “GPC distributions”, i.e.  $w(\log M)$ , where the thin line is the original macroinitiator and the thick line is the polymer after chain extension. (b) MWDs of polymer after chain extension displayed as GPC distribution and number distribution  $P(M)$ . Reprinted (adapted) with permission from ref 409. Copyright 2006 Wiley-VCH Verlag GmbH & Co.

Even if the macroinitiator is 100% living, a chain extension may be unsuccessful for a number of reasons. For example, if the macroinitiator concentration is too low, chain transfer to monomer may give rise to a high number fraction of new chains, resulting in a low MW tail which may be confused with dead macroinitiator.<sup>79</sup> Moreover, in PRE-based CLRP such as NMP and ATRP, the ratio  $[P^*]/[\text{deactivator}]$  increases with decreasing initial macroinitiator concentration, causing very significant termination during the chain extension if the initial macroinitiator concentration (i.e., the concentration of the polymer to be extended) is too low.<sup>11</sup> If a chain extension is carried out with a second monomer (block copolymer synthesis), the order of monomer addition can be crucial. For example, a PS-TIPNO macroinitiator cannot be efficiently extended with *n*BA, despite the fact that chain extension with isoprene works satisfactorily. However, *Pn*BA-TIPNO initiated polymerization of styrene gives well-defined block copolymer. These results are believed to be related to the relative rates of initiation and polymerization for the two monomers.<sup>80,81</sup> In the case of ATRP chain extensions involving different monomer types, the relative rates of cross-propagation (i.e., the first propagation step of the macroinitiator to be extended) and homopropagation of the extended polymer must be carefully considered. If homopropagation of the second monomer is significantly faster than cross-propagation, the resulting MWD becomes bimodal. The technique of halogen exchange can be used to overcome such difficulties.<sup>82–84</sup> The order of monomer addition is also important in RAFT polymerization. Fragmentation of a RAFT adduct radical comprising one PS arm and one PMMA arm predominantly occurs to release the PMMA radical, and thus polymerization of MMA using PS-dithiocarbonate does not proceed well, whereas PMMA-dithiocarbonate + styrene does.<sup>11,85</sup> One of the advantages of TERP is that the order of monomer addition is of less importance.<sup>43</sup>

The simultaneous use of UV and RI detectors can be useful when examining chain extensions by GPC. For example, in the case of styrene and acrylate or methacrylate copolymers,

the RI detector “sees” both monomer units whereas the UV detector only “sees” styrene, and thus homopolymer can be detected.

Contrary to what is frequently stated in the literature,  $M_n \approx M_{n,th}$  does not constitute proof of a successful chain extension, but it merely indicates that the total number of chains has remained constant, because  $M_n$  is only affected by the number of chains (unlike  $M_w$ ). A high fraction of dead original macroinitiator means that the living macroinitiator species will be extended more at the expense of the dead macroinitiator species; that is, it only affects the distribution of monomer units, not  $M_n$ .

It is in theory possible to accurately estimate livingness by NMR,<sup>65,86</sup> although this is often difficult in practice due to the low concentrations of end groups, especially for high MW polymer. More accurate methods involve the use of alkoxyamines with a chromophore attached to either the initiating fragment or the nitroxide,<sup>87</sup> and fluorescence labeling of nitroxyl-terminated polymer.<sup>88</sup> Another approach<sup>89,90</sup> constitutes heating a solution of the polymer in the presence of air, allowing the alkoxyamine species to thermally dissociate to release free nitroxide, whereas the carbon-centered radicals are scavenged by oxygen.<sup>91</sup> The livingness of the original polymer can be calculated from the amount of released nitroxide as measured by electron paramagnetic resonance (EPR) spectroscopy.

## 1.5. Importance of CLRP

Polymer chemists have long strived for precise control over macromolecular structure. Prior to the development of CLRP, this was not possible in radical polymerization. CLRP enables preparation of polymer of predetermined MW and narrow MWD, block copolymers, and more complex macromolecular architectures such as star- and comb-shaped polymers, as well as introduction of end functionality. In addition, CLRP is more versatile with regard to monomer type than living ionic polymerizations. CLRP can also be applied to cross-linking polymerizations, whereby more well-defined and homogeneous network structures can be prepared. The advent of CLRP has led to the preparation of a wide range of new polymeric materials with a range of potential applications such as surfactants, lubricants, adhesives, additives, thermoplastic elastomers, as well as biomedical and electronic applications.<sup>10,15,23,92,93</sup> Moreover, CLRP is valuable with regard to increasing the understanding of structure–property relationships of polymeric materials.

One of the main applications of CLRP is the synthesis of block copolymers.<sup>10,81,83,92,94</sup> CLRP carried out in a single step results in copolymers of very different microstructure compared to those formed from a conventional radical copolymerization. In a conventional radical copolymerization, the composition of the chains varies with conversion due to the relative monomer consumption rates, but the chains have no overall composition gradient. In CLRP, all chains have the same overall monomer composition, but with a composition gradient along the chain dictated by the relative monomer consumption rates. The monomer reactivity ratios are not affected by NMP,<sup>95–97</sup> ATRP,<sup>98–102</sup> or RAFT<sup>103</sup> (although, in RAFT, the apparent reactivity ratios may change as a result of the RAFT process itself altering the ratios of propagating radicals).

CLRP has also led to the development of various novel approaches to study fundamental mechanistic/kinetic aspects of conventional radical polymerization as well as polymer-

izations in dispersed systems. For example, chain-length dependent termination kinetics have been studied using RAFT,<sup>104–107</sup> and particle nucleation in precipitation/dispersion polymerizations has been investigated employing NMP.<sup>108,109</sup>

## 1.6. Dispersed Systems

Radical polymerization can be conducted in various dispersed systems, e.g. emulsion,<sup>78,110</sup> miniemulsion,<sup>8,9,111</sup> microemulsion,<sup>112–114</sup> precipitation, dispersion,<sup>115,116</sup> and suspension polymerizations. The continuous phase is usually, but not always, water (the descriptions below are based on water being the continuous phase). The characteristics of the dispersed systems described below apply to conventional, nonliving systems, and some of these characteristics may change in the case of CLRP. For example, dispersion CLRP often yields broad particle size distributions, whereas nonliving dispersion polymerizations normally result in close to monodisperse particles. An **emulsion polymerization** starts with a stirred mixture of water, initiator (usually water-soluble), monomer, and emulsifier. Polymer particles are formed in the aqueous phase via micellar or homogeneous nucleation during interval I (0–10% conversion). During interval II (10–40% conversion), monomer droplets and monomer-swollen particles coexist, and monomer diffuses from droplets to particles as monomer is consumed in the particles by polymerization. In interval III (conversion > 40%), monomer droplets no longer exist, and the system consists of monomer-swollen particles in an aqueous continuous phase. Emulsion polymerization normally yields particle diameters  $d \approx 100\text{--}600$  nm with relatively narrow particle size distributions. In a **miniemulsion polymerization**, a mixture of water, emulsifier, monomer, water- or oil-soluble initiator, and usually a hydrophobe (e.g., hexadecane) is subjected to external shear forces via ultrasonication or microfluidization, resulting in thermodynamically unstable but kinetically stable (on the time scale of the polymerization) monomer droplets. In an ideal miniemulsion (usually not the case), each monomer droplet is converted to a polymer particle. The particle size distribution is normally relatively broad with  $d \approx 60\text{--}200$  nm. A **microemulsion** is a thermodynamically stable transparent or translucent emulsion that forms on mixing of an aqueous emulsifier solution (much higher emulsifier content than in an emulsion polymerization) with monomer and sometimes a cosurfactant such as 1-pentanol. Microemulsion polymerization normally results in particles with  $d \approx 10\text{--}60$  nm. In a **precipitation polymerization**, all ingredients are initially soluble in the continuous phase. As polymer chains grow, they reach a critical chain-length at which precipitation occurs, resulting in formation of particles with  $d \approx 100\text{--}600$  nm. A **dispersion polymerization** is the same as a precipitation polymerization except that a stabilizer is present. Precipitation occurs, leading to formation of unstable precursor particles, which subsequently coalesce and adsorb stabilizers, resulting in stable particles. Dispersion polymerizations often yield narrower particle size distributions than precipitation polymerizations with  $d \geq 1$   $\mu\text{m}$ . A **suspension polymerization** is a mixture of water, emulsifier, monomer, and an oil-soluble initiator where polymerization proceeds in the monomer droplets, yielding large particles ( $d \geq 1$   $\mu\text{m}$ ).

## 2. CLRP in Dispersed Systems

### 2.1. Colloidal Stability

This section focuses on aspects of colloidal stability that are of particular significance with regard to CLRP.

#### 2.1.1. Ostwald Ripening

Emulsions (except microemulsions) are thermodynamically unstable and strive to minimize the interfacial energy by reducing the total interfacial area in the system via coalescence and Ostwald ripening.<sup>111,117</sup> Coalescence is minimized by use of a suitable surfactant. Ostwald ripening refers to monomer diffusion from small droplets/particles (particle = monomer droplet that contains polymer, or only polymer) to large droplets/particles. This process results in the larger droplets/particles increasing in size and the smaller droplets/particles decreasing in size (and the eventual disappearance of small droplets), and it can give rise to a bimodal particle/droplet size distribution. In general, Ostwald ripening is reduced by addition of a low MW hydrophobe (“cosurfactant” or “costabilizer”) such as hexadecane or cetyl alcohol.<sup>111,118,119</sup> Polymeric hydrophobes have also been reported to suppress Ostwald ripening.<sup>120</sup> The rate of diffusion (between monomer droplets/particles through the aqueous phase) of the hydrophobe is much lower than that of the monomer, which causes the monomer concentration to be higher in the thus formed larger droplets/particles than in the smaller ones (due to the hydrophobe being left behind in the small droplets/particles). This in turn causes the monomer chemical potential to be higher in the larger droplets/particles than in the smaller ones, and this effect counteracts the reduction in interfacial area, thus limiting Ostwald ripening.<sup>117</sup>

There are several reports describing colloidal instability in RAFT miniemulsion systems prior to polymerization (i.e., not related to superswelling—see below).<sup>121–124</sup> Qi and Schork<sup>125</sup> showed theoretically for a nonpolymerizing system that the stability of an aqueous miniemulsion is influenced by the presence of low concentrations of control agents used in CLRP (e.g., RAFT agent, metal complex in ATRP, nitroxide in NMP) through the effect on the rate of Ostwald ripening. If the hydrophobicity of the control agent is the same or higher than that of the costabilizer, the stability of the miniemulsion with regard to Ostwald ripening is improved in the presence of the control agent. However, if the control agent is less hydrophobic than the costabilizer, the miniemulsion becomes less stable.

#### 2.1.2. Superswelling

The chain concentrations and MWDs in CLRP are very different from those in a conventional nonliving radical polymerization. In CLRP, the MWDs are narrow ( $M_w/M_n < 1.5$ ) and the total concentration of polymer chains is higher than that in a nonliving radical polymerization.<sup>11,65</sup> Moreover, ideally, all chains are initiated at the start of the polymerization and grow simultaneously to eventually reach high MW (in a nonliving radical polymerization, chains are continuously initiated and grow to high MW within seconds throughout the polymerization). Consequently, there is a very high concentration of low MW oligomers present at low conversion in CLRP. This high concentration of oligomers and absence of high MW polymer at low conversion can



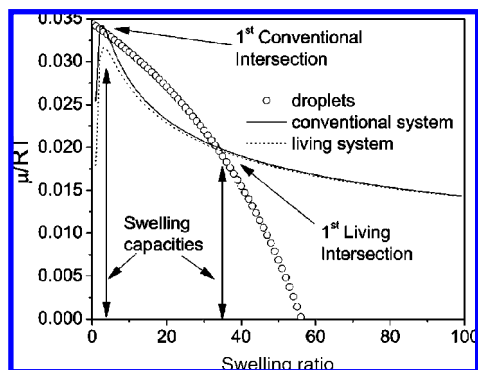


**Figure 2.** Monomer chemical potential ( $\mu$ ) at 75 °C vs degree of swelling of monomer (MMA) droplets (circles), polymer particles in conventional radical polymerization (full line), and polymer particles in CLRP (dotted line;  $M_{n,th}(100\% \text{ conversion}) = 10^4 \text{ g mol}^{-1}$ ;  $[\text{RAFT}]_0/[\text{MMA}]_0 = 0.01$ ) with 4 wt % hexadecane at 0.1% MMA conversion for polymer particles with an unswollen diameter of 60 nm, calculated using the model of Luo et al.<sup>126</sup> Reproduced (adapted) from ref 7 by permission of the Royal Society of Chemistry. Copyright 2006.

have a deleterious effect on colloidal stability as a result of “superswelling”,<sup>126</sup> which is generally of little or no concern in a nonliving miniemulsion polymerization.

Pure polymer particles can swell with a low MW compound so that the particle volume increases by approximately a factor of 1.5–5.<sup>127</sup> Oligomers are very effective swelling agents and can vastly increase the degree of swelling of polymer particles with monomer to beyond even a factor of 100.<sup>127,128</sup> The high concentration of low MW oligomers in CLRP at low conversion can under certain thermodynamic conditions give rise to superswelling,<sup>126</sup> where large amounts of monomer diffuse from non-nucleated monomer droplets to oligomer-containing droplets/particles. If the superswelling is severe enough, formation of very large particles ( $> 1 \mu\text{m}$ ) occurs, where buoyant forces dominate and a separate organic phase forms as an upper layer of the emulsion (this problem has often been encountered in RAFT emulsion and miniemulsion polymerization<sup>7,129–132</sup>); that is, the emulsion degrades. Moreover, redistribution of monomer but not control agent (RAFT agent, nitroxide etc.), caused by superswelling, alters the ratio of monomer/control agent at the polymerization loci, resulting in broad MWD and often also poor livingness.

The occurrence of superswelling can be understood within the framework of the theoretical model of Luo et al.<sup>126</sup> The monomer chemical potential in a nucleated droplet is lower than that in a monomer droplet, and monomer will diffuse from droplets to particles until the chemical potential of the droplets equals that of the particles at equilibrium. Figure 2 shows the chemical potentials of droplets and particles vs the degree of swelling calculated by McLeary and Klumperman<sup>7</sup> using the model of Luo et al.<sup>126</sup> for a conventional MMA miniemulsion polymerization ( $[\text{MMA}]/[\text{RAFT agent}] = 100$ ) employing 4 wt % hydrophobe for  $d = 60 \text{ nm}$  at 75 °C and 0.1% MMA conversion. Swelling occurs until the point is reached where the droplet and particle lines intersect. In the conventional system, this occurs at relatively low swelling. In CLRP, the chemical potential of the particles is reduced as a result of the presence of oligomers in high concentration, and the lines only intersect at much higher swelling—“superswelling”.

Droplet and particle chemical potentials are sensitive to a number of experimental factors, and as such, superswelling

can be avoided in a number of ways. In a miniemulsion, the extent of superswelling decreases as the number of polymer particles increases relative to the number of monomer droplets. Therefore, to avoid superswelling, it is important that monomer droplet nucleation (transformation of a monomer droplet to a polymer particle, i.e. generation of some polymer in a droplet) occurs rapidly. In miniemulsion NMP and ATRP, nucleation occurs as a result of an activation event inside a monomer droplet (except when an aqueous phase initiator is employed) as opposed to when an aqueous phase radical enters a droplet as in conventional miniemulsion polymerization. Problems with superswelling are thus likely to occur for systems with low activation rate and when each droplet contains only a low number activating species (e.g., alkoxyamine in the case of NMP), i.e. for high  $M_{n,th}$  and small particle sizes. It has been shown in conventional nonliving radical miniemulsion polymerization that addition of a small amount ( $< 1 \text{ wt } \%$  relative monomer) of high MW polymer to the organic phase can improve droplet stability and enhance monomer droplet nucleation, leading to higher  $R_p$ .<sup>8,133–137</sup> This approach has also been employed in miniemulsion NMP.<sup>138–143</sup>

If the particle diameter is above some critical level, superswelling does not occur.<sup>126</sup> For example, in an MMA miniemulsion with 1 wt % nucleated droplets, interfacial tension = 25 mN/m, 50 °C, molar ratio of control agent to monomer = 0.01, initial weight ratio of costabilizer to monomer in a particle = 0.02, and 10% MMA conversion based on initial MMA amount in a particle, superswelling occurs for  $d = 60 \text{ nm}$ , but not for  $d = 100 \text{ nm}$ . The theory of Luo et al.<sup>126</sup> also dictates that superswelling can be minimized by increasing the amount of hydrophobe and reducing the amount of control agent (RAFT agent, nitroxide, etc.), i.e. by increasing  $M_{n,th}$  (assuming this does not affect the droplet nucleation rate), by employing oligomeric/polymeric RAFT agents instead of low MW RAFT agents, and by decreasing the interfacial tension by postaddition of surfactant.<sup>144</sup>

### 2.1.3. Entry/Exit Considerations

In a miniemulsion polymerization, colloidal stability may be compromised if the transformation of a monomer droplet to a polymer particle is too slow (see above). In an emulsion polymerization in intervals I and II on the other hand, monomer droplet nucleation is not desirable. In a nonliving radical polymerization, the rate of monomer droplet nucleation (both in miniemulsion and emulsion polymerization) is governed by entry kinetics in the sense that once entry has occurred, the entered small radical will with extremely high probability grow to a high MW polymer. However, the rate at which an entered small radical grows to a high MW polymer is much lower in CLRP due to the dynamic activation–deactivation equilibrium only allowing intermittent chain growth, and the entered radical may exit prior to reaching a MW high enough to render it sufficiently hydrophobic to make exit impossible. The significance of exit of oligomers will of course increase with increasing hydrophilicity of the control agent. This idea was originally proposed by McLeary and co-workers<sup>7</sup> and is consistent with colloidal instability not being observed when using xanthates as RAFT agents in emulsion polymerization.<sup>145–150</sup> Xanthates have low exchange constants (i.e., the radical addition rates to xanthates are lower than those to normal RAFT agents such as CDB),<sup>11,32,151</sup> which allows the entering



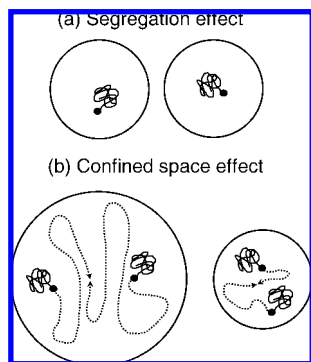


**Figure 3.** Schematic illustrations of (a) the segregation effect and (b) the confined space effect in a compartmentalized reaction system.

radical to grow to a considerable length prior to adding to a RAFT agent, thus minimizing RAFT oligomer exit. The use of xanthates also minimizes superswelling because of the reduction in the oligomer concentration.

The situation is particularly problematic in the case of high reactivity low MW RAFT agents, because the radical expelled on fragmentation of the RAFT intermediate radical generated by addition of an entering radical or propagating radical to the RAFT agent may easily exit (depending on the hydrophilicity).<sup>152–155</sup> This may be part of the reason why colloidal instability has been a major problem during implementation of RAFT in aqueous dispersed systems,<sup>7,129–132</sup> perhaps more so than for other CLRP systems such as NMP and ATRP.

## 2.2. Theoretical Aspects of CLRP in Dispersed Systems

### 2.2.1. General Considerations

This section is devoted to the understanding that has emerged from modeling and simulations of CLRP in dispersed systems. The theoretical studies described deal with CLRP in dispersed systems in the absence of particle formation; that is, the number of particles/droplets remains constant. This corresponds to miniemulsion or seeded emulsion polymerization with no transfer of reactants between particles and no secondary nucleation.

One of the intrinsic features of polymerization in dispersed systems is compartmentalization,<sup>78</sup> which refers to the confinement of reactants to compartments, e.g. polymer particles dispersed in a continuous phase. There are two types of compartmentalization effects: the *segregation effect* and the *confined space effect* (Figure 3).<sup>156</sup> The segregation effect refers to two species located in separate particles being unable to react. The confined space effect refers to two species located in the same particle reacting at a higher rate in a small particle than in a large particle.

The reaction rate between two species located in the same particle increases with decreasing particle size, expressed in terms of the pseudo-first-order rate coefficient  $k/N_A v_p$  ( $k$  is the rate coefficient for a bimolecular reaction in  $M^{-1} s^{-1}$  and  $v_p$  is the particle volume). The confined space effect is a concentration effect—the concentrations ( $\text{mol/dm}^3$ ) of a propagating radical and a deactivator in a particle containing a single propagating radical and a single deactivator increase with decreasing particle size according to  $\bar{n}/N_A v_p$ , where  $\bar{n}$  denotes the number of propagating radicals or deactivator species per particle ( $\bar{n} = 1$  in this example).

For compartmentalization effects to be significant, the number of reactants per particle must be sufficiently low. This requirement is fulfilled if the particles are sufficiently small and/or the concentration of reactants is sufficiently low. In a bimolecular reaction, the above requirement must be fulfilled with regard to both species. In a conventional emulsion polymerization under zero-one conditions,<sup>78</sup> termination is affected by compartmentalization but propagation is not, because a particle contains a very high number of monomer molecules. In CLRP, termination is often affected by segregation, and deactivation may be influenced by the confined space effect depending on the deactivator concentration. In both NMP and ATRP, the confined space effect may influence deactivation. However, the confined space effect is not operative on deactivation in RAFT (i.e., reaction between a propagating radical and a RAFT agent), because the RAFT agent concentration is too high. Another important factor is whether the reactants are generated in pairs or not. In NMP and ATRP, activation generates a propagating radical and deactivator as a pair in the same particle, and therefore, the confined space effect dominates over the segregation effect with regard to deactivation. Propagating radicals are not generated in pairs, and thus, the segregation effect dominates for termination. The rate of activation is not affected by compartmentalization in either NMP or ATRP. In NMP, activation is a first-order reaction and thus unaffected by compartmentalization. In ATRP, the activation step is bimolecular, but the alkyl halide and Cu(I)/ligand complex concentrations are both too high for compartmentalization to be operative under normal conditions. Compartmentalization in CLRP always leads to improved livingness because of less termination due to segregation, but the level of control (i.e.,  $M_w/M_n$ ) may be better or worse than that in bulk/solution depending on the particular system (mainly depending on  $N_{\text{cycles}}$  a chain experiences growing to a given DP).

### 2.2.2. CLRP Based on the Persistent Radical Effect (PRE)

**2.2.2.1. Compartmentalization.** CLRP systems based on the PRE<sup>68–70,75</sup> are exemplified by NMP and ATRP. The propagating radicals are segregated in the same way as in a conventional radical polymerization. The situation is however more complex if the deactivator (nitroxide in NMP, Cu(II)/ligand complex in ATRP) is also compartmentalized. This occurs if (i) the deactivator concentration is sufficiently low and (ii) the rate of transport of deactivator between particles is sufficiently low. Criterion (i) is easily understood by considering that the confined space effect is operative if the deactivator concentration in a single particle is greater than that in the corresponding bulk system.<sup>157</sup> Transport between particles refers to exit from one particle and diffusion through the continuous phase followed by entry into another particle—if this process is sufficiently rapid, deactivator species are not confined to a single particle.

**2.2.2.1.1. Deactivator with Relatively High Water Solubility.** In the case of sufficiently water-soluble deactivators that can move relatively freely between particles, compartmentalization only acts on propagating radicals. This case was treated theoretically for the NMP system styrene/SG1/90 °C by Charleux.<sup>158</sup> By assuming that the activation–deactivation equilibrium is the same as in a homogeneous system ( $K = [P^*][T^*]/[PT]$ ) and that spontaneous (thermal) initiation of styrene<sup>159</sup> is negligible

$$[T^*]_{\text{bulk}}^2 = [T^*]_{\text{disp}}^2 + \frac{2k_t}{N_A \nu_p k_{\text{deact}}} ([T^*]_{\text{disp}} - [T^*]_0) \quad (2.1)$$

where the subscripts disp and 0 denote the dispersed system and initial concentrations (organic phase), respectively. For sufficiently small particles ( $d < 500$  nm),  $[T^*]_{\text{disp}} < [T^*]_{\text{bulk}}$  because of reduced termination due to segregation, resulting in higher  $R_p$  and livingness, but also higher  $M_w/M_n$ . The increase in  $M_w/M_n$  is caused by the reduced deactivation rate (because  $[T^*]_{\text{disp}} < [T^*]_{\text{bulk}}$ ), resulting in a greater number of monomer units added per activation–deactivation cycle. Consequently,  $N_{\text{cycles}}$  is reduced, resulting in broader MWD.<sup>11</sup> These findings also apply to ATRP when the deactivator is not compartmentalized.

**2.2.2.1.2. Deactivator with Relatively Low Water Solubility.** The effects of compartmentalization on NMP<sup>156,160</sup> and ATRP<sup>161</sup> in dispersed systems with negligible deactivator exit (partitioning) have been investigated by Zetterlund and Okubo using modified two-dimensional Smith–Ewart equations originally derived by Butte et al.,<sup>162</sup> accounting for compartmentalization of both propagating radicals and deactivator as well as spontaneous (thermal) initiation<sup>159</sup> of styrene (S):

$$\begin{aligned} \frac{dN_i^j}{dt} = & N_A \nu_p k_{\text{act}} [\text{PT}] \{N_{i-1}^{j-1} - N_i^j\} + 0.5k_{i,\text{th}} [\text{S}]^3 N_A \nu_p \{N_{i-2}^j - \\ & N_i^j\} + \frac{k_t}{N_A \nu_p} \{(i+2)(i+1)N_{i+2}^j - (i)(i-1)N_i^j\} + \\ & \frac{k_{\text{deact}}}{N_A \nu_p} \{(i+1)(j+1)N_{i+1}^{j+1} - (i)(j)N_i^j\} \quad (2.2) \end{aligned}$$

In eq 2.2,  $N_i^j$  denotes the number of particles containing  $iP^*$  and  $jT^*$ , PT denotes alkoxyamine, and  $k_{i,\text{th}}$  is the rate coefficient for thermal initiation of styrene. An analogous equation has been derived for ATRP.<sup>161</sup>

Figure 4 shows  $[P^*]$  in the organic phase ( $R_p$  is proportional to  $[P^*]$  via  $R_p = k_p[P^*][S]$  because propagation is not affected by compartmentalization) as a function of  $d$  for styrene/TEMPO using a PS-TEMPO macroinitiator with and without thermal initiation at 125 °C for different particle diameters ( $d$ ). In the presence of thermal initiation, the system behaves as in bulk for particles with  $d > 65$  nm, but for smaller particles,  $[P^*]$  decreases dramatically with decreasing  $d$ . In the absence of thermal initiation, there is a maximum in  $[P^*]$  for  $35 < d < 65$  nm, but for  $d < 35$  nm, the system behaves the same as in the presence of thermal initiation. The dramatic decrease in  $[P^*]$  for  $d < 35$  nm is caused by the confined space effect on deactivation and geminate termination of thermal radicals. Activation generates  $P^*$  and  $T^*$  in pairs, and deactivation occurs rapidly in a small particle (for such small particles, the vast majority of particles contain no  $P^*$  and no  $T^*$ ). The same is true for thermal radicals generated in pairs, which undergo rapid geminate termination in small particles. For  $d < 35$  nm, the confined space effect acting on both deactivation and geminate termination of thermal radicals generated in pairs far outweighs the segregation effect on termination. The slope of the straight line is equal to 3 because  $[P^*]$  is proportional to the deactivation time in a particle containing one  $P^*$  and one  $T^*$  (deactivation time =  $N_A \nu_p / k_{\text{deact}}$ ). The maximum in  $[P^*]$  in the absence of thermal initiation is caused by segregation of  $P^*$ , causing a reduction in termination rate. In the absence of thermal initiation, all radicals are generated via PS-TEMPO activation and are thus not generated in pairs

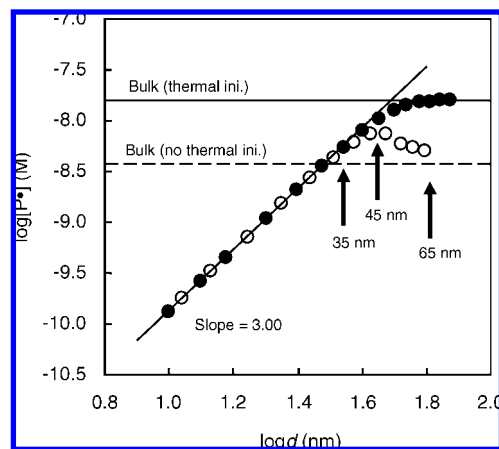


**Figure 4.** Simulated propagating radical concentrations ( $[P^*]$ ; 10% conversion) for TEMPO-mediated radical polymerization of styrene ( $[\text{PS-TEMPO}]_0 = 0.02$  M) with (●) and without (○) thermal initiation at 125 °C for different particle diameters ( $d$ ). The horizontal lines show  $[P^*]$  in the corresponding bulk systems. Reprinted with permission from ref 156. Copyright 2006 American Chemical Society.

in the same particles. Consequently, the segregation effect then plays a more significant role on termination than in the presence of thermal initiation.

In the particle size range where  $[P^*]_{\text{disp}} < [P^*]_{\text{bulk}}$ , i.e. where the confined space effect dominates, both the livingness and the level of control ( $M_w/M_n$ ) are superior to the case for bulk. The improved livingness is due to reduced termination caused by segregation.  $M_w/M_n$  is largely governed by  $N_{\text{cycles}}$  that a chain experiences growing to a given MW;  $M_w/M_n$  decreases with increasing  $N_{\text{cycles}}$ . Thus,  $M_w/M_n$  is expected to be lower than in bulk in the particle size range where the confined space effect dominates (rapid deactivation leads to fewer monomer units added per cycle). In the particle size range where  $[P^*]_{\text{disp}} > [P^*]_{\text{bulk}}$ , i.e. where segregation dominates, the livingness is again higher than in bulk. However, the control is poorer as a result of the low  $[T^*]_{\text{disp}}$  (due to low termination rate), allowing a high number of monomer units adding per activation–deactivation cycle.

The principles outlined above apply also to ATRP,<sup>161</sup> with the Cu(II)/ligand complex playing the role of the nitroxide.

The particle size range where either effect dominates (confined space effect or segregation effect) depends very strongly on the rates of activation and deactivation. For styrene/TEMPO/125 °C, the NMP equilibrium constant is relatively low,<sup>11</sup> and segregation of  $P^*$  plays a relatively minor role (the contribution of thermal radicals generated in pairs is strong). However, segregation of  $P^*$  exerts a much stronger effect in NMP/ATRP systems with a higher equilibrium constant. In such systems (e.g., styrene/TIPNO/125 °C, styrene/EBiB/CuCl/dNbpy2/70 °C),<sup>163</sup> very high  $R_p$ , high livingness, but broad MWDs are predicted unless the particles are very small ( $d < \text{approximately } 20$  nm). Compartmentalization may thus lead to either a decrease in both  $R_p$  and  $M_w/M_n$  or an increase in both  $R_p$  and  $M_w/M_n$  depending on the particular system, whereas the livingness always improves by compartmentalization.<sup>163</sup> Compartmentalization effects also depend on the absolute concentration of dormant chains. The critical particle size at which compartmentalization effects become significant increases with decreasing concentration of dormant chains.<sup>160</sup>

Compartmentalization in CLRP in dispersed systems has also been investigated by Tobita using Monte Carlo

simulations.<sup>157,164,165</sup> The results were in good agreement with those obtained by Zetterlund and Okubo.<sup>156</sup> The Monte Carlo technique revealed an additional feature of dispersed CLRP systems based on PRE; the fluctuation in the number of deactivators between different particles can lead to higher  $[P^*]$  in the organic phase than predicted from the average deactivator concentration.<sup>164</sup> This in turn results in different MWDs in different particles, causing overall MWD broadening. This effect is significant if the number of deactivators per particle is less than approximately 10, and the maximum effect (i.e., increase in  $[P^*]$ ) is approximately 100%.<sup>164</sup> It is important to note that the modified Smith–Ewart simulations<sup>156,160,161</sup> described above are based on particle averages, and fluctuation effects are therefore not accounted for. As such, it is clear that the maximum in  $[P^*]$  and concomitant loss in control can occur even in the absence of fluctuation effects as a result of the segregation effect on termination, because such  $[P^*]$  maxima were observed in the Smith–Ewart simulations. Moreover, recent Smith–Ewart simulations for NMP and ATRP with higher activation/deactivation equilibrium constants have revealed  $[P^*]$  maxima much greater than 100%.<sup>163</sup>

**2.2.2.2. Deactivator Partitioning.** Depending on the deactivator partitioning coefficient between the continuous (aqueous) phase and the organic phase (particles/monomer droplets), a significant amount of deactivator may be located in the aqueous phase, and this may have significant effects on the polymerization.

Cunningham and co-workers<sup>166</sup> modeled the interfacial mass transfer of TEMPO between the organic and aqueous phases under conditions pertaining to NMP in miniemulsion, concluding that phase transfer equilibrium is reached in  $<10^{-4}$  s for  $d \leq 300$  nm. The time to phase equilibrium increased with increasing droplet size, but the TEMPO equilibrium concentrations were unaffected by the droplet size. Cunningham and co-workers<sup>167</sup> also carried out simulations of miniemulsion NMP of styrene for TEMPO and OH-TEMPO at 135 °C based on a kinetic model accounting for nitroxide partitioning. The water solubility of OH-TEMPO is much higher than that of TEMPO; the partition coefficients between styrene and water are 2.2 and 98.8, respectively ( $= [\text{nitroxide}]_{\text{styrene}}/[\text{nitroxide}]_{\text{aq}}$ ).<sup>166,168</sup> but the  $k_{\text{act}}$  values are very similar.<sup>169</sup> The values of  $R_p$ , MW, and  $M_w/M_n$  were barely affected by replacing TEMPO with OH-TEMPO. However, when thermal initiation of styrene was not included in the model,  $R_p$  was markedly higher for OH-TEMPO than TEMPO.<sup>167</sup>

Theoretical work by Zetterlund and Okubo<sup>170</sup> clarified that, at phase transfer equilibrium, deactivator partitioning does not affect the polymerization once the stationary state with respect to  $[P^*]$  has been reached. However, in the pre-stationary state, the deactivation rate is reduced due to exit of nitroxide, resulting in an increase in  $[P^*]$  (and  $R_p$ ) and thus more termination. In simple terms, at the stationary state, the nitroxide that has been “lost” to the aqueous phase has been “replaced” in the organic phase by “additional” termination to make up for the loss. The above rationale holds if the nitroxide does not undergo reactions in the aqueous phase. Consequently, a more complex situation is anticipated when using a water soluble initiator such as KPS. The situation in ATRP<sup>171</sup> is analogous to that in NMP, although it is more complicated because the activation step is bimolecular, involving a Cu(I)/ligand complex, which may also partition to the aqueous phase.

The time to reach the stationary state ( $t_{\text{ss}}$ ) (initial deactivator concentration = 0) is given by<sup>11</sup>

$$t_{\text{ss}} = \frac{(k_t K^2 [\text{PT}]_0^2)^{1/2}}{3R_{i,\text{th}}^{3/2}} \quad (2.3)$$

where  $K$  is the CLRP equilibrium constant and  $R_{i,\text{th}}$  is the rate of thermal (spontaneous) initiation. The stationary state is reached within a few minutes for styrene/TEMPO at 125 °C.<sup>11</sup> However, for NMP and ATRP systems with a higher  $K$  and/or when  $R_{i,\text{th}}$  is lower (e.g., styrene/SG1/125 °C<sup>11</sup> and styrene/EBiB/CuBr/dNbpy2/90 °C<sup>171</sup>), the polymerization is essentially completed in the pre-stationary state due to the high  $t_{\text{ss}}$ . In such systems, deactivator partitioning may strongly affect the polymerization depending on the partition coefficient. If  $R_{i,\text{th}} = 0$ , there is no stationary state ( $t_{\text{ss}} = \infty$ ) and nitroxide partitioning affects the polymerization throughout the entire conversion range.

The theoretical findings with regard to deactivator partitioning in NMP and ATRP are consistent with experimental data.<sup>170</sup>  $R_p$ ,  $M_n$ , and  $M_w/M_n$  are barely affected when TEMPO is replaced by OH-TEMPO in styrene miniemulsion NMP,<sup>167,172</sup> because the polymerizations proceed in the stationary state. On the other hand, miniemulsion polymerization of *n*BA at 135 °C is faster using the macroinitiator PS-(OH-TEMPO) than PS-TEMPO.<sup>173</sup> Due to the low value of  $R_{i,\text{th}}$  for acrylates, a stationary state is not reached and thus there is a significant effect of partitioning. ATRP usually proceeds in the pre-stationary state, and thus partitioning effects are observed in the case of significant partitioning of the Cu(II)/ligand complex.<sup>171</sup>

Modeling and simulations by Cunningham and co-workers<sup>174,175</sup> of TEMPO-mediated polymerization of styrene in miniemulsion at 135 °C (not accounting for compartmentalization effects) using the water-soluble initiator KPS indicated that both  $R_p$  and the livingness could be improved by decreasing the solids content as a result of nitroxide partitioning.

The modeling studies of compartmentalization effects on NMP and ATRP described in section 2.2.1.2 did not account for exit (partitioning) of deactivator; that is, the results obtained are only applicable to systems with highly hydrophobic deactivators where exit can be neglected. In a real system, some exit will occur even for quite hydrophobic deactivators. The confined space effect on deactivation will thus be counteracted by exit of deactivator. The time for deactivation to occur is significantly longer than the phase equilibrium times for styrene/TEMPO,<sup>166</sup> suggesting that exit of nitroxide can compete with deactivation. This also applies to the fate of thermal radicals generated in pairs by thermal initiation of styrene inside particles—some fraction of these radicals may undergo exit instead of geminate termination in small particles.<sup>157,176</sup> Moreover, the presence of deactivator in the aqueous phase would reduce the rate of re-entry, enhancing the effect of exit of thermal radicals and monomeric radicals generated by chain transfer to monomer.<sup>176</sup>

**2.2.2.3. Comparison with Experiment.** **2.2.2.3.1. Compartmentalization in NMP.** TEMPO-mediated polymerization of styrene often gives very similar results in miniemulsion and bulk.<sup>177–183</sup> In most such miniemulsion systems,  $d \approx 80 - 200$  nm, and the particles are thus not small enough for compartmentalization to play a significant role.<sup>156,160</sup> Moreover, particle size distributions in miniemulsion are often relatively broad,<sup>8,11,178</sup> and most polymer would then form in the larger particles, further minimizing compart-



mentalization effects. There are however numerous examples where  $R_p$  in miniemulsion/microemulsion NMP is different from that in bulk,<sup>139,143,176,184–188</sup> but many factors are at play and it is usually difficult to attribute deviations to one factor only. Factors other than compartmentalization and nitroxide partitioning that may affect NMP in dispersed systems include the interface effect on deactivation,<sup>185,188–190</sup> exit of small radicals (from chain transfer to monomer and/or thermal initiation of styrene),<sup>176</sup> enhanced (spontaneous) radical generation,<sup>184,186,191</sup> the Laplace pressure inside the particles,<sup>192</sup> as well as effects related to the monomer concentration at the polymerization locus.

Evidence of compartmentalization effects in miniemulsion NMP has been obtained by Cunningham and co-workers<sup>176</sup> for the TEMPO-mediated miniemulsion polymerization of styrene at 135 °C in the absence of hexadecane. As  $d_w$  decreased from 180 to 50 nm with increasing Dowfax 8390 concentration,  $R_p$  decreased and the livingness increased, but  $M_w/M_n$  remained relatively unaffected.  $R_p$  in miniemulsion was lower than that in bulk, but the bulk system exhibited intermediated livingness. These results (except the livingness in bulk) are consistent with the confined space effect on deactivation and geminate termination of styrene thermal radicals, and less termination due to segregation. In the presence of hexadecane, the reduction in  $R_p$  for small particles was weaker than that without hexadecane.<sup>176</sup> Okubo and Zetterlund<sup>187</sup> reported reduced  $R_p$  (compared to bulk) in microemulsion NMP of styrene at 125 °C using TEMPO ( $d_n = 44–68$  nm) and SG1 ( $d_n = 21–27$  nm). The reduction in  $R_p$  was smaller for SG1 than for TEMPO, consistent with exit of nitroxide competing more effectively with deactivation for SG1, as expected based on its higher water solubility, thus weakening the confined space effect. No substantial evidence of compartmentalization effects in SG1-mediated polymerizations in emulsion<sup>193,194</sup> and miniemulsion<sup>139</sup> has been observed. This is most likely because the relatively high water solubility of SG1 counteracts the confined space effect on deactivation,<sup>194</sup> and the particle sizes have not been sufficiently small for significant segregation effects on termination. Somewhat higher  $R_p$  in miniemulsion than bulk has however been observed in SG1-mediated polymerizations of styrene, attributed to segregation of propagating radicals and/or SG1 partitioning and/or decomposition of SG1 in the aqueous phase.<sup>143</sup>

**2.2.2.3.2. Compartmentalization in ATRP.** Examination of the literature on ATRP in dispersed systems with regard to compartmentalization meets with the same problems as for NMP. There are limited data where particle size effects are investigated or where comparison is made with the corresponding bulk/solution polymerization. Matyjaszewski et al.<sup>195</sup> reported that, for the reverse ATRP system  $nBMA/AIBN/CuBr_2/dNbpy/190$  °C, the polymerization behavior was close to identical with ( $d = 235$  nm) and without ( $d = 1070$  nm) hexadecane.  $R_p$  was lower in miniemulsion than in bulk, but it is unlikely that the confined space effect on deactivation (which would reduce  $R_p$ ) would be operative for such large particles, and it is more likely that the main factor was the lower initiation efficiency in miniemulsion. The corresponding direct ATRP miniemulsion system was also unaffected by decreasing the particle size from  $d = 1.5$   $\mu\text{m}$  to 300 nm. Matyjaszewski and co-workers<sup>196</sup> also investigated  $nBMA/EBIB/CuBr_2/BPMODA/AIBN$  (SR&NI system) miniemulsion polymerization ( $d = 252$  nm), reporting no difference compared to bulk. Very similar results in

miniemulsion and bulk were also obtained with  $nBA$  ( $d = 270$  and 305 nm depending on ligand). Again, these results indicate that smaller particles are needed for compartmentalization effects to play a significant role in these systems, consistent with theory.<sup>161</sup> Microemulsion ATRP has been reported,<sup>197,198</sup> but nothing conclusive can be said about compartmentalization because the corresponding bulk systems were not studied. Simms and Cunningham<sup>199</sup> recently reported very high MWs ( $M_n = 989900$ ,  $M_w/M_n = 1.25$ ) for the redox initiated reverse ATRP of  $nBMA$  ( $d_w < 110$  nm). Current understanding indicates that such high MWs cannot be obtained with good control/livingness in the corresponding bulk/solution system, and it is speculated that compartmentalization<sup>200</sup> as well as the nature of the redox initiation system are important factors.

### 2.2.3. CLRP Based on Degenerative Transfer

CLRP systems based on degenerative transfer include RAFT, TERP, and ITP. This section focuses exclusively on RAFT, although some of the conclusions would apply to other degenerative transfer systems (in particular with regard to effects of chain-length dependent termination). RAFT polymerization in bulk/solution is often (but not always) accompanied by both inhibition and retardation.<sup>19,21,22</sup> Inhibition in bulk/solution can be ascribed to the pre-equilibrium, whereas retardation effects are currently not fully understood.<sup>22</sup> The ongoing scientific debate on retardation in bulk/solution centers around the behavior of the RAFT intermediate radicals.<sup>22,201,202</sup> Inhibition/retardation in the presence of a RAFT agent is usually stronger in miniemulsion and seeded emulsion systems than in bulk/solution.<sup>7,144,152–155,203,204</sup> The extent of deactivator partitioning in NMP and ATRP depends on the hydrophobicity of the deactivator. Low MW RAFT agents may partition to the aqueous phase, and this would be a concern at low conversion (prior to consumption of the initial RAFT agent) as well as for wider conversion ranges when using low reactivity, low MW RAFT agents.

**2.2.3.1. Compartmentalization.** Degenerative transfer CLRP systems are affected differently by compartmentalization than systems based on the PRE. Segregation of propagating radicals is a factor if the particles are sufficiently small. However, the confined space effect is not operative on the deactivation reaction because the concentration of the “deactivator” is too high (in RAFT, the “deactivator” corresponds to the RAFT agent (the RAFT end group)).<sup>157</sup> A reduction in particle size does not lead to an increase in the RAFT agent concentration for realistic particle sizes and RAFT agent concentrations (see section 2.2.1).

Luo et al.<sup>204</sup> analyzed the kinetics of RAFT polymerization in a dispersed system using an adapted two-dimensional Smith–Ewart equation as the starting point, distinguishing between propagating radicals and RAFT intermediate radicals. Assuming that the RAFT equilibrium itself is unaffected by compartmentalization and that the system is zero–one with respect to the total number of radicals, they derived eq 2.4 for the total number of radicals per particle ( $\bar{n}_{\text{tot}}$ ):

$$\bar{n}_{\text{tot}} = \frac{\rho}{2\rho + kf_n} \quad (2.4)$$

where  $\rho$  and  $k$  are the entry and exit rate coefficients, respectively, and  $f_n$  is the number fraction of propagating radicals relative to the total number of radicals (eq 2.4 was also modified to account for “RAFT-induced” exit). When

$f_n = 1$ , eq 2.4 reduces to the expression for a so-called “simple zero–one system”.<sup>78</sup> Under zero–one conditions with respect to  $\bar{n}_{\text{tot}}$ , there is an intrinsic retardative effect of the RAFT agent:

$$\frac{\bar{n}_{\text{RAFT}}}{\bar{n}_0} = (1 + 2\bar{n}_0 K[\text{KRAFT}]_0)^{-1} \quad (2.5)$$

In eq 2.5,  $\bar{n}_{\text{RAFT}}$  and  $\bar{n}_0$  are the numbers of propagating radicals per particle for polymerization with and without RAFT agent, respectively. This treatment rests on the assumption that crosstermination between a propagating radical and a RAFT intermediate radical occurs at a rate sufficiently high for crosstermination to be considered instantaneous. The rate coefficient for crosstermination ( $k_t'$ ) has been estimated experimentally for the styrene/PS-dithiobenzoate system ( $k_t' = 0.8k_t$ ), suggesting that this assumption is reasonable.<sup>205</sup> The transformation of a propagating radical to a RAFT intermediate radical by addition to a RAFT agent means that, during some fraction of the total time this particle spends containing one radical (i.e., the time that passes until another radical enters), propagation does not occur, because the RAFT intermediate radical does not propagate. Therefore, some fraction of particles containing one radical are “inactive”. The extent of retardation of this origin is expected to increase in magnitude with decreasing fragmentation rate coefficient of the RAFT intermediate radical. This effect is intrinsic to RAFT and is not present for CLRP systems operating based on the persistent radical effect. Luo et al.<sup>204</sup> used eq 2.5 to estimate  $K$  for styrene/CPDB and obtained a value in close agreement with that obtained in bulk, demonstrating how a dispersed system can be exploited to extract kinetic information.

Peklak and Butte<sup>153</sup> modeled RAFT (low MW RAFT agent) in a seeded emulsion using population balance equations and assuming a zero–one system. The RAFT intermediate radicals were not considered, i.e. the reversible transfer reaction was modeled simply as an exchange process. The authors concluded that inhibition is caused by entering  $z$ -mer radicals adding to RAFT agent, followed by expulsion of the RAFT leaving group, which has a high probability of exit. Prescott et al.<sup>154</sup> investigated RAFT polymerization of styrene in dispersed systems by use of a Smith–Ewart approach that also included aqueous phase kinetics and phase transfer events, and they reported that the inhibition periods observed experimentally can be explained by RAFT-induced exit of  $z$ -mer radicals, exit of the RAFT leaving group radical (low MW RAFT agent), and addition of the RAFT leaving group radical to the RAFT end group (regenerating the original RAFT agent). Peklak and Butte<sup>153</sup> concluded that retardation occurs as a result of RAFT-induced exit, originally proposed by Prescott et al.,<sup>206</sup> whereby an entering  $z$ -mer adds to a RAFT agent to generate a  $z$ -mer RAFT agent. Subsequent radical addition to such a  $z$ -mer RAFT agent expels the  $z$ -mer, which may then exit or propagate (or add to another RAFT agent). However, although this process undoubtedly influences the kinetics in some way, it is in our opinion unclear how the presence of any RAFT agent changes the overall probability of exit of an entering  $z$ -mer, which is ultimately governed by the relative rates of exit and propagation (to a chain-length where exit can no longer occur). Addition to a RAFT agent prior to propagation/exit does not alter the probability of exit that the entering  $z$ -mer experiences once it is subsequently expelled from the RAFT agent by addition of another radical. Comparison of the rate

of exit of a  $z$ -mer from a particle with and without  $z$ -mer RAFT agents is in this sense somewhat misleading,<sup>206</sup> because the increased exit rate observed in the presence of a  $z$ -mer RAFT agent occurs simply as a result of the  $z$ -mers consumed on generation of these  $z$ -mer RAFT agents not having exited (i.e., the  $z$ -mer exit is essentially delayed, with the cumulative number of exit events occurring being unaltered). RAFT-induced exit should be distinguished from “frustrated entry”,<sup>148</sup> which refers to RAFT-induced exit involving low MW surface active RAFT agents, whereby the rate of addition to a RAFT agent by an entering radical is enhanced due to the high concentration of RAFT agent near the interface.

Monte Carlo simulations by Tobita and Yanase<sup>157,165</sup> (not considering aqueous phase kinetics and exit/entry, and assuming chain-length independent  $k_t$ ) revealed that  $R_p$  increased with decreasing particle size, attributed to the segregation effect on termination. This effect was much stronger if it was assumed that RAFT intermediate radicals terminate with propagating radicals (cross-termination) with the same  $k_t$  as termination between two propagating radicals. As pointed out by the authors, RAFT polymerization in miniemulsion with different particle sizes may thus provide a means of settling the ongoing debate as to whether cross-termination occurs significantly or not in RAFT.<sup>22</sup>

**2.2.3.2. Chain-Length Dependent Termination.** Butte et al.<sup>207</sup> investigated compartmentalization effects in a dispersed system for a generic degenerative transfer system (discussed below in terms of a high MW RAFT agent) using population balance equations based on the Smith–Ewart equations<sup>208</sup> and the concept of a distinguished particle distribution<sup>209</sup> (zero–one not assumed). The RAFT exchange reaction was modeled as an exchange process without consideration of RAFT intermediate radicals. The results revealed the importance of the reaction of an entering radical with a high MW RAFT agent, generating a long radical. As a short radical enters a particle already containing a radical, it may either terminate or add to a RAFT agent. The probability of the second radical terminating ( $P(\text{term})$ ) prior to addition to a dormant species increases with decreasing particle size:

$$P(\text{term}) = \frac{k_t/N_A v_p}{k_t/N_A v_p + k_{\text{ex}}[\text{RAFT}]} \quad (2.6)$$

where  $k_{\text{ex}}$  is the rate coefficient for the overall RAFT exchange process. The time that passes before termination occurs between two radicals located in a particle is equal to the inverse of the pseudo-first-order rate coefficient for termination ( $N_A v_p/k_t$ ),<sup>78</sup> and as such the termination rate increases with decreasing particle size—this is the confined space effect<sup>156</sup> on termination. The reaction rate between the entering radical and a RAFT agent does however not change with particle size because  $[\text{RAFT}]$  is too high for the confined space effect to be operative (section 2.2.1). Since transfer to a RAFT agent, generating a long radical, would be followed by long-long termination,  $P(\text{term})$  also corresponds to the probability of short–long termination (if the second radical does not add to a RAFT agent, short–long termination occurs). Monte Carlo simulations by Prescott<sup>210</sup> also showed that, in a RAFT system with a high MW RAFT agent, the smaller the particles, the greater is the fraction of short–long termination events relative to the total number of termination events; that is,  $k_t$  itself (not  $k_t/N_A v_p$ ) increases with decreasing particle size due to the chain-length dependence of  $k_t$ . In other words, the effect of particle size on

radical lifetimes (the confined space effect) is enhanced by the presence of a RAFT agent because of the chain-length dependence of  $k_t$ .

Monte Carlo simulations by Prescott<sup>154,210</sup> revealed that a RAFT agent may influence whether the system obeys zero-one kinetics or not because of the chain-length dependence of  $k_t$ .<sup>76,211</sup> Termination is diffusion controlled,<sup>76,211</sup> and shorter chains diffuse more rapidly than longer chains ("short" = DP  $\leq$  10; "long" = DP  $\geq$  100). In a zero-one system in the absence of a RAFT agent, termination occurs between an entering short radical and a long radical already present in the particle. RAFT agents with a high chain transfer constant can have a profound effect on the kinetics, whereas low chain transfer constant RAFT agents only exert a minor influence. All radicals are short at low conversion, and all termination events are thus short-short, and as such considerably faster than short-long events (which would be the case in the absence of RAFT agent). As the conversion increases, the dormant chains grow, and thus the corresponding radicals also become longer. Moreover, entering short radicals rapidly add to the high reactivity RAFT agent (which is now of considerable DP), thus generating longer radicals, resulting in long-long termination, i.e. slower than short-long termination. The end result is that, in comparison to a system without RAFT agent, a RAFT system is more likely to be zero-one at low conversion (because termination is faster than without RAFT agent) and less likely to be zero-one at high conversion (because termination is slower than without RAFT agent). This general trend is in agreement with experimental findings by Luo et al.<sup>204</sup>

**2.2.3.3. Comparison with Experiment.** Due to the sheer complexity of RAFT polymerization in dispersed systems (exit of RAFT agent leaving radical, RAFT-induced exit, effects of chain length dependent termination, and issues related to local concentrations of reactants), it is difficult to extract information on compartmentalization from experimental data. The task is also complicated by the fact that the RAFT mechanism is at this point not fully understood, in particular with regard to the behavior of the RAFT intermediate radicals.<sup>22,201,202,212,213</sup> However, in general, RAFT in miniemulsion is faster than in bulk, consistent with segregation of propagating radicals.<sup>203,204,214</sup> The confined space effect on deactivation is not operative in RAFT (section 2.2.1).<sup>157</sup> Moreover, retardation (compared to in the absence of RAFT agent) is usually stronger in dispersed systems than in bulk/solution.<sup>7,144,152-155,203,204</sup> This is consistent with the intrinsic retardative effect of RAFT in a zero-one system proposed by Luo et al.<sup>204</sup> (there are however other possible reasons for more extensive RAFT retardation in dispersed systems).

## 2.3. Miniemulsion Polymerization (Incl. Suspension Polymerization)

### 2.3.1. Nitroxide-Mediated Radical Polymerization (NMP)

**2.3.1.1. General Considerations.** In a miniemulsion polymerization, monomer droplets are converted to polymer particles as the polymerization proceeds, and transport of nitroxide or low MW alkoxyamine through the aqueous phase between the monomer phase and the polymer particles (as in an *ab initio* emulsion polymerization) is therefore not a concern. Miniemulsion NMP can be broadly divided into two categories: (i) Aqueous phase initiation,<sup>138,139,143,181,182,215-217</sup> and (ii) oil phase initiation.<sup>139-142,172,173,178,180,181,184-186,188,216-223</sup>

NMP can be carried out using a radical initiator and a nitroxide (e.g., BPO/TEMPO), or by employing a preformed alkoxyamine species as unimolecular initiator. In the case of aqueous phase initiation, the initiator/nitroxide or the alkoxyamine is initially located in the aqueous phase. Subsequently, propagation to a  $z$ -mer occurs,<sup>78</sup> followed by entry into a monomer droplet leading to droplet nucleation. Entry may occur by a  $z$ -meric alkoxyamine and/or by a  $z$ -meric radical and nitroxide. The extent of aqueous phase termination can have an important effect on the MW, as it affects the number of chains initiated (the initiation efficiency).<sup>143,182</sup> Systems based on oil phase initiation are inherently simpler, because aqueous phase kinetics plays only a minor role.

The pH of the aqueous phase can sometimes be important. In the case of aqueous phase initiation in miniemulsion NMP using the redox initiation system KPS/Na<sub>2</sub>S<sub>2</sub>O<sub>5</sub>, SG1 is consumed by side reactions at acidic pH, and buffering is required to optimize the system in terms of control/livingness.<sup>138,139</sup> Miniemulsion copolymerization of styrene and AA using the water-soluble alkoxyamine A-Na also proceeds poorly due to SG1 decomposition in the aqueous phase at low pH.<sup>143</sup> In TEMPO-based miniemulsion polymerizations, buffering is not a requirement.<sup>6</sup>

Proper choice of surfactant can be crucial. The very vast majority of miniemulsion NMPs have been carried out using SDBS or Dowfax 8390. SDS is not suitable for TEMPO-mediated radical polymerization of styrene, which may be related to its degradation at high temperature.<sup>224</sup> SDS has however been used successfully in SG1-mediated miniemulsion polymerization of styrene at 90 °C,<sup>138,139</sup> and the surfactant mixture SDS/Forafac has been employed successfully for *n*BA at 112 °C<sup>141</sup> and 115 °C,<sup>140</sup> as well as for the copolymerization of styrene/*n*BA at 120 °C<sup>141</sup> and 115 °C.<sup>140</sup> There are to date no reports on the use of nonionic or cationic emulsifiers in miniemulsion NMP.

In general, miniemulsion polymerizations require the addition of a suitable hydrophobe to suppress Ostwald ripening.<sup>111,118,119</sup> In the case of miniemulsion NMP, that role can (to some extent) be fulfilled by an alkoxyamine macroinitiator such as PS-TEMPO, thus alleviating the need for addition of e.g. hexadecane.<sup>74,111,186,217</sup> The addition of a small amount of high MW polymer (<1 wt % rel. monomer) may also aid in monomer droplet stabilization and enhance droplet nucleation.<sup>8,133-137</sup>

**2.3.1.2. TEMPO-Based Systems.** TEMPO can effectively mediate radical polymerization of styrene and styrenic monomers but can in general not be employed for NMP of other vinyl monomers such as acrylates (see below), methacrylates, or vinyl esters. TEMPO-based miniemulsion NMP of styrene has been carried out successfully for a number of different systems: (i) TEMPO/BPO,<sup>172,173,177,181,217</sup> (ii) KPS/TEMPO,<sup>167,168,181,182,215,217</sup> (iii) PS-TEMPO,<sup>74,173,178-180,184-186,188,217</sup> and (iv) the low MW TEMPO-based alkoxyamine BST.<sup>167,184</sup> The use of the more water-soluble OH-TEMPO has also been investigated.<sup>167,168,172,173,181</sup> These polymerizations in general proceed well, resulting in good control/livingness comparable to that of bulk/solution. In all the studies cited above, the anionic surfactants SDBS or Dowfax 8390 were employed. Due to the relatively low equilibrium constant ( $K = 2.1 \times 10^{-11} \text{ M}^{-1}$  at 125 °C) for TEMPO/styrene, polymerizations are generally carried out at >120 °C. TEMPO-based NMP of styrene has also been



carried out as a suspension polymerization at 122 °C using a mixed surfactant system PVA/SDS.<sup>225</sup>

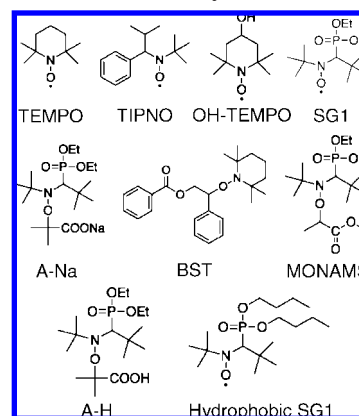
The initiator/TEMPO ratio is an important experimental parameter for both oil phase<sup>177</sup> and aqueous phase initiation.<sup>182</sup> If the ratio is too high, the amount of TEMPO is insufficient to ensure controlled/livingness, whereas the opposite results in an induction period (applies also to bulk/solution).<sup>182,219</sup> Moreover, in the case of the water-soluble initiator KPS, the initiator efficiency decreases with increasing KPS concentration as a result of increased termination in the aqueous phase.<sup>182</sup> Initiation using an oil phase alkoxyamine species such as a PS-TEMPO macroinitiator is simpler in the sense that the initial number of chains is well-defined.

Theory dictates that nitroxide partitioning between the organic and aqueous phases is not expected to influence NMP in dispersed systems in the stationary state using oil phase initiation, although a significant increase in  $R_p$  and partial loss of control/livingness may occur in the prestationary state (section 2.2).<sup>170</sup> In the case of aqueous phase initiation, the situation is more complex, because nitroxide in the aqueous phase then partakes in activation–deactivation in the aqueous phase.<sup>181</sup> In agreement with theory, NMP of styrene in miniemulsion proceeds very similarly for TEMPO and OH-TEMPO,<sup>167,172,181</sup> despite the much higher water solubility of the latter.<sup>166,168</sup> The alkoxyamines corresponding to the ethylbenzene radical and TEMPO and OH-TEMPO have very similar rate coefficients for thermal dissociation (differing by <20%).<sup>169</sup>

One of the drawbacks of CLRP systems based on dissociation–combination is that  $R_p$  is often relatively low compared to that for a conventional radical polymerization. In bulk/solution,  $R_p$  can be increased by use of various additives such as organic acids and organic acid salts that consume free TEMPO.<sup>226–229</sup> This approach has also been employed in miniemulsion. Addition of camphorsulfonic acid (CSA) in batch mode at the beginning of the polymerization to both TEMPO and OH-TEMPO-mediated miniemulsion polymerizations of styrene results in similar increases in  $R_p$  accompanied by relatively minor broadening of the MWD.<sup>172</sup> The effects of CSA are weaker than those in bulk, presumably as a result of CSA partitioning between the organic and aqueous phases. Continuous addition of an aqueous solution of ascorbic acid (which also consumes TEMPO) has also been investigated, resulting in higher final conversions than those for batch mode addition of CSA, and narrow MWDs.<sup>183,217</sup> The livingness increased on addition of ascorbic acid despite the increase in  $R_p$ . This is because the main formation mechanism of dead chains is in fact alkoxyamine decomposition (disproportionation; Scheme 7),<sup>169,230</sup> which is a first-order reaction, the extent of which thus increases with increasing polymerization time (Figure 5).<sup>167</sup>

Continuous addition of ascorbic acid has also been exploited in TEMPO-mediated miniemulsion polymerization of styrene at 100 °C, resulting in good livingness but poor control ( $M_w/M_n = 1.4–1.6$ ; poor control due to a relatively low  $N_{cycles}$  experienced by each chain during its growth).<sup>74</sup> Another technique to increase  $R_p$  while maintaining reasonable control/livingness is to add a high temperature radical initiator (e.g., dicumyl peroxide), which decomposes slowly and thus provides a continuous supply of radicals.<sup>71,73,231</sup> This approach has also been applied relatively successfully to TEMPO-mediated miniemulsion polymerization of styrene

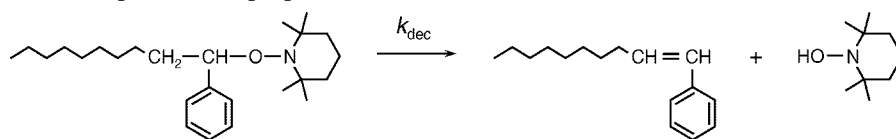
## Scheme 6. Nitroxides and Alkoxyamines



at 100 °C, using the water-soluble initiators VA-085 and VA-060,<sup>74,183</sup> as well as to TEMPO-mediated suspension polymerization of styrene.<sup>225</sup> Microwave-assisted OH-TEMPO-mediated miniemulsion polymerization of styrene has also been carried out, resulting in somewhat higher  $R_p$  and satisfactory control/livingness.<sup>232</sup>

Recent work has indicated that  $R_p$  in TEMPO-mediated styrene miniemulsion polymerization using SDBS as surfactant at 135 °C increases with the SDBS concentration (at similar particle size distributions;  $d_v \approx 120$  nm), whereas the MWDs are not significantly affected.<sup>184,186</sup> This has been speculated to be caused by SDBS participating in radical generation. No such surfactant concentration effects were observed for Dowfax 8390.<sup>180,186</sup> There is also experimental evidence that the particle size can influence both  $R_p$  and the control/livingness. For TEMPO-mediated styrene miniemulsion polymerizations using SDBS as surfactant at 125 °C,  $R_p$  increased at the expense of lower control/livingness with decreasing particle size ( $70 < d_n < 170$  nm).<sup>185,188</sup> Similar particle size effects have been observed in monomer-free aqueous miniemulsion model systems consisting of a PS-TEMPO macroinitiator dissolved in toluene/tetradecane (SDBS/125 °C).<sup>189</sup> The high MW shoulder arising from termination by combination increased with decreasing particle size. It has been suggested that an interface effect is operative,<sup>185,188–190</sup> consistent with TEMPO exhibiting interfacial activity, according to which some fraction of TEMPO is adsorbed at/preferentially located near the interface between the aqueous and the organic phases, resulting in a reduced deactivation rate, and thus higher  $R_p$  and lower control/livingness.

As discussed in section 2.2, theory dictates that compartmentalization effects are expected in TEMPO-mediated radical polymerization of styrene in dispersed systems for  $d < 110$  nm (depending on the concentration of dormant chains).<sup>156,160</sup> In most cases, styrene/TEMPO miniemulsion polymerization using PS-TEMPO,<sup>178,180</sup> BPO/TEMPO,<sup>177,181</sup> or KPS/TEMPO<sup>181–183</sup> results in  $R_p$  similar to that in bulk.<sup>65</sup> The particle size distribution in a miniemulsion is normally relatively broad, and thus even if  $d_n < 110$  nm, most polymer would form in larger particles,<sup>178</sup> and thus compartmentalization would not be important. Cunningham and co-workers showed that, in the TEMPO-mediated radical polymerization of styrene in miniemulsion at 135 °C using Dowfax 8390,  $R_p$  decreased and the livingness increased with decreasing particle size ( $54 < d_w < 185$  nm),<sup>176</sup> consistent with the confined space effect and segregation (compartmentalization).<sup>156</sup>

**Scheme 7. Alkoxyamine Decomposition (Disproportionation)**

TEMPO-mediated polymerization of acrylates in bulk/solution only proceeds to low conversion mainly due to excessive buildup of free TEMPO. By use of various additives that consume TEMPO,<sup>233–235</sup> it is however possible to achieve satisfactory results. Successful TEMPO-mediated radical polymerization of *n*BA in aqueous miniemulsion at 135 °C has been reported by use of addition of ascorbic acid (which consumed free TEMPO).<sup>235,236</sup> Miniemulsion NMP of *n*BA at 135 °C proceeds much faster and to higher conversion with OH-TEMPO than TEMPO due to partitioning of OH-TEMPO to the aqueous phase.<sup>173</sup> The stationary state is not expected to be reached on the polymerization time scale in this system, and consequently there is a significant effect of nitroxide partitioning on the kinetics (section 2.2.2.2).<sup>170</sup>

**2.3.1.3. SG1-Based Systems.** Aqueous miniemulsion NMP using the more versatile nitroxide SG1 or SG1-based alkoxyamines has been performed for styrene<sup>138–141,143</sup> and *n*BA<sup>140–143,218</sup> as reviewed by Charleux and Nicolas.<sup>237</sup>

SG1-mediated miniemulsion polymerization of styrene at 90 °C using AIBN results in less control and a higher initial  $R_p$  than in bulk,<sup>139</sup> probably mainly due to SG1 partitioning to the aqueous phase. A ratio of  $[\text{SG1}]/[\text{AIBN}] \approx 1.2$  gave the best results in terms of good control/livingness and a reasonable (not too low)  $R_p$ . Nitroxide partitioning results in a reduced nitroxide concentration in the particles during the prestationary state (no such effect during the stationary state), and SG1-mediated polymerization of styrene at 90 °C proceeds exclusively in the prestationary state (section 2.2.2.2).<sup>170</sup> There are at present no data available on the partitioning of SG1 between water and styrene, but significantly higher water solubility than TEMPO is anticipated. The initiator efficiency (the fraction of the initial alkoxyamine species that are converted to polymer chains) is significantly lower than unity in the SG1-mediated miniemulsion polymerization of *n*BA at 112 °C using the oil-soluble low MW alkoxyamine MONAMS.<sup>142</sup> Increasing the temperature to 125 °C or using a *Pn*BA-SG1 macroinitiator results in enhanced initiator efficiency, consistent with the reduction in initiator efficiency being related to exit of the primary

radical<sup>142,216</sup> (or the oligomeric species formed on addition of one or more *n*BA units) generated upon thermal dissociation of MONAMS and/or the initiation rate (which increases with temperature).

SG1-mediated miniemulsion polymerization of styrene using the redox initiation system KPS/Na<sub>2</sub>S<sub>2</sub>O<sub>5</sub> at 90 °C<sup>138</sup> proceeds at a rate similar to SG1-mediated styrene polymerization in bulk at 120 °C;<sup>238</sup> that is, rate enhancement is observed in miniemulsion. The use of a more hydrophobic analogue of SG1 (butyl- instead of ethyl groups; Scheme 6) resulted in lower  $R_p$ , consistent with SG1 partitioning between the aqueous and organic phases playing an important role.<sup>138</sup> As a consequence of SG1 partitioning, the MWDs were relatively broad ( $M_w/M_n \approx 1.69\text{--}2.47$ ). Increasing the solids content led to narrower MWDs due to the reduced effect of SG1 partitioning. SG1 is consumed by side reactions at acidic pH, and thus buffering is essential in order to obtain good control/livingness.<sup>138,139</sup>

SG1-mediated miniemulsion polymerizations of styrene and *n*BA have also been carried out using a water-soluble low MW alkoxyamine initiator (A-Na), the sodium salt of A-H.<sup>143</sup> Polymerizations were thus carried out at 112 °C using Dowfax 8390 at alkaline pH using sodium hydrogen carbonate as buffer (pH > 5.5 to avoid SG1 decomposition). Activation initially takes place in the aqueous phase, where chain growth occurs until the species is sufficiently hydrophobic to enter the monomer droplets/polymer particles.<sup>216</sup> Termination prior to entry results in loss of chains capable of continued growth, manifested as  $M_n > M_{n,\text{th}}$  (reduction in initiator efficiency). Both  $R_p$  and  $M_w/M_n$  were higher in miniemulsion than bulk (using A-H) for *n*BA, most likely due to SG1 partitioning and/or SG1 decomposition, although the MWDs were relatively narrow and  $M_n \approx M_{n,\text{th}}$ . Both for styrene and *n*BA, the miniemulsion polymerizations with the water-soluble A-Na were much slower than with the organic phase initiator A-H. In the case of styrene, the polymerization was very slow with a significant induction period, as well as poor initiator efficiency. The equilibrium constant  $K$  is much higher for styrene than *n*BA,<sup>11</sup> and therefore the aqueous phase concentration of radicals will be much higher for styrene, which results in more termination and consequently a lower initiator efficiency. Moreover, the propagation rate of styrene is low in the aqueous phase due to a low styrene concentration and the relatively low  $k_p$ . In the case of *n*BA,  $K$  is much lower and aqueous phase propagation is faster (higher *n*BA concentration in the aqueous phase and higher  $k_p$  than styrene), and thus very high initiator efficiencies are obtained. Consistent with this rationale, the addition of a small amount of MA to the styrene system resulted in considerable improvement in the initiator efficiency.

$R_p$  in miniemulsion for SG1-mediated polymerizations of styrene<sup>139</sup> and *n*BA<sup>140,141</sup> with  $d > 100$  nm are relatively similar to those in bulk,<sup>139,238</sup> indicating the absence of significant compartmentalization effects (section 2.2.2).

According to NMR and MALDI-TOF analyses, chain transfer to polymer in SG1-mediated polymerization of *n*BA in both bulk and miniemulsion at 112 °C proceeds mainly by the intramolecular mechanism (backbiting; as opposed

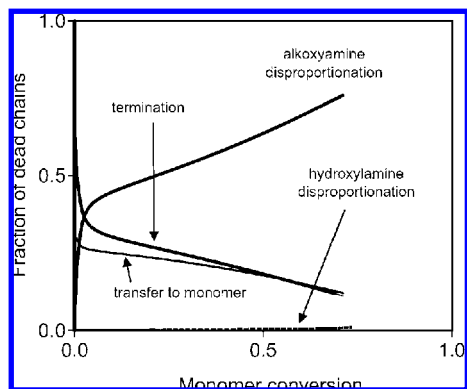


**Figure 5.** Simulated fractions of dead chains formed by different mechanisms as indicated for TEMPO-mediated radical polymerization of styrene in aqueous miniemulsion at 135 °C. Reprinted with permission from ref 167. Copyright 2003 Elsevier Ltd.

to intermolecular chain transfer), with the majority of chains having the ideal structure with one initiator fragment and one SG1 end group.<sup>218</sup>

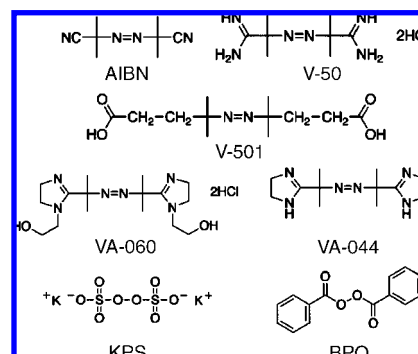
### 2.3.2. Atom Transfer Radical Polymerization (ATRP)

**2.3.2.1. General Considerations.** When implementing ATRP in aqueous dispersed systems, an obvious concern is how the ATRP process itself is affected by the presence of water. ATRP can be carried out successfully in aqueous solution, as recently reviewed by Tsarevsky and Matyjaszewski.<sup>239</sup> However, various side reactions may occur. The nature of the solvent influences the structure of the Cu complex—less polar solvents (e.g., hydrophobic monomers) favor formation of  $\text{Cu}(\text{bpy})_2^+ \text{CuBr}_2^-$ , whereas polar solvents such as water favor formation of  $\text{Cu}(\text{bpy})_2^+ \text{Br}^-$ . Less polar solvents lead to a reduction in the apparent  $k_{\text{act}}$ ,<sup>240–242</sup> because only half of the Cu of the complex  $\text{Cu}(\text{bpy})_2^+ \text{CuBr}_2^-$  is in the active form  $\text{Cu}(\text{bpy})_2^+$ .<sup>241</sup> Deactivator dissociation occurs as a result of low stability of the Cu complexes in protic media, leading to formation of inactive Cu(II) complexes that are unable to deactivate propagating radicals.<sup>243</sup> The ATRP equilibrium is thus shifted more toward the active state, and consequently, the overall effect is an increase in  $R_p$  and partial loss of control/livingness with increasing solvent polarity.<sup>239,241</sup> The loss in control/livingness can be overcome by addition of excess deactivator<sup>243–248</sup> or halide salts.<sup>243</sup> Other side reactions that may occur in the presence of water include disproportionation of Cu(I) complexes, generating Cu(II) and Cu(0), and substitution or elimination reactions of the alkyl halide initiators.<sup>239</sup> The effects of water itself on  $R_p$  and control/livingness in aqueous dispersed ATRP are relatively minor because the main locus of polymerization is the organic phase, and by proper choice of ligand, the Cu(I) and Cu(II) complexes partition primarily to the organic phase.

In an ideal miniemulsion polymerization, each monomer droplet is converted to one polymer particle without migration of components through the aqueous phase.<sup>8,111</sup> In a real miniemulsion system, some droplet/particle coagulation occurs, and the addition of a hydrophobe (e.g., hexadecane) is required to minimize Ostwald ripening.<sup>111,118,119</sup> Okubo and co-workers<sup>249,250</sup> carried out miniemulsion ATRP of *i*BMA using the hydrophobic ligand dNbpy2 at 40 °C without addition of a specific hydrophobe. Good colloidal stability with approximately constant particle size throughout the polymerization as well as good control/livingness suggested that the ligand may have fulfilled the role of a hydrophobe. However, Matyjaszewski et al.<sup>195</sup> reported markedly larger particle sizes in the miniemulsion reverse ATRP of *n*BMA at 90 °C using dNbpy1 without (1070 nm) than with hexadecane (235 nm), indicating the ligand was unable to prevent Ostwald ripening. It has been reported that a hydrophobe/monomer molar ratio > 1:250 is required to prevent Ostwald ripening;<sup>251</sup> that is, in most cases, the ligand content would be high enough, and failure of the ligand to prevent Ostwald ripening can then be attributed to excessive water solubility.<sup>195</sup> In the vast majority of miniemulsion ATRP reported, hexadecane has been employed as hydrophobe.

Various transition metals can be employed in ATRP,<sup>10,17,18</sup> but to date all miniemulsion ATRP systems investigated are based on copper. A complicating issue when implementing direct ATRP in miniemulsion is the sensitivity of the Cu(I) complex to oxidation on exposure to air during the emulsification process.<sup>195</sup> It is technically difficult to perform

Scheme 8. Radical Initiators



emulsification under anaerobic conditions, and for this reason reverse ATRP,<sup>195,199,252–255</sup> SR&NI ATRP,<sup>196,256,257</sup> and AGET ATRP<sup>171,258–263</sup> have been employed with success because these approaches are less sensitive to oxygen.

The choice of emulsifier is crucial in miniemulsion ATRP. Anionic emulsifiers are incompatible with ATRP because they deactivate the Cu complexes; the sulfate anion of the anionic emulsifier SDS has been speculated to react with copper(II) bromide to form copper(II) sulfate and sodium bromide.<sup>264,265</sup> Good colloidal stability as well as satisfactory control/livingness have been obtained using mainly nonionic (Brij 98,<sup>195,196,199,252,256–260,266</sup> Tween 80,<sup>249,250</sup> and PVA<sup>171</sup>) emulsifiers but also the cationic emulsifier CTAB.<sup>254</sup>

Miniemulsion ATRP has been carried out successfully for styrene,<sup>171,196,250,256,259,260,263,266,267</sup> MMA,<sup>199,266</sup> *n*BMA,<sup>195,196,199,252,254,255,257,263,266</sup> MA,<sup>256,267</sup> *n*BA,<sup>196,256–260,263,266,268</sup> *t*BA,<sup>266</sup> OEOMA,<sup>261,262,269,270</sup> and HEMA.<sup>271</sup>

**2.3.2.2. Initiation Systems.** **2.3.2.2.1. Direct ATRP.** Application of high shear forces is necessary for the preparation of a miniemulsion,<sup>8,111</sup> which comprises submicron-sized monomer droplets dispersed in a continuous (usually aqueous) phase. The normal approach is to employ strong agitation via ultrasonication or by use of a microfluidizer, a process which normally takes at least 10 min. In direct ATRP, the transition Cu complex is in its lower oxidation state prior to polymerization, and the presence of air (oxygen) will inevitably result in partial or complete oxidation to the corresponding Cu(II) complex (i.e., the deactivator). Therefore, emulsification in the case of direct ATRP must be carried out under a nitrogen atmosphere<sup>195</sup> or alternatively for a very short time.<sup>250</sup> In the direct ATRP system *n*BMA/EBiB/CuBr/dNbpy1, conversion reached >70% in 2 h at 70 °C with good control/livingness.<sup>195</sup> However, (partial) Cu(I) complex oxidation renders direct ATRP unsuitable for miniemulsion implementation and makes kinetic studies difficult.

**2.3.2.2.2. Reverse ATRP.** The problem of Cu(I) complex oxidation can be avoided by use of reverse ATRP, which starts with a radical initiator, which may be water-soluble, and a Cu(II) complex.<sup>10,272,273</sup> An induction period is observed until initiator decomposition causes the initially high Cu(II) concentration to decrease to a level that allows polymerization. The emulsion changes color from green (Cu(II)) to brown (Cu(I)) in the initial stage of the polymerization.

Reverse ATRP in miniemulsion has been carried out for *n*BMA<sup>195,199,252–255</sup> and MMA<sup>199</sup> with both good control/livingness and colloidal stability. Matyjaszewski et al.<sup>195</sup> carried out reverse ATRP of *n*BMA in miniemulsion (CuBr<sub>2</sub>/



AIBN/dNbpy1/Brij 98/90 °C) with reasonable control/livingness and good colloidal stability ( $d = 235$  nm). The initiator efficiency was lower in miniemulsion than in bulk, probably because of lower deactivator concentration in miniemulsion due to partitioning as well as exit of primary radicals followed by termination in the aqueous phase. Better agreement between  $M_n$  and  $M_{n,th}$  was obtained with the water-soluble azoinitiator V-50 ( $d = 190$ – $300$  nm), partly caused by more rapid initiator decomposition than with AIBN. Reverse ATRP can lead to a relatively broad MWD if the initiator decomposition is too slow, as new chains are generated throughout the polymerization. Li and Matyjaszewski<sup>252</sup> also carried out reverse ATRP of *n*BMA in miniemulsion (CuBr<sub>2</sub>/VA-044/Brij 98/70 °C) with high activity TREN-based ligands (high  $k_{act}$  and  $K$ ), obtaining good control/livingness and colloidal stability ( $d = 190$ – $300$  nm) and no induction period, as opposed to the case with the lower activity dNbpy1 complex. When the emulsifier concentration was too high, control/livingness was largely lost for very hydrophobic TREN-based ligands, due to micellar nucleation (as well as droplet nucleation), resulting in polymerization loci with an insufficient concentration of deactivator due to aqueous phase transport limitations of the hydrophobic ligand complex. Compared to the dNbpy1 system at 90 °C, less emulsifier was required due to the lower temperature of 70 °C, made possible by use of a complex with high catalytic activity.

Cunningham and Simms<sup>254</sup> reported successful reverse ATRP of *n*BMA using the cationic emulsifier CTAB (CuBr<sub>2</sub>/EHA<sub>6</sub>TREN/VA-044) at 90 °C, although some phase separation was observed at conv. < 75%. The use of Brij 98 led to severe coagulation at 70 °C but colloidal stability at 60 °C. This discrepancy with the work of Matyjaszewski and co-workers,<sup>195</sup> who reported successful use of Brij 98 at temperatures at high as 90 °C, was attributed to the smaller particle sizes generated by Cunningham and Simms ( $d = 126$  nm) due to different emulsification techniques. CTAB loadings as low as 1 wt % relative to monomer provided colloidal stability, i.e. considerably lower than that for Brij 98.

Cunningham and Simms<sup>199,255</sup> found that reverse ATRP of *n*BMA and MMA in miniemulsion using the redox initiation system ascorbic acid/hydrogen peroxide (CuBr<sub>2</sub>/EHA<sub>6</sub>TREN/Brij 98/60 °C) allows formation of extremely high MW polymer with narrow MWD (e.g.,  $M_n = 989900$ ,  $M_w/M_n < 1.25$ ;  $d_w \approx 100$  nm). Based on current CLRP understanding,<sup>11</sup> such high MW polymer cannot be prepared while still maintaining good control/livingness. Such high MWs could not be obtained by using low concentrations of VA-044, suggesting that the explanation is somehow related to the redox initiation system, although compartmentalization is also likely to play a role.<sup>200</sup>

Despite the advantages of reverse ATRP over direct ATRP in miniemulsion, reverse ATRP is associated with various inherent disadvantages (also in bulk/solution) such as an induction period, often relatively broad MWDs, difficulty in predicting the MW, requirement of a large amount of Cu(II) complex, as well as being limited to synthesis of linear polymer (because the structure of the radical initiator determines the polymer structure), and block copolymers are not accessible.<sup>10</sup> It is of course possible to prepare block copolymer by addition of a second monomer after completion

of a first stage polymerization by reverse ATRP, but this second stage polymerization then becomes direct ATRP by definition.

**2.3.2.2.3. SR&NI and AGET ATRP.** In order to overcome the problems of reverse ATRP, alternative initiation systems have been employed. SR&NI (Simultaneous Reverse and Normal Initiation) ATRP<sup>10,274</sup> is a combination of direct and reverse ATRP, where alkyl halide, Cu(II) complex, and radical initiator are initially present. Compared to reverse ATRP, SR&NI ATRP allows lower Cu complex content, and more complex polymer architectures are accessible. Pure block copolymers are however not accessible via SR&NI ATRP. AGET (Activators Generated by Electron Transfer) ATRP<sup>10,259</sup> starts with alkyl halide, Cu(II) complex, and a reducing agent such as ascorbic acid, which reduces the Cu(II) complex to the corresponding Cu(I) complex, followed by direct ATRP. Miniemulsion ATRP synthesis of well-defined polymers of various architectures (linear, block, gradient, and star-shape polymers) have been reported using SR&NI<sup>196,256,257</sup> and AGET<sup>171,258–263,266</sup> ATRP.

It is desirable to reduce the catalyst concentration in ATRP formulations, as the Cu complex contaminates the polymer product. This can be achieved by use of high activity complexes (e.g., TREN-based ligands) in direct ATRP, but in reverse ATRP, a stoichiometry limitation is imposed on the initial Cu(II) complex concentration based on the radical initiator concentration. Li et al.<sup>196</sup> obtained good control/livingness and colloidal stability ( $d = 252$  nm) in SR&NI miniemulsion ATRP of *n*BMA using the ligands BPMODA or tNtpy (EBiB/AIBN/CuBr<sub>2</sub>/Brij 98/80 °C), which are hydrophobic and have high catalytic activity, but not with EHA<sub>6</sub>TREN due to excessive partitioning to the aqueous phase. Compared to a reverse ATRP process, the amount of CuBr<sub>2</sub>/ligand was reduced by a factor of 5–8. ATRP of various monomers (*n*BMA, *n*BA, and styrene) in miniemulsion employing SR&NI has been carried out successfully.<sup>196,256,257</sup> Diblock, triblock, and 3-arm star block copolymers have also been prepared in miniemulsion using this technique with tNtpy or BPMODA at 60 °C, employing mono-, di-, and trifunctional macroinitiators with good control/livingness ( $M_w/M_n = 1.18$ – $1.37$ ). However, 2-dimensional chromatography revealed the presence of a small amount of homopolymer of the second monomer generated by AIBN radicals during the block copolymer synthesis, which is an inevitable drawback of SR&NI ATRP.<sup>256</sup>

AGET ATRP, which relies on a reducing agent such as ascorbic acid to reduce the Cu(II) complex instead of radicals from a radical initiator, allows preparation of pure block copolymer in the absence of homopolymer of the second monomer. Matyjaszewski and co-workers<sup>259</sup> carried out AGET ATRP in miniemulsion of *n*BA and styrene using ascorbic acid as reducing agent (EBiB/CuBr<sub>2</sub>/BPMODA/Brij 98/80 °C). Ascorbic acid, which is water-soluble, reduces Cu(II) located in the aqueous phase at/near the monomer droplet surface, generating the less water-soluble Cu(I), which partitions to the monomer droplets. The amount of ascorbic acid added is crucial—too much results in compromised control/livingness, whereas an insufficient amount causes very low  $R_p$ . As anticipated, AGET ATRP allowed the synthesis of high purity block copolymers and star copolymers of MA and styrene,<sup>259,267</sup> as well as various gradient copolymers.<sup>266</sup> An additional advantage of AGET ATRP is that, by employing an excess of reducing agent, the reducing agent consumes the oxygen as well as reduces

**Table 1. Partitioning of CuBr<sub>2</sub>/2dNbpy1 and CuBr/2dNbpy1 in *n*BMA and Water with *n*BMA/Water (w/w) = 15/100 (from Ref 253) <sup>a</sup>**

		CuBr <sub>2</sub> /2dNbpy1			CuBr/2dNbpy1		
		2.5 × 10 <sup>-3</sup> M	1.0 × 10 <sup>-2</sup> M	2.5 × 10 <sup>-2</sup> M	1.0 × 10 <sup>-2</sup> M	2.5 × 10 <sup>-2</sup> M	3.0 × 10 <sup>-2</sup> M
Γ <sup>a</sup>	rt	0.2	1.6	11.9	160	160	71
Γ <sup>a</sup>	90 °C	N.A.	0.2	0.4	19	21	13

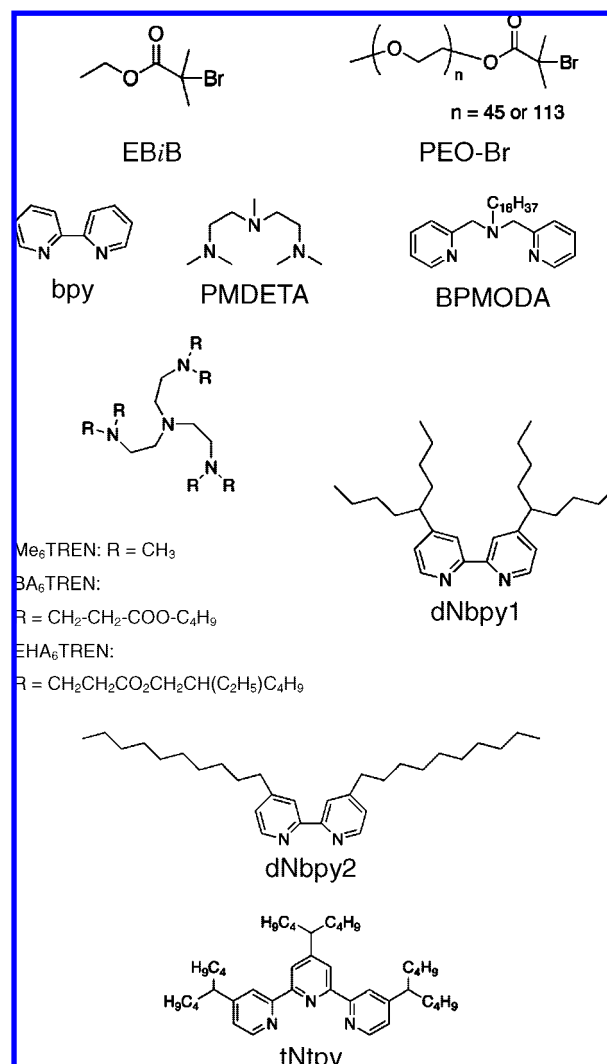
<sup>a</sup> Γ = [Cu]<sub>org</sub>/[Cu]<sub>aq</sub>.

the Cu(II) complex, thus eliminating the need for deoxygenation.<sup>260</sup> Charleux and co-workers<sup>263</sup> used an amphiphilic diblock copolymer, poly(ethylene oxide)-*b*-PS, as emulsifier and macroinitiator in AGET ATRP of *n*BMA, styrene, and *n*BA in miniemulsion (CuBr<sub>2</sub>/ascorbic acid/BPMODA/80 °C). The presence of free emulsifier in polymer particles can have adverse effects on film properties (emulsifier migration<sup>275,276</sup>), and covalently linking the emulsifier to the polymer is thus desirable and may also improve colloidal stability.

AGET ATRP in miniemulsion has also been applied to synthesis of well-defined hybrid materials.<sup>258,268</sup> Core-shell hybrid particles using functionalized silica particles as macroinitiator were prepared in miniemulsion, thereby minimizing macrogelation due to bimolecular termination (coupling) of chains by exploiting compartmentalization, thus increasing the yield.<sup>258</sup> The same miniemulsion approach has also been employed for efficient synthesis of molecular brushes.<sup>268</sup>

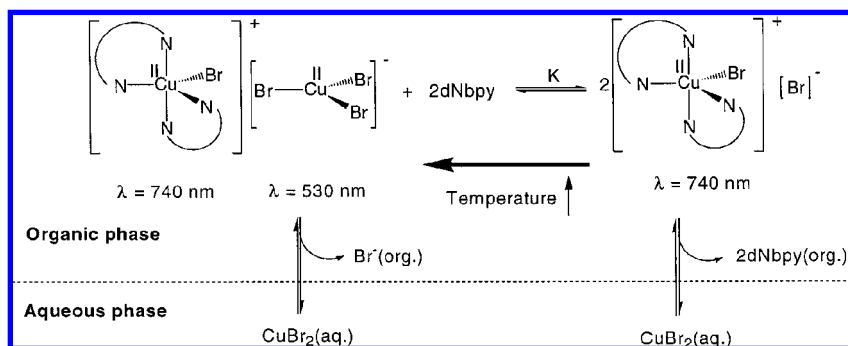
**2.3.2.3. Partitioning Effects.** Excessive deactivator (Cu(II)) partitioning to the aqueous phase results in the deactivator concentration at the polymerization locus being too low, and control/livingness is lost.<sup>196,264,265,277</sup> However, most ligands employed in bulk/solution, such as bde, bpy, PMDETA, and Me<sub>6</sub>TREN, have high water solubility (low partitioning coefficient, Γ = [X]<sub>org</sub>/[X]<sub>aq</sub>). For example, in the *n*BMA/EBiB/CuCl/Brij 98 system at 85–90 °C using bpy as ligand, *M*<sub>n</sub> (64000) ≫ *M*<sub>n,th</sub> (8500) at 30% conversion and *M*<sub>w</sub>/*M*<sub>n</sub> = 2.08.<sup>277</sup> Replacing bpy with the more hydrophobic dNbpy1 led to *M*<sub>w</sub>/*M*<sub>n</sub> = 1.24–1.31 and much better agreement between *M*<sub>n</sub> and *M*<sub>n,th</sub>.<sup>277</sup> Therefore, more hydrophobic ligands that are more suitable for aqueous miniemulsion have been developed, e.g. dNbpy, EHA<sub>6</sub>TREN, BPMODA, and tNtpy.

Even when using very hydrophobic ligands which themselves only partition negligibly to the aqueous phase, significant Cu(I) and Cu(II) partitioning may still occur if the binding affinity of the ligand toward Cu is not sufficiently strong.<sup>253</sup> Matyjaszewski and Charleux and co-workers<sup>253</sup> measured the partitioning of Cu(I) and Cu(II) species and dNbpy1 between *n*BMA and water (Table 1). The ligand itself partitioned negligibly to the aqueous phase, yet as much as 20–30% of Cu(I) and 80–99% of Cu(II) species were located in the aqueous phase at 90 °C (partitioning experiments with 15 wt % *n*BMA, 85 wt % water). The water solubility of CuBr is very low, as evidenced by Γ<sub>CuBr</sub> > 10, whereas Γ<sub>CuBr<sub>2</sub></sub> < 1 at 90 °C. Γ<sub>CuBr<sub>2</sub></sub> decreased with decreasing overall concentration of Cu(II)/2dNbpy1 and with increasing temperature. Γ<sub>CuBr</sub> appeared to increase somewhat with decreasing overall concentration of Cu(I)/2dNbpy1 and also decreased with increasing temperature. Thus, for both Cu(I) and Cu(II), partitioning to the aqueous phase increases with increasing temperature. Cu(I) species are most likely to exit to the aqueous phase in the form of CuBr<sub>2</sub><sup>-</sup>.<sup>253</sup> With regard to Cu(II), some Cu(II) would exit in the form of a complex with dNbpy1, but the concentration of Cu(II) in this form in the aqueous phase is much lower than the total Cu(II)

**Scheme 9. ATRP Initiators and Ligands**

concentration in the aqueous phase. It was deduced from UV–vis analysis that the CuBr<sub>2</sub>/2dNbpy1 complex dissociates to CuBr<sub>3</sub><sup>-</sup> and [Cu(dNbpy1)<sub>2</sub>Br]<sup>+</sup> (Scheme 10), and CuBr<sub>3</sub><sup>-</sup> subsequently dissociates to CuBr<sub>2</sub> and Br<sup>-</sup>. Moreover, the CuBr<sub>2</sub>/2dNbpy1 complex dissociates to form CuBr<sub>2</sub> and dNbpy1. CuBr<sub>2</sub> has very high water solubility and readily partitions to the aqueous phase, and thus the high (apparent) Γ value for CuBr<sub>2</sub>/2dNbpy1 is not due to the water solubility of CuBr<sub>2</sub>/2dNbpy. Partitioning causes the dNbpy/Cu(II) ratio in the organic phase to increase, creating an excess of ligand. Only Cu(II) complexes with cations of the form [Cu(II)(dNbpy)<sub>2</sub>Br]<sup>+</sup> are believed to function as deactivators in ATRP.<sup>278</sup>

The influence of partitioning has been quantified by Kagawa et al.<sup>171</sup> in the miniemulsion AGET ATRP of styrene (*d* = 500 nm) (EBiB/CuBr<sub>2</sub>/dNbpy2/ascorbic acid/PVA/90 °C) using experiments and simulations based on the partitioning data discussed above. According to both simulations

**Scheme 10. Partitioning of Cu(II) Species** (Reprinted with permission from ref 253. Copyright 2000 American Chemical Society.)

and experiment,  $R_p$  and  $M_w/M_n$  were higher in miniemulsion than in the corresponding solution polymerization as a result of a decrease in deactivator concentration in the organic phase (Figure 6). Simulations indicated quantitatively that a decrease in  $N_{\text{cycles}}$  as well as an increase in termination caused the increase in  $M_w/M_n$ , both direct results of the reduced deactivator concentration. Simulations also revealed  $R_p$  to be independent of Cu(II) partitioning in the stationary state (consistent with earlier findings in NMP<sup>170</sup>) but increasing with increasing Cu(II) partitioning in the prestationary state. The present ATRP proceeds exclusively in the prestationary state, and thus, Cu(II) partitioning leads to a decrease in Cu(II) in the particles (section 2.2.2.2).

**2.3.2.4. Inverse Miniemulsion Systems.** Inverse miniemulsion polymerization (W/O emulsion; hydrophobic continuous phase, hydrophilic dispersed phase) enables synthesis of water-soluble and hydrophilic polymer. The first application of ATRP in an inversion miniemulsion was reported by Matyjaszewski and co-workers,<sup>261,262</sup> who employed AGET ATRP to prepare poly[oligo(ethylene glycol) monomethyl ether methacrylate] particles with good control/livingness and colloidal stability ( $d \approx 200$  nm). The nonionic emulsifier Span 80, which has a low HLB value of 4.3, resulted in good colloidal stability. Considering both water solubility and Cu halide complex activity, TPMA and bpy were used as ligands. The use of EBiB as initiator led to inferior control/livingness, most likely due to poor solubility

in the dispersed phase. The water-soluble PEO-Br was instead employed as initiator. As described in section 2.3.2.1, the presence of water can lead to loss of control/livingness. However, TPMA forms an active Cu complex without dissociation in water.<sup>279</sup>

Di- and triblock copolymers (PEO-*b*-PHEMA and PHEMA-*b*-PEO-*b*-PHEMA)<sup>271</sup> as well as hydrophilic polymer gels<sup>262</sup> have been prepared by inverse miniemulsion AGET ATRP. Matyjaszewski and co-workers<sup>269,270</sup> also employed miniemulsion AGET ATRP for synthesis of cross-linked hydrophilic polymer particles for drug delivery applications.

### 2.3.3. RAFT Polymerization

**2.3.3.1. General Considerations.** RAFT is one of the most versatile of the current CLRP techniques, and the number of papers describing RAFT in aqueous dispersed systems exceeds that of other CLRP methods. The control agent is attached to the polymer chain as an end group (except in the initial stage of the polymerization using low MW RAFT agents) and is thus unable to partition between the aqueous and organic phases (unlike in NMP and ATRP, where the nitroxide and metal complexes, respectively, may partition significantly to the aqueous phase). Implementation of RAFT in aqueous dispersed systems, especially miniemulsion, thus initially seemed relatively straightforward. However, significant difficulties related to colloidal stability have had to be overcome.

Miniemulsion RAFT polymerizations have to date been reported for styrene,<sup>122–124,131,132,144,203,204,214,280–293</sup> 4-acetoxystyrene,<sup>294</sup> MMA,<sup>280,281,283,284,291,295,296</sup> nBMA,<sup>123,131,281,295,297–299</sup> EHMA,<sup>131,281</sup> various fluorinated alkyl methacrylates,<sup>297,299</sup> nBA,<sup>123,124,155,290,300</sup> MAA,<sup>281,300</sup> VAc,<sup>121,301</sup> acrylamide,<sup>302</sup> as well as vinyl saccharide monomers based on D-glucose and D-fructose.<sup>295</sup> Miniemulsion RAFT copolymerizations have also been reported; for example, styrene/MMA<sup>303</sup> and BMA/fluorinated methacrylates<sup>304</sup> and numerous block copolymers have been synthesized, e.g. PMMA-*b*-PS,<sup>280,283</sup> PS-*b*-PnBA,<sup>124,280,290</sup> PnBA-*b*-PS,<sup>290</sup> PBMA-*b*-poly(dodecafluoroheptyl methacrylate),<sup>297</sup> poly(fluoroalkyl methacrylate)-*b*-PnBMA,<sup>299</sup> PEHMA-*b*-P(MMA-*co*-MAA),<sup>281</sup> as well as diblock and triblock copolymers involving methacrylates and vinyl saccharide monomers based on D-glucose and D-fructose.<sup>295</sup> Schork and co-workers reported that miniemulsion RAFT polymerizations of styrene and nBA can be implemented in continuous polymerization systems consisting of a train of stirred tank reactors (CSTRs)<sup>124,292,305</sup> as well as a tubular reaction system,<sup>122,123,285</sup> both for homopolymerization and block copolymer synthesis.

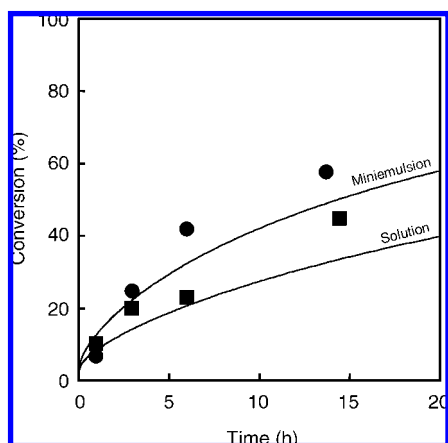


**Figure 6.** Simulated (solid lines) and experimental (■, ●) conversion vs time for solution (■) and miniemulsion (●) ATRP of styrene at 90 °C ([styrene]<sub>0</sub> = 4.36 M, [PBr]<sub>0</sub> = 0.022 M, [CuBr]<sub>0</sub> = 0.044 M, [dNbpy]<sub>0</sub> = 0.088 M). Partitioning coefficients in miniemulsion ( $\Gamma_{\text{CuBr}} = [\text{CuBr}]_{\text{org}}/[\text{CuBr}]_{\text{aq}}$  and  $\Gamma_{\text{CuBr}_2} = [\text{CuBr}_2]_{\text{org}}/[\text{CuBr}_2]_{\text{aq}}$ ):  $\Gamma_{\text{CuBr}} = 3.2$  and  $\Gamma_{\text{CuBr}_2} = 0.14$ . Reprinted with permission from ref 171. Copyright 2007 American Chemical Society.



RAFT polymerization has also been carried out successfully in suspension.<sup>306</sup>

**2.3.3.2. Hydrolysis of RAFT Agent.** Depending on the experimental conditions, hydrolysis of the dithiocarbonyl moiety of the RAFT agent may be significant. The rate of hydrolysis increases with increasing pH of the aqueous phase as well as with temperature.<sup>307–310</sup> Dithioester RAFT agents are more susceptible to hydrolysis than trithiocarbonate RAFT agents.<sup>311</sup> Prescott et al.<sup>310</sup> reported that only minimal degradation of PPPDTA occurred at 50 °C in an ethanol/water mixture, but as much as 30% decomposition occurred in 1 h at 85 °C. However, in a dispersed system, the RAFT agent partitions between the aqueous and the organic phases, and the extent of hydrolysis will thus decrease with increasing hydrophobicity of the RAFT agent. Therefore, for most RAFT agents employed in dispersed systems, hydrolysis is not a significant problem.

**2.3.3.3. Colloidal Stability.** Miniemulsion RAFT polymerization suffers from severe colloidal instability in the form of a clear, usually colored, organic layer that grows in size during polymerization unless appropriate experimental conditions are employed.<sup>131,132,281</sup> This is believed to be caused by superswelling (section 2.1.2).<sup>126</sup> Slow/inefficient monomer–droplet nucleation favors superswelling, and as such the nucleation process plays a crucial role.<sup>9</sup> Superswelling can be avoided/minimized<sup>126</sup> by use of (i) oligomeric/polymeric RAFT agents instead of low MW RAFT agents;<sup>286</sup> (ii) a high amount of hydrophobe (“costabilizer”, e.g. hexadecane); (iii) a low amount of control agent (RAFT agent, nitroxide, etc.), i.e. high  $M_{n,th}$ ; (iv) large droplets/particles; or (v) low interfacial tension by postaddition of surfactant.<sup>144</sup> Miniemulsion RAFT polymerization has been performed successfully for a wide variety of systems with satisfactory colloidal stability under conditions where superswelling is not significant.<sup>121–124,155,204,280–283,285–287,289,291–293,295–304</sup>

Anionic (SDS),<sup>122–124,144,155,203,204,214,280,282–285,287–289,291,292,295–297,299,300,303,304</sup> cationic (e.g., CTAB),<sup>123,283,286,291</sup> and nonionic<sup>122,281,297,302</sup> (e.g., Brij 98) surfactants have been employed successfully in miniemulsion RAFT polymerization. Some early reports concluded that ionic surfactants are unsuitable,<sup>131,281</sup> resulting in colloidal instability consistent with superswelling. Superswelling is however very sensitive to recipe variations, and it has been suggested that the somewhat larger particles usually obtained with nonionic surfactants are less conducive to superswelling.<sup>126,286</sup> Surfmers (polymerizable surfactants) have also been successfully employed in miniemulsion RAFT polymerization.<sup>291</sup> RAFT miniemulsion homopolymerizations of styrene<sup>282</sup> and MMA<sup>296</sup> have also been employed for synthesis of carboxylic acid functionalized particles by use of a functionalized RAFT agent, resulting in enhanced colloidal stability due to a significant fraction of the carboxylic acid groups being located at the particle surface (electrostatic stabilization).<sup>312,313</sup>

**2.3.3.4. Inhibition and Retardation.** The main feature of the RAFT mechanism is the equilibrium between propagating radicals and polymer chains containing a RAFT end group, which involves the formation of an intermediate radical (Scheme 5). The kinetic features of the pre-equilibrium and the main equilibrium may be significantly different depending primarily on the nature of the small radical released upon fragmentation of the low MW RAFT agent intermediate radical.<sup>19,21,22,284</sup> A comprehensive description of the behavior of the intermediate radicals remains to emerge, in particular with regard to the origin of the retardation usually

observed in the presence of a RAFT agent in bulk/solution. Retardation is believed to be caused by cross-termination between propagating and intermediate radicals (of the main equilibrium) and/or slow fragmentation of intermediate radicals (of the main equilibrium).<sup>22,201,202</sup> Additional reaction steps involving the intermediate radicals have been proposed<sup>212,213</sup> but remain to be verified.

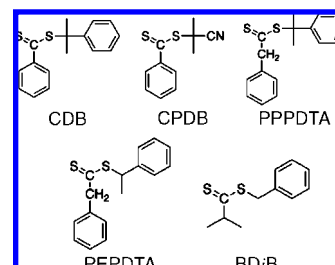
Inhibition in RAFT polymerization in bulk/solution is related to the pre-equilibrium—inhibition is not observed when using oligomeric/polymeric RAFT agents.<sup>22</sup> Inhibition in bulk/solution has been proposed to have its origin in the rate of addition to monomer of the leaving group radical<sup>284,314</sup> and its propensity to participate in termination reactions,<sup>314</sup> as well as to slow fragmentation of the intermediate radical.<sup>315,316</sup> Inhibition in miniemulsion RAFT polymerization using low MW RAFT agents is often more severe than in bulk as a result of exit to the aqueous phase of the leaving group radical of the RAFT agent.<sup>152–155</sup> As such, the extent of inhibition depends on the hydrophobicity of the leaving group radical.

The mechanisms of retardation in RAFT polymerization in bulk/solution are expected to be operative also in miniemulsion. However, the extent of retardation in miniemulsion can be more severe than in bulk/solution.<sup>203,204,214</sup> This has been attributed to a number of causes:

(i) If the system is zero–one,<sup>78</sup> by definition, particles contain either zero or one radical, because the appearance of a second radical would be followed by instantaneous termination. Assuming that intermediate radicals undergo cross-termination, a propagating radical and an intermediate radical cannot coexist in the same particle. In the presence of a RAFT agent, no propagation would occur in the particles containing one radical in the form of an intermediate radical, thus causing retardation relative to the case in the absence of RAFT agent (where propagation occurs in all particles with one radical).<sup>204,286</sup> Theoretical work by Prescott et al.<sup>154,210</sup> has shown that the presence of a RAFT agent may influence whether zero–one kinetics are obeyed or not (section 2.2.3.2.). Luo et al.<sup>204</sup> observed that, in the styrene miniemulsion polymerization mediated by a polymeric RAFT agent derived from PEPDTA under zero–one conditions, significant retardation occurred relative to bulk. In bulk, the presence of this RAFT agent has a very small effect on  $R_p$  (the benzyl substituent as the “Z group”<sup>21</sup> poorly stabilizes the intermediate radical, leading to rapid fragmentation).<sup>64</sup>

(ii) Exit to the aqueous phase (as opposed to initiation and propagation within the particle) of the radical released upon fragmentation of a low MW RAFT agent intermediate radical, followed by aqueous phase termination and/or termination after re-entry into a particle containing one radical (the latter in the case of a zero–one system).<sup>131,154</sup> This is not a factor in the case of oligomeric/polymeric RAFT agents because the expelled radical is too hydrophobic to

**Scheme 11. RAFT Agents**



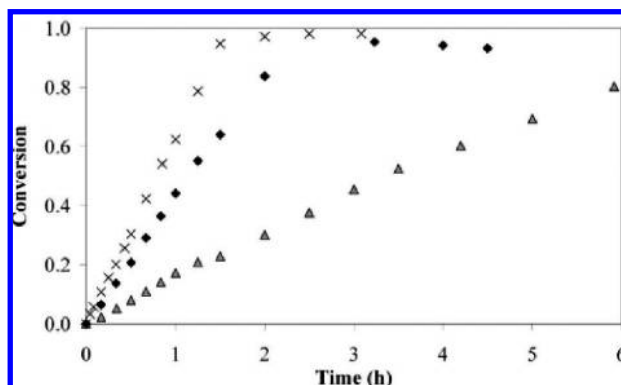


**Figure 7.** Fractional conversion vs time for KPS-initiated miniemulsion polymerization of styrene at 75 °C without RAFT agent (x), in the presence of low MW RAFT agent PEPDTA (Δ) and polymeric RAFT agent PS-PEPDTA (◆) at initial concentrations of 0.03 M. Reprinted with permission from ref 203. Copyright 2002 American Chemical Society.

exit.<sup>204,280,288</sup> The extent of retardation decreases with increasing hydrophobicity of the expelled radical.<sup>203,280</sup> This is illustrated in Figure 7, which shows conversion–time for styrene miniemulsion polymerization using PEPDTA as well as its polymeric analogue PS-PEPDTA. Use of PS-PEPDTA leads to much less retardation than PEPDTA, consistent with the expelled radical being too hydrophobic to undergo exit for PS-PEPDTA. McLeary et al.<sup>283</sup> showed that, in the miniemulsion RAFT polymerization of styrene, an increase in the water solubility of the RAFT leaving radical resulted in an increase in  $M_w/M_n$ . However, in the case of high reactivity RAFT agents, the above is not causing significant retardation but only inhibition, because the initial RAFT agent is consumed early in the reaction.<sup>129,154</sup> An additional cause of retardation in miniemulsion systems using an aqueous phase initiator and in emulsion polymerizations proposed by Prescott et al.<sup>206</sup> is so-called “RAFT-induced exit” (section 2.2.3.1), whereby an entering  $z$ -mer adds to a RAFT agent to generate a  $z$ -mer RAFT agent. Subsequent propagating radical addition regenerates the  $z$ -mer radical, which may then exit, and this has been argued to lead to an increase in the rate of exit of  $z$ -mers.<sup>153,206</sup> Such RAFT-induced exit should be distinguished from “frustrated entry”,<sup>148</sup> which refers to a reduction in the entry rate caused by chain transfer of a  $z$ -mer to a surface active RAFT agent located at the oil–aqueous interface, thereby increasing the probability of exit (i.e., unsuccessful entry of the  $z$ -mer). In this case, the rate of addition to a RAFT agent by an entering radical is increased due to the high concentration of RAFT agent near the interface. Xanthates have been proposed to be surface active as a result of their canonical forms involving ionized species.<sup>148,284</sup>

(iii) In a nonliving miniemulsion polymerization,  $R_p$  increases with an increase in the monomer droplet nucleation efficiency, i.e. an increase in the number of particles.<sup>8,133–137</sup> This would be expected to be the same in the case of RAFT (but not necessarily for NMP and ATRP—section 2.2.2). The number of particles has been reported to be lower in the presence of a RAFT agent compared to in its absence.<sup>144,203,204,214</sup> This has been proposed to be caused by a reduced monomer droplet nucleation efficiency<sup>203,204</sup> and/or a less efficient emulsification due to the viscosity increase of the oil phase imparted by the RAFT agent.<sup>204</sup> In the case of a high reactivity, low MW RAFT agent with a relatively hydrophilic leaving group radical, the RAFT agent may cause a reduction

in nucleation efficiency due to exit of the expelled radical. However, Luo et al.<sup>204</sup> observed a reduction in particle number also using an oligomeric RAFT agent, i.e. where no such exit would occur.

**2.3.3.5. Control/Livingness.** In general, miniemulsion RAFT polymerization usually results in somewhat inferior or similar control/livingness compared to bulk/solution. The livingness is difficult to determine quantitatively, but the level of control is readily assessed from  $M_w/M_n$ . The main culprit with regard to loss of control is the redistribution of monomer (and low MW RAFT agent) between non-nucleated monomer droplets and nucleated droplets (polymer particles) that occurs as a result of superswelling,<sup>126,214</sup> which can give rise to bimodal MWDs.<sup>132,144,155</sup> Superswelling results in “storage” of monomer and initial RAFT agent in superswollen “oligomer particles”, which supply monomer and RAFT agent to the “normal particles”.<sup>144,214</sup> This results in a lower consumption rate of the initial RAFT agent than in bulk and broadening of the MWD and  $M_n > M_{n,th}$  except at high conversion. Even in the absence of superswelling, the low rates of monomer droplet nucleation rates often seen in RAFT miniemulsion systems<sup>204,317</sup> create a situation where monomer diffusion may occur from droplets to particles, resulting in different [RAFT]/[monomer] ratios in different particles/droplets and thus broad MWDs.<sup>126</sup> Low droplet nucleation rates also lead to RAFT agent remaining unreacted until late in the polymerization, causing low MW tailing.<sup>214</sup> Such effects have also been observed in RAFT microemulsion polymerization.<sup>318,319</sup> Compartmentalization in RAFT miniemulsion, i.e. segregation of propagating radicals, would lead to reduced levels of termination when the number of propagating radicals per particle is sufficiently low (as evidenced by RAFT miniemulsion polymerizations proceeding faster than their bulk counterparts<sup>204,214,280,289</sup>), and this would potentially lead to improved control/livingness in miniemulsion compared to bulk.<sup>280</sup> However, it appears that the negative effects of mainly superswelling and monomer diffusion in general outweigh compartmentalization effects. The confined space effect<sup>156,160,161</sup> is normally not operative in RAFT miniemulsion due to the high concentration of RAFT agent<sup>157</sup> (to be compared with the much lower concentration of nitroxide in NMP and Cu(II) complex in ATRP).

Miniemulsion RAFT polymerization of styrene,<sup>293</sup> MMA,<sup>293,320</sup> and  $n$ BMA<sup>298</sup> in the presence of  $\beta$ -cyclodextrin has been reported to lead to improved control (lower  $M_w/M_n$ ) under appropriate conditions, attributed to enhanced transport of RAFT agent across the aqueous phase as a result of  $\beta$ -cyclodextrin solubilizing the hydrophobic RAFT agent by complexation within the hydrophobic cavity of  $\beta$ -cyclodextrin. In general, partitioning to the aqueous phase of the control agent has mainly negative effects on CLRP in miniemulsion, because the organic phase is the polymerization locus. However, there may be cases where a certain water solubility of the RAFT agent is beneficial because it counteracts the effect monomer diffusion between droplets/particles (Ostwald ripening, superswelling) has on the [control agent]/[monomer] ratio in particles.

RAFT miniemulsion polymerization of  $n$ BA was found to be sensitive to the structure of the RAFT agent.<sup>155</sup> Satisfactory control/livingness was obtained using BDIB, which is characterized by low stability of the intermediate radical. The sensitivity was speculated to be related to a complex interplay of the high  $k_p$  of  $n$ BA, the exit charac-

teristics of the leaving group, and mass transfer between monomer droplets/particles.

One of the general disadvantages of CLRP in both homogeneous and dispersed systems is that it is normally difficult to prepare high MW polymer, and in the very vast majority of publications, DP values > approximately 500 are rarely targeted. This is because the probability of any *individual* chain undergoing termination or side reactions such as transfer increases with increasing DP.<sup>11</sup> In RAFT, the problem one encounters when designing a recipe for high MW is that  $R_p$  becomes too low as a result of the low initiator concentration required to ensure that most chains have RAFT end groups. Compartmentalization (segregation of propagating radicals) offers a potential solution to this problem, as the ensuing reduction in termination rate leads to an increase in both  $R_p$  and livingness. Yang et al.<sup>289</sup> attempted to synthesize high MW PS (target DP = 557) using RAFT miniemulsion polymerization employing PEPDTA. Although there was evidence of compartmentalization,  $M_w/M_n$  was relatively broad. However, by use of a semibatch miniemulsion approach, whereby the polymerization was carried out with additional monomer being added at 80% conversion,  $M_n = 57417$  and  $M_w/M_n = 1.38$  were achieved. Although the corresponding bulk data were not reported, this may illustrate how the inherent characteristics of a dispersed system can be exploited to improve CLRP. The reasons for improved control in the semibatch system may be related to (i)  $N_{cycles}$  a chain experiences during its growth ( $M_w/M_n$  decreases with increasing number of cycles<sup>11</sup>), which increases with decreasing monomer concentration and/or (ii) changes in monomer/RAFT agent diffusion behavior between droplets/particles and/or (iii) reduced superswelling in the semibatch approach. A similar improvement in control in semibatch vs batch seeded emulsion RAFT polymerization was also observed by Smulders et al.<sup>149</sup> in seeded emulsion polymerization using xanthates.

There is to date only one report describing an inverse<sup>321</sup> RAFT miniemulsion polymerization resulting in formation of hydrophilic polymer particles. Schork and co-workers<sup>302</sup> carried out inverse RAFT miniemulsion polymerization of acrylamide using cyclohexane as the continuous phase and obtained the best results using a water-soluble radical initiator. Some loss of control at high conversion was observed, attributed to RAFT agent hydrolysis (often a problem in aqueous homogeneous RAFT polymerizations).<sup>322</sup>

## 2.4. Emulsion Polymerization

### 2.4.1. Nitroxide-Mediated Radical Polymerization (NMP)

**2.4.1.1. General Considerations.** Implementation of NMP in an *ab initio* emulsion polymerization has proved to be a significant challenge, meeting with problems with both colloidal stability and control/livingness. In an emulsion polymerization, the locus of polymerization is the polymer particles, which form during the nucleation stage at low conversion. Successful emulsion NMP requires that significant monomer droplet nucleation does not occur and that the nitroxide is able to diffuse across the aqueous phase to the particles, while at the same time the partitioning of nitroxide between the organic and aqueous phases allows the nitroxide concentration in the particles to be sufficiently high.

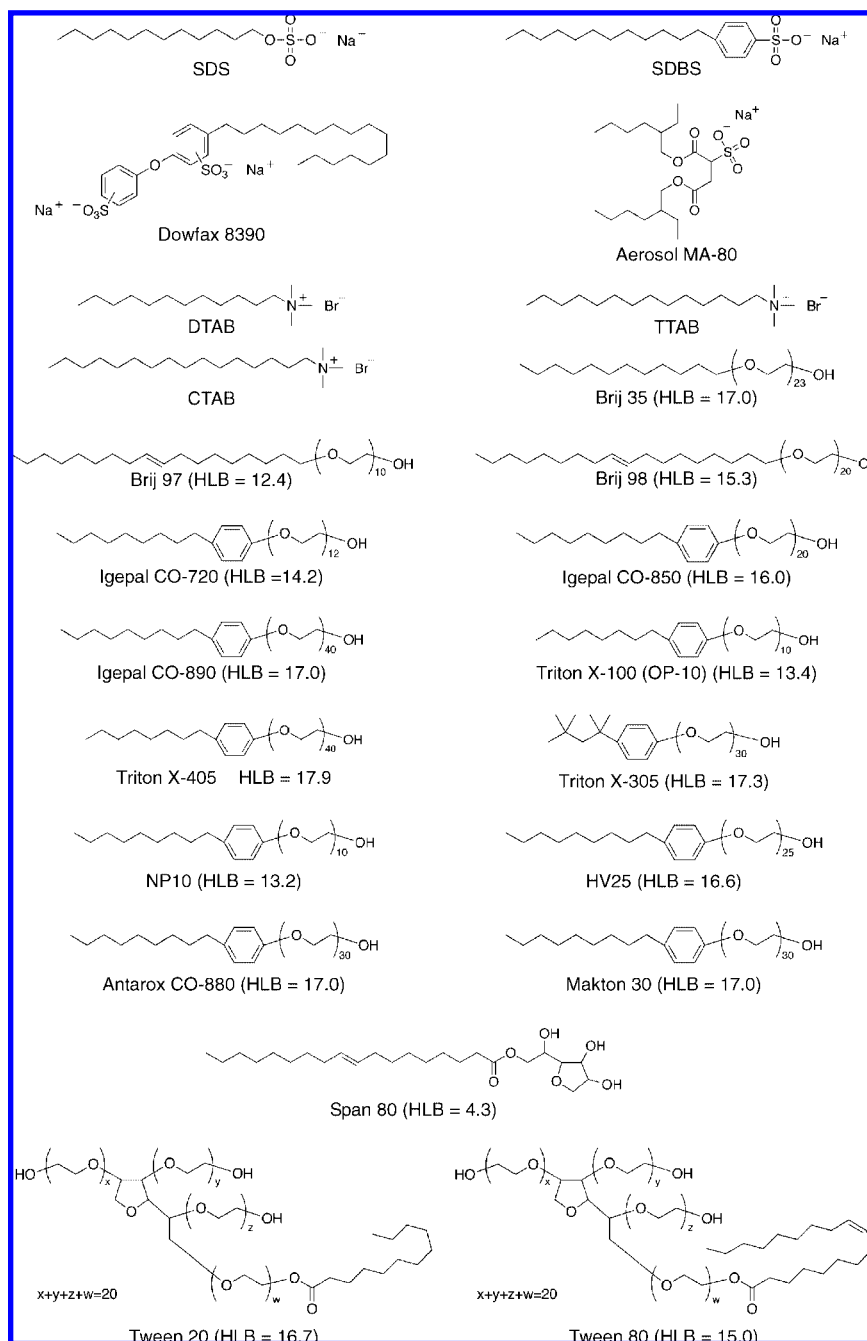
True *ab initio* emulsion NMP, whereby all ingredients are charged initially and both colloidal stability and good control/livingness are displayed, has been achieved by use of the self-assembly approach<sup>237,323,324</sup> as well as by use of two nitroxides of widely different hydrophobicities in the same system.<sup>325</sup> Various seeded emulsion NMPs have also been carried out successfully, whereby the nucleation stage is completed in the absence of a monomer phase.<sup>193,326–328</sup>

**2.4.1.2. Ab Initio Emulsion NMP.** The first attempts at *ab initio* emulsion NMP met with limited success, mainly because of problems associated with nucleation and nitroxide partitioning.<sup>139,224,329</sup> *Ab initio* emulsion NMP of styrene at 120 and 135 °C has been attempted using KPS and a variety of TEMPO-based nitroxides: TEMPO, OH-TEMPO, di-*tert*-butyl nitroxide, 4-carboxy-TEMPO, 4-benzoyloxy-TEMPO, and 4-amino-TEMPO.<sup>224,329</sup> Very low conversions and/or emulsion instability were observed in all cases, except for amino-TEMPO<sup>224</sup> and acetoxy-TEMPO<sup>329</sup> (both with SDS), in which cases intermediate conversion levels and stable emulsions were obtained, as well as some evidence of control/livingness. The relative success obtained with amino-TEMPO and acetoxy-TEMPO may be related to their partitioning characteristics between the oil and aqueous phases. *Ab initio* emulsion NMP of styrene at 135 °C has also been attempted with a TEMPO/KPS-based water-soluble alkoxyamine and SDBS, resulting in promising control/livingness but unstable emulsions.<sup>327</sup> *Ab initio* emulsion NMP of styrene and *n*BA at 120 and 112 °C (Dowfax 8390), respectively,<sup>326</sup> employing the low MW water-soluble alkoxyamine A-Na resulted in controlled/living polymerization but unstable emulsions at conversions > 50%, probably as a result of droplet nucleation caused by oligomeric alkoxyamines partitioning between the aqueous phase and the monomer droplets.<sup>326</sup> Similar problems occurred when the difunctional water-soluble alkoxyamine DIAMA-Na was employed.<sup>193</sup> *Ab initio* emulsion polymerizations of styrene using KPS and SG1 at 90 °C have also been unsuccessful, with poor control and coagulation.<sup>328</sup>

Cunningham and co-workers<sup>325</sup> recently employed two nitroxides, TEMPO and the extremely hydrophobic 4-stearoyl-TEMPO, in *ab initio* emulsion polymerization of styrene (KPS/SDBS/135 °C). Polymerizations employing only TEMPO resulted in 25 wt % coagulation, where the coagulum comprised a mixture of small ( $\approx 500$  nm) and large ( $> 1 \mu\text{m}$ ) particles. However, good control/livingness was obtained ( $M_w/M_n = 1.19$ ) and the MWDs of the coagulum, and dispersed particles were virtually identical. When using both nitroxides in a suitable ratio (4-stearoyl-TEMPO/TEMPO = 1.33), particles with  $d_n = 45$  nm formed without coagulum, and the control/livingness was excellent. TEMPO diffuses from the droplets to the micelles where polymerization occurs, but 4-stearoyl-TEMPO is too hydrophobic to diffuse through the aqueous phase and remains in the droplets. If the amount of 4-stearoyl-TEMPO is high enough, it acts as an inhibitor and prevents polymerization in the droplets (4-stearoyl-TEMPO could be replaced with any sufficiently hydrophobic inhibitor, not necessarily a nitroxide). Thus, in addition to providing an elegant way to perform TEMPO/styrene *ab initio* emulsion polymerization, this work demonstrates that the (main) problem with regard to colloidal instability for the TEMPO/styrene system is polymerization in the droplets; that is, spontaneous (thermal) initiation of styrene<sup>159</sup> plays a crucial role. Thermodynamic modeling of the seeded emulsion polymerization of styrene (Interval II)



## Scheme 12. Emulsifiers

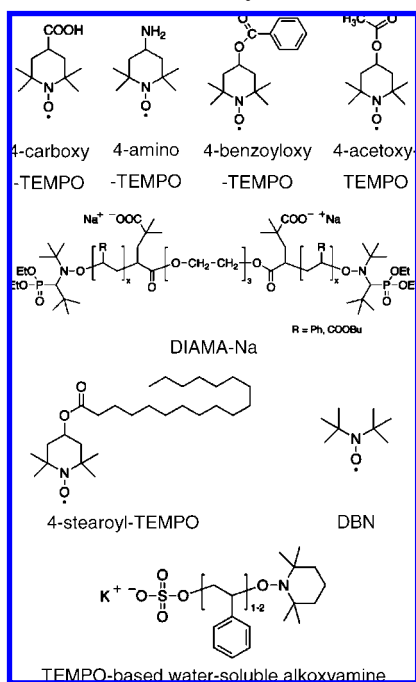


at 120 °C mediated by TEMPO also showed that thermal initiation of styrene results in high MW polymer formation in monomer droplets, causing monomer droplet stabilization against monomer diffusion.<sup>330</sup> Consequently, these droplets (<1  $\mu\text{m}$ ) do not merely act as monomer reservoirs as in a conventional emulsion polymerization but remain in the system and ultimately cause coagulation and poor control. Moreover, it was demonstrated how the seed particle size strongly influenced the obtained particle size distributions, with the majority of polymer formation in fact occurring in the monomer droplets when small seed particles ( $d < 50$  nm) were employed.

**2.4.1.3. *Ab Initio* Emulsion NMP Based on Self-Assembly.** Charleux and co-workers developed an *ab initio* emulsion NMP system that relies on self-assembly into micelles of SG1-terminated poly(sodium acrylate)-based amphiphilic diblock copolymer, which forms *in situ* during the polymeriza-

tion.<sup>323,324</sup> The original macroinitiator is PAA-SG1, which exists as SG1-terminated poly(sodium acrylate) under alkaline conditions. Use of the macroinitiator under acidic conditions results in poor control/livingness due to SG1 decomposition at low pH.<sup>138,139,143</sup> The initial polymerization mixture comprises the main components of macroinitiator, hydrophobic monomer (styrene or *n*BA), and water (no surfactant), and the monomer exists in the aqueous phase and as monomer droplets. Initiation subsequently occurs in the aqueous phase, and an amphiphilic diblock copolymer is formed, the critical micelle concentration (cmc) of which decreases with increasing hydrophobic block length (i.e., increasing conversion). Self-assembly into micelles occurs, which subsequently swell with monomer that diffuses from the droplets through the aqueous phase. Upon further polymerization, the amphiphilic block copolymers become too hydrophobic to exit into the aqueous phase, and fixed

## Scheme 13. Nitroxides and Alkoxyamines



structures (polymer particles) are formed. The poly(sodium acrylate) segments of the diblock copolymer extend into the aqueous phase providing electrosteric stabilization.

Using this approach, *ab initio* emulsion NMP of styrene and *n*BA can be performed at 120 °C with solids contents of 20 wt %, with the usual criteria of CLRP being fulfilled (in general,  $M_w/M_n < 1.5$  for conversion  $< 60\%$ ). The macroinitiator eventually becomes the surfactant, and therefore, the particle size and  $M_n$  cannot be varied independently. An increase in the macroinitiator concentration leads to a reduction in both  $M_n$  and particle size.<sup>324</sup> Although  $M_n$  increased with conversion, the macroinitiator efficiencies were well below unity, as indicated by  $M_n > M_{n,th}$ . The final particle diameters were less than 100 nm (Figure 8). The size of such particles is pH-sensitive; at pH  $> 7$ , the shell was a stretched polyelectrolyte brush that effectively stabilized the particles, whereas, at pH = 4, the hairy layer collapsed onto the particle surface, resulting in unstable particles.

The above concept has also been successfully applied to RAFT polymerization (section 2.4.3.2.5).<sup>311,331,332</sup> However, in the case of RAFT, starved-feed conditions are necessary to ensure the absence of monomer droplets. RAFT polymerization requires the addition of a radical initiator, and some fraction of these radicals will add to the hydrophobic monomer in the aqueous phase and generate radicals capable of entry into monomer droplets prior to chain transfer with a RAFT agent, thus leading to undesired droplet nucleation. The NMP process thus has an inherent advantage over RAFT with regard to the implementation of controlled-radical mediated self-assembly in that no radical initiator is required, because radicals are generated directly from the macroinitiator.<sup>324</sup>

**2.4.1.4. Seeded Emulsion NMP.** Seeded emulsion polymerization is inherently simpler than *ab initio* emulsion polymerization because the nucleation step is avoided. Seeded emulsion NMP of styrene at 125 °C using an oil phase low MW TEMPO-based alkoxyamine and the anionic surfactant Aerosol MA-80 proceeded with some control/

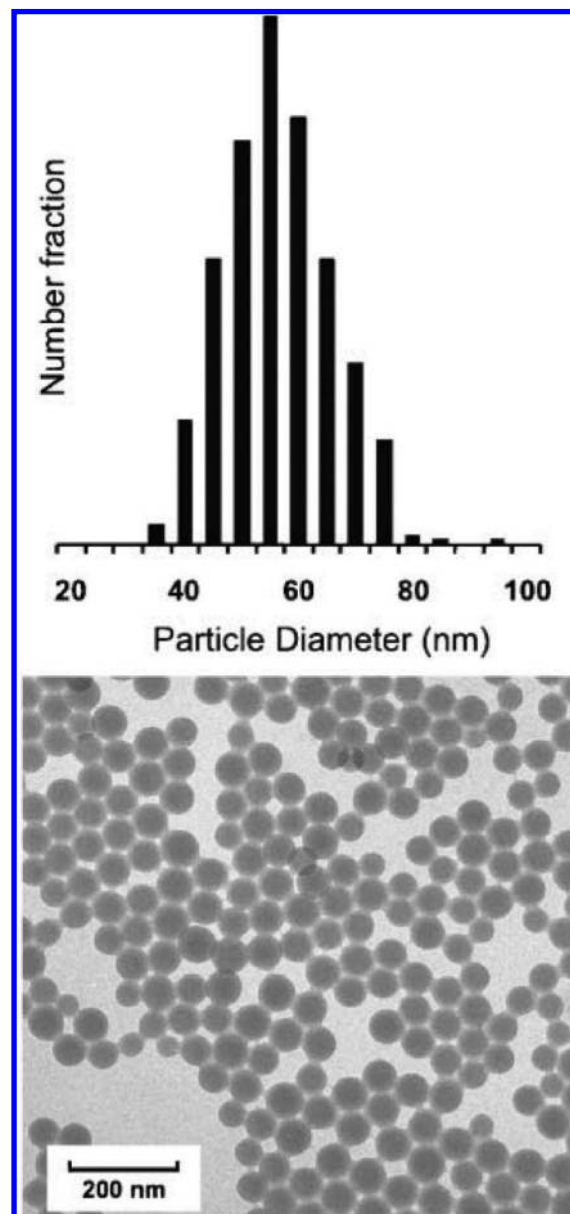


**Figure 8.** Particle size distribution and TEM photograph of PS particles obtained by SG1-mediated *ab initio* emulsion NMP employing a SG1-terminated poly(sodium acrylate) macroinitiator at 120 °C. Reprinted with permission from ref 323. Copyright 2005 Royal Society of Chemistry.

livingness, although the MWDs were relatively broad ( $M_w/M_n \approx 1.45$ ) and  $M_n < M_{n,th}$ .<sup>333</sup>

Styrene and *n*BA were polymerized successfully by seeded NMP at 120 and 112 °C, respectively, employing a living seed of P*n*BA-SG1 prepared from a very dilute aqueous emulsion of monomer using a high Dowfax 8390 concentration with the low MW water-soluble alkoxyamine A-Na.<sup>326</sup> Most monomer is located in the monomer-swollen micelles and the aqueous phase, and monomer droplet nucleation is thus avoided (microemulsion-like conditions). Monomer was subsequently introduced in one shot to swell the seed particles. The polymerizations were carried out at pH  $> 6$  using sodium hydrogen carbonate as buffer in order to ensure a sufficiently high degree of ionization of A-H to A-Na and to avoid SG1 decomposition at low pH, giving particle diameters of 250–600 nm (broad particle size distribution). Seeded NMPs of styrene and *n*BA were also carried out in the same way, but replacing A-Na with the difunctional

water-soluble alkoxyamine DIAMA-Na, resulting in good control/livingness.<sup>193</sup> As a result of the increased electrostatic repulsion between particles due to the presence of two negatively charged groups in each alkoxyamine species, considerably smaller particles and narrower particle size distributions were obtained. This strategy has also been implemented for styrene and *n*BA under semibatch conditions (using A-Na or DIAMA-Na), with significantly reduced overall polymerization time.<sup>334</sup>

Cunningham and co-workers<sup>328</sup> reported a similar two-stage approach in surfactant-free emulsion polymerization of styrene using SG1 and KPS at 90 °C with a small amount of styrene (1.5% of total styrene) added initially and the remainder added after 3.5 h (over 10 min). Good colloidal stability ( $d_w = 121$  nm) with only minor coagulation as well as good livingness were obtained, but fairly poor control as evidenced by  $M_w/M_n = 1.77$  at close to 60% conversion. Different [chains]/[SG1] ratios in different particles was proposed as the main reason.

Successful seeded emulsion NMP of styrene at 135 °C (in the absence of monomer droplets) using a PS-TEMPO macroinitiator and PVA as surfactant have been reported by Georges and co-workers by use of a microprecipitation technique to generate the initial seed and subsequent swelling with styrene.<sup>327</sup>

## 2.4.2. Atom Transfer Radical Polymerization (ATRP)

**2.4.2.1. General Considerations.** A relatively extensive body of work on ATRP emulsion polymerization exists in the literature. The presence of water can have a significant effect on the ATRP process itself (section 2.3.2.1.),<sup>239</sup> but these effects are relatively minor in aqueous dispersed systems due to the main locus of polymerization being the organic phase. The implementation of ATRP in an *ab initio* emulsion system using direct ATRP initially led to significant problems with poor colloidal stability,<sup>264,265,335–337</sup> mainly due to complications associated with the nucleation step. It was however soon realized that reverse ATRP is a more suitable approach. Reverse ATRP *ab initio* emulsion systems have been demonstrated to proceed with both good control/livingness and colloidal stability. However, the initiator efficiencies tend to be very low ( $M_n > M_{n,th}$ ).<sup>253,337–341</sup> Seeded emulsion ATRP can in general be carried out in a fairly straightforward manner with good colloidal stability and control/livingness under appropriate conditions.<sup>249,250,252,342–345</sup>

In order to obtain satisfactory control/livingness in emulsion ATRP, it is crucial that the metal complexes are present in appropriate concentrations at the polymerization loci, i.e. the polymer particles, and it is difficult to adjust both the amount and rate of transfer of reagents from monomer droplets to micelles/particles throughout the polymerization. This requires sufficiently rapid transport from the droplets to the particles through the aqueous phase (kinetic factors), as well as favorable partition coefficients (thermodynamic factors). These fundamental requirements are the same for NMP and RAFT. The choice of emulsifier is pivotal—nonionic and cationic emulsifiers have thus far given the most satisfactory results, whereas anionic emulsifiers are incompatible with ATRP.<sup>264,265,339,342</sup> Copper is by far the most commonly employed metal in ATRP,<sup>10</sup> and all successful reports of emulsion ATRP deal with Cu-based systems.

**2.4.2.2. *Ab Initio* Emulsion ATRP.** **2.4.2.2.1. Emulsifiers.** ATRP appears to be compatible with both nonionic and cationic emulsifiers but incompatible with anionic emulsi-

fiers. *Ab initio* emulsion ATRP of *n*BA<sup>265</sup> and *n*BMA<sup>339</sup> with the anionic emulsifier SDS resulted in essentially no control/livingness, speculated to be caused by interaction between CuBr<sub>2</sub> and SO<sub>4</sub><sup>2-</sup> of SDS in the aqueous phase.<sup>264,265,342</sup>

The use of the cationic emulsifiers DTAB and TTAB in *ab initio* ATRP of EHMA resulted in either poor colloidal stability (DTAB) or broad MWDs (TTAB).<sup>336</sup> DTAB has also been employed in *ab initio* ATRP of *n*BMA with good control/livingness but poor colloidal stability.<sup>265</sup> Nonionic emulsifiers do not interact with Cu(II) in a detrimental manner and have thus far been the emulsifiers of choice in most studies. A wide range of nonionic emulsifiers have been employed with various degrees of success: Brij 97,<sup>264,265,336,337</sup> Brij 98,<sup>253,264,265,336,337,341,342,344,346,347</sup> Brij 35,<sup>339</sup> Tween 20,<sup>337,346</sup> Tween 80,<sup>249,250,336,343</sup> Antarox CO-880,<sup>335</sup> Igepal CO-720,<sup>337</sup> Igepal CO-850,<sup>337</sup> Igepal CO-890,<sup>342</sup> HV25,<sup>337</sup> Makon 30,<sup>337</sup> Triton X-405,<sup>337</sup> NP 10,<sup>337</sup> OP-10,<sup>339,348</sup> PEG,<sup>264</sup> and PVA-co-PVAc.<sup>342</sup>

**2.4.2.2.2. Direct ATRP.** In direct ATRP, the polymerization mixture initially contains the initiator (an alkyl halide) and the Cu complex in its lower oxidation state (e.g., CuBr/ligand).<sup>10</sup> The general trend in direct ATRP in *ab initio* emulsion systems is that good control/livingness is obtained but that colloidal stability is relatively poor, often with  $d \approx 1$   $\mu$ m and broad particle size distributions.<sup>265,335,336,346</sup> These polymerizations are likely to proceed in a manner akin to a suspension/mini-emulsion polymerization,<sup>264,265,337</sup> because the initiator (e.g., EBiB) will be primarily located in the monomer droplets and very significant monomer droplet nucleation is thus highly probable. Droplet nucleation results in large particles, and concomitant micellar nucleation (giving smaller particles) thus results in broad particle size distributions.

Gaynor et al.<sup>264</sup> reported *ab initio* Cu-based emulsion ATRP of *n*BA, *n*BMA, styrene, and MMA using nonionic emulsifiers and various ligands. Ligands rendering excessively water-soluble Cu complexes (e.g., bpy) yielded uncontrolled polymerizations, whereas good control/livingness was obtained with sufficiently hydrophobic ligands (e.g., dNbpy).<sup>264,265,277,348</sup> Loss of control, as well as an accompanying increase in  $R_p$ , is caused by the Cu(II) concentration in the particles being too low due to partitioning to the aqueous phase.<sup>171,265</sup> The colloidal stability was in general poor, as evidenced by extensive coagulation, the exception being the combination Brij 98/*n*BMA, which gave a stable emulsion.<sup>264</sup> The particles were large, generally greater than 1  $\mu$ m.

Jousset et al.<sup>337</sup> investigated direct ATRP of MMA in *ab initio* emulsion using the ligand dNbpy1 and a variety of nonionic emulsifiers at 60 °C. Brij 97 led to significant coagulation at low conversion, with as much as 40 wt % coagulum based on the initial amount of monomer at the end of the polymerization. The use of Brij 98 resulted in less coagulation (19 wt % coagulum) than for Brij 97, and when increasing the Brij 98 concentration to 25 wt % relative to monomer, coagulation at low conversion was avoided. Emulsifiers of various HLB values were investigated for alkylphenoethoxylates (NP10, Igepal CO-720, Igepal CO-850, HV25, Makon 30, and Triton X-405). The extent of coagulation decreased with increasing HLB value but went through a minimum at a certain HLB value. In this particular direct ATRP system, the emulsifier HV25 (HLB = 16.6) gave the best results both in terms of colloidal stability and MW control, with no coagulation for 18 wt % emulsifier relative to monomer ( $d \approx 800$  nm).



Zhu and Eslami<sup>336</sup> studied Cu-based *ab initio* emulsion ATRP of EHMA with the ligand dNbpy2. In general, good control/livingness was achieved, but the colloidal stability was poor, and large particles were obtained (300–1000 nm). The best results were obtained with Brij 98 and Tween 80. Increasing the temperature from 50 to 70 °C had a detrimental effect on colloidal stability. In the case of nonionic emulsifiers, an increase in temperature leads to more extensive coagulation because the concentration of emulsifier in the aqueous phase is reduced as a result of emulsifier dehydration, which causes the emulsifier to partition more toward the organic phase.<sup>253,336,337</sup> Therefore, a large amount of emulsifier is needed at high temperature.

All of the above studies employed hydrophobic initiators (e.g., EBiB). However, Matyjaszewski et al.<sup>265</sup> also carried out *ab initio* emulsion ATRP using either EBiB or the water-soluble 2-hydroxyethyl 2-bromoisobutyrate (OH-EBiB) as initiator, reporting satisfactory control/livingness in both cases but severe coagulation in the case of the water-soluble initiator.

Copolymerizations of MMA/*n*BA and MMA/*n*BMA as well as block copolymer synthesis employing macroinitiators using direct ATRP in *ab initio* emulsion have also been reported to proceed with good control/livingness.<sup>346</sup>

Direct ATRP in *ab initio* emulsion has also been applied to the synthesis of hyperbranched polyacrylates.<sup>347</sup>

**2.4.2.2.3. Reverse ATRP.** In reverse ATRP, the polymerization mixture initially contains a radical initiator and the Cu complex in its higher oxidation state.<sup>10</sup> The advantage of using reverse ATRP is that the nucleation process is anticipated to proceed similarly to in a conventional nonliving emulsion polymerization in the aqueous phase, and as such monomer droplet nucleation would be avoided. Monomer droplet nucleation is believed to be the main reason for the poor colloidal stability and broad particle size distributions obtained in direct ATRP in *ab initio* emulsion systems. Radicals would be generated on initiator decomposition in the aqueous phase followed by monomer addition until the propagating radicals attain surface activity,<sup>78</sup> and these oligoradicals would subsequently enter monomer-swollen micelles, leading to nucleation. The entering radicals would be deactivated by reaction with CuBr<sub>2</sub>/ligand located in the micelles, generating dormant species. Reverse ATRP in *ab initio* emulsion has yielded much better results than direct ATRP with regard to colloidal stability and particle size distributions (more narrow).<sup>253,337–341</sup>

Matyjaszewski and co-workers<sup>253,341</sup> carried out reverse ATRP of *n*BMA in *ab initio* emulsion using water-soluble initiators and Brij 98. The use of KPS required the addition of a buffer to prevent KPS decomposition (which changes the pH, reducing the initiation efficiency and *R<sub>p</sub>*).<sup>341</sup> The buffer is however believed to have compromised the colloidal stability. Such problems were avoided with the azoinitiators V-50 and VA-044, resulting in good colloidal stability, small particles with a relatively narrow particle size distribution (*d<sub>n</sub>* = 85 nm; *d<sub>w</sub>*/*d<sub>n</sub>* = 1.36), as well as good control/livingness (*M<sub>w</sub>*/*M<sub>n</sub>* = 1.28 at 84% conversion).<sup>341</sup> The cmc of Brij 98 is  $6 \times 10^{-6}$  M,<sup>237</sup> i.e. consistent with micellar nucleation. However, the initiator efficiencies were as low as 30%,<sup>253</sup> mainly due to termination of oligomeric radicals in the aqueous phase, with a possible minor contribution from deactivation of oligomeric radicals in the aqueous phase by CuBr<sub>2</sub>.<sup>253,341</sup> Due to the low water solubility of CuBr, subsequent activation in the aqueous phase would be slow,

leading to highly delayed growth of dormant water-soluble species in the aqueous phase (CuBr<sub>2</sub> is much more water-soluble than CuBr). In addition,  $\beta$ -hydrogen abstraction from oligomeric radicals in the aqueous phase by CuBr<sub>2</sub> may also occur.<sup>253,349</sup> In the case of the water-soluble azoinitiator V-50, the amount of emulsifier did not greatly affect the MWs or *R<sub>p</sub>*, but the particle size decreased with increasing emulsifier content (13 wt % Brij 98 rel. monomer: *d<sub>n</sub>*  $\approx$  190 nm).<sup>253</sup> At 90 °C, 90% of the initiator V-50 has decomposed in 30 min, and thus radical generation occurs mainly via the ATRP activation throughout most of the polymerization (as is normal in reverse ATRP). An induction period is observed, during which initiator decomposition occurs, generating radicals that consume CuBr<sub>2</sub> until its concentration is sufficiently low for polymerization to occur.

Sufficient hydrophobicity of the ligand is an important criterion also in reverse ATRP to prevent excessive partitioning of the Cu complexes to the aqueous phase. Peng et al.<sup>339</sup> investigated reverse ATRP of *n*BMA in *ab initio* emulsion using the nonionic emulsifier Brij 35 and CuCl with ligands of different hydrophobicity. Control/livingness was not obtained for the ligands bpy and bde, whereas good control/livingness resulted using the more hydrophobic dNbpy1.

Jousset et al.<sup>337</sup> carried out reverse ATRP of MMA in *ab initio* emulsion at 80 °C using the nonionic emulsifier HV25 and the water-soluble azoinitiator VA-044, employing CuBr<sub>2</sub> or CuCl<sub>2</sub>. The polymerizations proceeded with good control/livingness with no coagulation when using 10 wt % HV25 (rel. MMA) and *d<sub>n</sub>* = 43–48 nm, but low initiator efficiencies were obtained, as previously observed for *n*BMA.<sup>253</sup> The cmc of HV25 was determined as  $2.5 \times 10^{-4}$  M, i.e. consistent with micellar nucleation.

**2.4.2.3. Seeded Emulsion ATRP.** The objective of seeded emulsion ATRP is often to prepare block copolymers. The first block (macroinitiator) can be prepared either in a separate reaction step and purified<sup>346,350</sup> or in a first emulsion or miniemulsion polymerization step to create seed particles, followed by addition of the second monomer to swell the seed particles, and second stage polymerization as a seeded emulsion polymerization.<sup>249,250,252,343,345</sup> Addition of the second stage monomer can in principle be done after the first monomer is completely consumed. However, the second monomer is often added before complete conversion in the first step in order to obtain higher livingness (the livingness decreases with increasing conversion). This gives a block copolymer where the second block is in fact a copolymer (gradient copolymer), which may lead to significantly different physical properties compared to those of a pure block copolymer.<sup>92,351</sup>

Many of the challenges associated with *ab initio* emulsion ATRP are avoided in seeded systems, because particle nucleation is complete and the reactants are already located in the particles (depending on partitioning coefficients). Direct ATRP in *ab initio* emulsion often yields extensive coagulation and broad particle size distributions, and consequently, alternative approaches have been employed to prepare seed particles, e.g. miniemulsion ATRP,<sup>249,250</sup> microemulsion ATRP,<sup>344</sup> and a nanoprecipitation technique.<sup>342</sup>

Okubo and co-workers<sup>249</sup> carried out seeded ATRP of *i*BMA using a seed (*d<sub>n</sub>*  $\approx$  200 nm) prepared by miniemulsion polymerization (>90% conversion) employing Tween 80 (EBiB/CuBr/dNbpy2). Subsequent swelling with styrene and seeded emulsion ATRP yielded block copolymer with narrow MWD (*M<sub>w</sub>*/*M<sub>n</sub>* = 1.28) and high blocking efficiency. The

optimum emulsifier content with respect to high  $R_p$ , satisfactory control/livingness, and colloidal stability was 6–10 wt % based on monomer.<sup>250</sup>

Eslami and Zhu<sup>343</sup> synthesized PMMA-*b*-PEHMA-*b*-PMMA by first preparing seed PEHMA particles by direct ATRP in *ab initio* emulsion using a bifunctional initiator (CuBr/dNbpy2) with Tween 80, followed by seeded ATRP of MMA. A temperature program (30 °C in the initial stage, thereafter 70 °C) was employed to avoid coagulation during the nucleation stage in the *ab initio* emulsion polymerization. Polymerization mainly occurred in the seed particles (i.e., no secondary nucleation or monomer droplet nucleation), as evidenced by a monomodal particle size distribution ( $d \approx 300$  nm).

Georges and co-workers<sup>342</sup> reported an alternative means of preparing seed particles by use of a nanoprecipitation technique (also applied to NMP<sup>327</sup> and RAFT<sup>352</sup>). A low MW ATRP macroinitiator was prepared in bulk and dissolved in acetone with (CuBr or CuCl)/BPMODA. The resulting solution was added dropwise to an aqueous emulsifier solution (best results were obtained with Brij 98). After removal of acetone, seeded ATRP was subsequently carried out by swelling the resulting nanoparticles with styrene, resulting in good control/livingness and colloidal stability ( $d_w \approx 220$  nm). An inherent disadvantage of this process is the oxidation of Cu(I) to Cu(II) during the preparation of seed particles and the evaporation of acetone.

Seeded ATRP of styrene and *n*BA with nanosized PnBA seed particles has also been investigated by Matyjaszewski and co-workers.<sup>344</sup> The seed particles were prepared by microemulsion AGET ATRP<sup>10</sup> (EBiB/CuBr<sub>2</sub>/BPMODA/ascorbic acid/Brij 98), and the second batch of monomer was added to the ongoing microemulsion polymerization. To minimize the amount of emulsifier in the final emulsion, the amount of monomer added in the initial microemulsion stage relative to the total amount was decreased. Good control/livingness ( $M_w/M_n = 1.2$ – $1.4$ ), high initiation efficiency ( $>90\%$ ), and colloidal stability ( $d = 120$  nm) were obtained using 10 wt % emulsifier (relative to monomer).

## 2.4.3. RAFT Emulsion Polymerization

**2.4.3.1. General Considerations.** RAFT is perhaps the most versatile CLRP, and much research has been devoted to its implementation in aqueous emulsion. An important difference between RAFT and the two other major CLRP techniques (NMP and ATRP) with respect to emulsion polymerization is that, with RAFT, monomer droplet nucleation is not a problem, because the radical generation mechanism is the same as that in a conventional, nonliving process. Radical entry into droplets is negligible compared to that into polymer particles due to the much larger total surface area of the particles.<sup>78</sup> However, implementation of RAFT in *ab initio* and seeded emulsion systems has been fraught with difficulties related to colloidal instability (coagulation or phase separation) and transport of the RAFT agent from the monomer droplets through the aqueous phase to the polymer particles.<sup>130,147,310,353</sup> The best results have been obtained using conditions that minimize superswelling,<sup>126,354</sup> notably with low reactivity RAFT agents (xanthates<sup>32</sup>) which yield good livingness but poor control (broad MWDs).<sup>145–147,150,355</sup> An elegant way of performing *ab initio* emulsion polymerization is by use of polymeric RAFT agents that undergo self-assembly as part of the nucleation step.<sup>311,331,332</sup> This

approach has also been employed for *ab initio* emulsion NMP<sup>323,324</sup> and TERP.<sup>356</sup>

Successful seeded RAFT emulsion polymerizations have been reported for styrene,<sup>146,148,149,206,284,310</sup> *n*BA,<sup>147,149,355</sup> and acetoacetoxyethyl methacrylate,<sup>147,355</sup> and *ab initio* emulsion RAFT polymerizations have been carried out with good results for styrene,<sup>145,147,150,311,357–359</sup> *n*BA,<sup>147,149,355</sup> EHA,<sup>145</sup> MMA,<sup>354,360–362</sup> and *n*BMA.<sup>284</sup> Retardation in RAFT emulsion polymerization in intervals II and III is believed to have the same origin as in miniemulsion (sections 2.2.3 and 2.3.3.4).

### 2.4.3.2. RAFT *ab Initio* Emulsion Polymerization.

**2.4.3.2.1. Superswelling.** Luo and Cui<sup>354</sup> simulated monomer swelling of particles comprising oligomers or polymer in CLRP, revealing that superswelling<sup>126</sup> (section 2.1.2) may cause particles in interval I to swell to become as large as 1  $\mu\text{m}$  as a result of the low DP at low conversion in CLRP. Superswelling in interval I may thus cause colloidal instability similarly to in miniemulsion (section 2.3.3.3), and accordingly the colloidal stability was predicted to be enhanced by increasing the initiator and surfactant concentrations and by increasing  $M_{n,\text{th}}$ . These predictions were experimentally verified using MMA/CPDB/KPS, resulting in successful *ab initio* RAFT emulsion polymerization.<sup>354</sup> However, at low RAFT agent concentrations (to increase  $M_{n,\text{th}}$ ), relatively broad MWDs were observed, speculated to be caused by different numbers of RAFT agents in different particles (also observed in RAFT miniemulsion<sup>289</sup>).

**2.4.3.2.2. Xanthates (MADIX).** Xanthates are a special type of RAFT agent (MADIX),<sup>32</sup> characterized by chain transfer constants considerably lower ( $C_{\text{ex}} = k_{\text{ex}}/k_p \approx 1$ ) than those for other RAFT agents. Consequently, relatively high MW polymer is formed already at low conversion, markedly reducing or even eliminating superswelling,<sup>119,339</sup> making MADIX relatively straightforward to implement in *ab initio* emulsion. However, due to the low  $C_{\text{ex}}$ , narrow MWDs are usually not attained (good livingness but poor control), because the  $N_{\text{cycles}}$  a chain experiences during its growth is too low.<sup>11</sup>

Charmot et al.<sup>145</sup> reported *ab initio* emulsion polymerizations of styrene, *n*BA, and EHA using the xanthate EEXP with KPS and SDS at 85 °C. The presence of xanthate did not cause retardation or influence particle size. Good livingness was observed, but the MWDs were broad ( $M_w/M_n > 2.1$ ) except for *n*BA ( $M_w/M_n = 1.4$ ), despite the use of monomer feed to reduce the instantaneous monomer concentration (to increase the rate of transfer relative to propagation). Monteiro et al. carried out *ab initio* emulsion polymerizations of styrene<sup>147,355</sup> and *n*BA<sup>146</sup> using the xanthate EXEB with KPS and SDS at 70 °C. Marked retardation with increasing xanthate concentration (no retardation in bulk) was proposed to be caused by exit of the xanthate leaving group radical, consistent with decreasing particle size ( $d_n = 31$ – $98$  nm) with increasing xanthate concentration (exit followed by re-entry into a micelle would increase the particle number). Retardation in the presence of chain transfer agents (CBr<sub>4</sub> and CCl<sub>4</sub>) in nonliving seeded emulsion polymerization is caused by exit of the thus generated small radicals,<sup>363,364</sup> and the exit rate increases with increasing water solubility of the exiting radical.<sup>365</sup> The low  $C_{\text{ex}}$  causes xanthate to remain to high conversion, thus expelling small radicals throughout the polymerization. The presence of xanthate in a styrene emulsion system leads to an increase in exit rate and a decrease in entry rate, speculated

to be caused by the surface activity of the xanthate ("frustrated entry"—sections 2.2.3.1 and 2.3.3.4),<sup>147,148</sup> due to canonical forms of xanthate involving ionized species.<sup>148,284</sup> The livingness was reasonably good, but the control was poor with  $M_w/M_n \approx 2$ , as expected when the main end-forming event is chain transfer;<sup>366</sup> that is, most chains only undergo one single activation–deactivation cycle. Some improvement was achieved by Monteiro et al.<sup>150</sup> by use of a fluorinated MADIX agent, ETFEXP, with, for xanthates, a relatively high  $C_{ex}$  (3.8) in styrene *ab initio* emulsion polymerization (SDS/sodium persulfate/70 °C) resulting in  $M_w/M_n = 1.5$  and  $M_n \approx M_{n,th}$  with good colloidal stability.

**2.4.3.2.3. RAFT Agent Partitioning and Diffusion.** Partitioning of the RAFT agent between droplets, particles, and the aqueous phase, as well as the rate of transport of RAFT agent from droplets to particles are crucial to the success of an *ab initio* RAFT polymerization.<sup>353,358,359,367,368</sup> If the rate of transport is too low and/or if a significant amount of RAFT agent is located in the droplets or the aqueous phase, the RAFT agent concentration in the particles will not be sufficiently high, resulting in poor control/livingness.<sup>130</sup> Moreover, if the RAFT agent is too water-soluble, it effectively acts as an inhibitor by increasing the time taken for surface active *z*-mers (which can enter particles<sup>78</sup>) to form by chain transfer in the aqueous phase.<sup>130,353</sup> The water solubility of the RAFT agent is thus an important parameter—the diffusion rate of a species from a monomer droplet through the aqueous phase and into a particle is proportional to its saturation concentration in water.<sup>369</sup> RAFT agents similar to PPPDTA<sup>310</sup> have been estimated to undergo transport sufficiently fast for this not to be a limiting factor.<sup>129</sup> Thus, when the RAFT agent concentration in the particles is too low, the origin is likely to be thermodynamic (i.e., unfavorable partitioning coefficients) rather than kinetic. This conclusion is also supported by simulations for TEMPO/styrene aqueous miniemulsions.<sup>166</sup>

Tauer and co-workers<sup>358,359</sup> investigated the effect of RAFT agent hydrophilicity in styrene *ab initio* emulsion polymerizations using SDS at 80 °C, employing the RAFT agents (in order of increasing water solubility<sup>359</sup>) CDB, PhEDB, BDB, and BDA (no data were presented for the corresponding bulk/solution systems, and the differences observed between RAFT agents/initiators may not be entirely accounted for by the effects of heterogeneity of the system). No significant problems with colloidal instability were reported (<9 wt % coagulum). The retardation relative to the system without RAFT agent increased with increasing hydrophilicity of the RAFT leaving group. The hydrophilicity of the RAFT leaving group also influenced the particle size, although no clear trend with hydrophilicity was observed, and particle size effects on  $R_p$  (section 2.2.3) may thus to some extent obscure the effect of the RAFT agent hydrophilicity. Tauer and co-workers<sup>359</sup> also showed that both the rate of transport of the RAFT agent to particles and the RAFT agent concentration in the particles at phase equilibrium increased with increasing RAFT agent hydrophilicity in the order CDB  $\approx$  PhEDB < BDB < BDA (the water solubility of CDB is  $10^{-4}$  to  $10^{-5}$  M,<sup>130</sup> i.e. much lower than that for styrene). These results correlate well with *ab initio* emulsion polymerization data, where  $M_n$  and  $M_w/M_n$  at the final conversion decreased with increasing water solubility of the RAFT agent:<sup>359</sup>  $M_n(\text{CDB}) \approx M_n(\text{PhEDB}) > M_n(\text{BDB}) > M_n(\text{BDA})$ ;  $M_w/M_n(\text{CDB}; 3.0) > M_w/M_n(\text{PhEDB}; 2.2) > M_w/M_n(\text{BDB}; 1.7) > M_w/M_n(\text{BDA}; 1.35)$ .  $M_n \approx M_{n,th}$  for the most

water soluble RAFT agent (BDA), and thus the RAFT agent concentration in the particles is lower than what the overall stoichiometry dictates for the other less water-soluble RAFT agents. The rate of transportation of BDB to polymer particles was higher with styrene than with MMA, illustrating the importance of monomer hydrophobicity.<sup>359</sup> The water solubility of the initiator also played an important role;<sup>358</sup> for CDB,  $R_p$  increased with increasing initiator water solubility, although  $M_w/M_n$  at the final conversion was only marginally affected.

Charleux and co-workers<sup>370</sup> reported emulsifier-free emulsion polymerization of styrene (90.3 mol %) and AA (9.7 mol %) using dibenzyltrithiocarbonate at 60 °C. Except at very high conversion,  $M_n > M_{n,th}$  and the MWD was broad (although  $M_w/M_n = 1.4$  was reached at >90% conversion and the livingness was good), attributed to problems with RAFT agent transport to the particles.

The rate of transport across the aqueous phase of RAFT agents of low water solubility can be increased by use of cyclodextrins, which have been shown to facilitate monomer transport from droplets to particles in emulsion polymerization of highly water-insoluble monomers by formation of host–guest complexes.<sup>371</sup> This approach has been employed with CDB, resulting in good control/livingness for MMA, and good livingness ( $M_n \approx M_{n,th}$ ) but poor control ( $M_w/M_n > 3$ ) for styrene.<sup>367</sup> Uzulina et al.<sup>130</sup> investigated emulsion polymerizations of styrene and MMA using a RAFT agent with a leaving group containing an amide functionality.  $M_n$  increased linearly with conversion close to  $M_{n,th}$ , but  $M_w/M_n$  was relatively broad (>1.5).

**2.4.3.2.4. Miscellaneous RAFT Emulsion Polymerizations.** Choe and co-workers<sup>360–362</sup> carried out *ab initio* emulsion photopolymerizations of MMA using a surface active RAFT agent (TBSMSB) functioning as initiator, chain transfer agent, and stabilizer at 60–80 °C (no surfactant or initiator added). No problems with colloidal instability were reported ( $d = 47.6$ –412 nm, depending on recipe). Interestingly,  $1.20 \leq M_w/M_n \leq 1.41$  and  $M_n$  increased linearly with conversion despite for CLRP unusually high MWs ( $338500 < M_n < 757400$ ). In general, such high MW polymer of narrow MWD is extremely difficult to prepare by CLRP.<sup>11</sup>

Comb-type copolymers have been synthesized by copolymerization of styrene and 2-hydroxyethyl acrylate-capped polyurethane macromonomer using the RAFT agent BD-MBA at 60 °C with good control/livingness.<sup>372</sup>

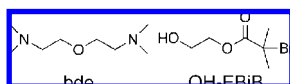
Urbani et al.<sup>368</sup> investigated emulsion polymerization of styrene using PEPDTA and Brij 98 at 70 °C using a "microemulsion-like" system with most monomer (>86.4%) initially located in "monomer-swollen micelles". Good control/livingness was obtained when  $M_{n,th} \leq 9000$  ( $51 \leq d_n \leq 161$  nm). Lack of control at  $M_{n,th} > 9000$  was attributed to superswelling resulting in different ratios of monomer to RAFT agent in different particles.

*Ab initio* RAFT emulsion polymerizations using plasma-initiation have been reported for MMA and octyl acrylate at 35 and 70 °C.<sup>373</sup> Good control/livingness was obtained to 49% conversion, after which colloidal instability was observed. The use of consecutive freeze–thaw cycles, which has been reported to influence the particle size distribution, has also been investigated in *ab initio* RAFT (and MADIX) polymerization.<sup>374</sup>

Charleux and co-workers<sup>370</sup> developed a phase inversion approach to obtain a dispersed system. Styrene (82.1 mol %) and AA (17.9 mol %) were copolymerized in bulk to



Scheme 14



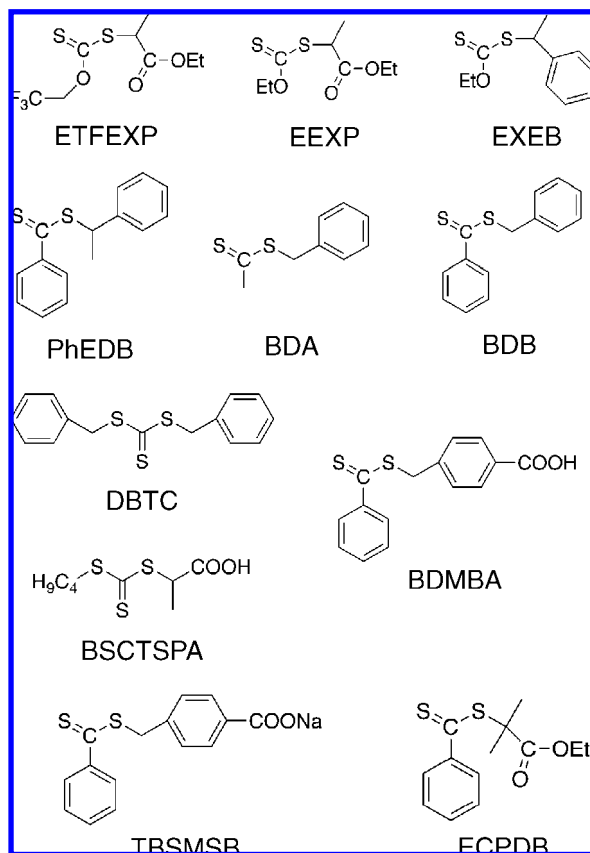
relatively low conversion employing DBTC at 60 °C, and subsequently an aqueous sodium hydroxide solution was added until phase inversion occurred, generating a dispersed organic phase, which could be successfully employed as seed for a second polymerization step of styrene and *n*BA, respectively. Good control/livingness ( $M_w/M_n \approx 1.2$ ) and colloidal stability ( $d = 140\text{--}180$  nm) were obtained.

**2.4.3.2.5. RAFT *ab Initio* Emulsion Polymerization Based on Self-Assembly.** Gilbert and co-workers<sup>311,331,332</sup> have developed a technique for performing RAFT *ab initio* emulsion polymerization based on nucleation via self-assembly of amphiphilic diblock copolymer formed *in situ*. In a first stage, a water-soluble monomer such as AA is polymerized to low DP (approximately five) in a controlled/living fashion in the aqueous phase using an amphiphilic RAFT agent (e.g., BSCTSPA) and a water-soluble radical initiator (e.g., V-501). Water solubility of the RAFT agent and initiator was ensured by addition of NaOH to achieve partial neutralization of the acid groups. Subsequent addition of a hydrophobic monomer such as *n*BA using a feed technique to ensure the absence of monomer droplets results in formation of surface active block copolymer that self-assembles into micelles. These micelles constitute the locus of polymerization upon further controlled addition of the hydrophobic monomer, resulting in formation of polymer particles (Scheme 16). Polymer thus forms via CLRP, without any problems with phase separation and colloidal instability. This approach ensures the presence of RAFT agent at the locus of polymerization, ideally in the interior of the particle, and no additional surfactant is added. The particle formation process has been modeled by Gilbert.<sup>332,375</sup>

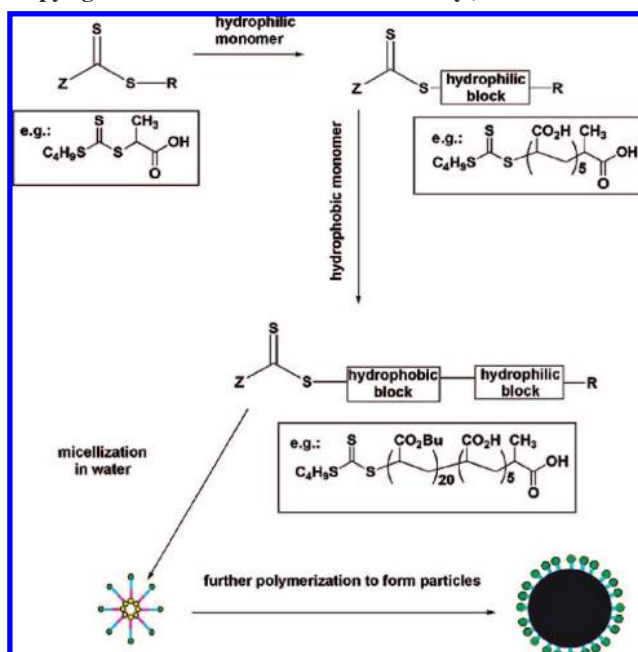
Hawckett and co-workers<sup>376</sup> investigated the nucleation mechanism in *ab initio* emulsion polymerizations of styrene and *n*BA using RAFT-capped poly(AA<sub>*x*</sub>-*b*-styrene<sub>*y*</sub>) copolymers ( $x \approx 10$ ,  $y \approx 0, 5, 10$ ) at 70 °C. Above the cmc (0.23 mM for  $x = 9$  and  $y = 5$ ), the mobility of the diblocks between micelles influences the nucleation process. The rate of exchange of diblocks between the micelles is on the same time scale as the nucleation process, and the mobility of diblocks depends mainly on the hydrophobicity of the diblocks. The higher the hydrophobicity and the higher the initiator concentration, the more likely it is that all micelles become nucleated. At low initiator concentrations and with a shorter hydrophobic block (i.e., more labile micelles), only some of the micelles are nucleated and become polymer particles, while the remaining micelles break up as their constituent diblocks migrate to new particles. This is evidenced by the fact that the number of RAFT moieties per particle ( $\approx 2700$ <sup>311</sup>) is much higher than the typical surfactant aggregation number ( $\approx 90$  for these types of diblock copolymers<sup>376</sup>).<sup>311,332,376</sup>

The particle surface can be functionalized according to the choice of the R group of the RAFT agent. To this end, the RAFT agent should have a hydrophilic R group and a hydrophobic Z group.<sup>311</sup> If monomer droplets are present, the amphiphilic diblock copolymer may adsorb onto monomer droplets, reducing monomer loss from the droplets and eventually resulting in monomer droplet nucleation.<sup>311</sup> The presence of a monomer phase is thus only a problem during the particle nucleation step.

Scheme 15. RAFT Agents



Scheme 16. RAFT *ab Initio* Emulsion Polymerization via Self-Assembly (Reprinted with permission from ref 311. Copyright 2005 American Chemical Society.)



The MWs increased with conversion, consistent with a controlled/living process, but the MWDs were relatively broad ( $M_w/M_n = 1.5$  at 67% conversion), speculated to be caused by termination, grafting reactions, as well as the monomer/RAFT agent ratio varying between particles. The particle size increased with conversion, as anticipated, with  $d_n = 60$  nm ( $d_w/d_n = 1.11$ ) at 67% conversion.<sup>311</sup> According to the postulated mechanism, the chains would

be surface anchored via the AA segment, whereas the hydrophobic chains would extend into the particle. However, the particle size was too great for the chains to reach into the center of the particle. This can be explained by a significant fraction of chains having their hydrophilic chain end buried within the particle, as well as by the presence of chains not formed via the RAFT mechanism (e.g., chain transfer to monomer).<sup>311</sup> Polymerizations were also carried out replacing *n*BA with MA in the hope its higher water solubility would result in more rapid aqueous phase propagation and thus less termination occurring prior to self-assembly. However, the MWDs were broader than those for *n*BA.<sup>311</sup>

**2.4.3.3. RAFT Seeded Emulsion Polymerization.** RAFT is easier to implement in seeded emulsion polymerization than in an *ab initio* system mainly because superswelling<sup>126</sup> is avoided. However, transport of RAFT agent to the polymer particles remains an issue.

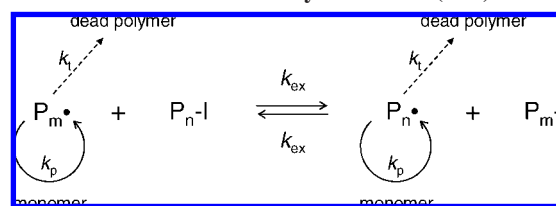
Moad et al.<sup>284</sup> carried out seeded starved-feed emulsion polymerizations of styrene at 80 °C, thereby avoiding the presence of a monomer-phase, with the best results obtained with BDB and BDA ( $M_w/M_n < 1.4$  at >99% conversion). PS-*b*-PMMA was also prepared by sequential monomer addition.

Monteiro et al.<sup>129</sup> performed seeded emulsion polymerizations of styrene using a PMMA seed (intervals II and III) and CDB and ECPDB (KPS/SDS/60 °C). Phase separation and poor control/livingness were observed. The retardation was greater for the RAFT agent with the more water soluble leaving group (ECPDB), consistent with the cause being exit of the radical leaving group. As stated above, superswelling is believed to be the main cause of colloidal instability in RAFT miniemulsion and emulsion systems. However, superswelling should not occur in a seeded polymerization due to the presence of high MW polymer in the particles. The presence of highly water insoluble species (the RAFT agent) in the droplets in interval II may prevent complete disappearance of the droplets and ultimately cause phase separation/coagulation. This would be exacerbated if the initial RAFT agent is to some extent transformed to oligomeric RAFT agents in the monomer droplets.<sup>154</sup> Moreover, it has been suggested that high reactivity RAFT agents may lead to significant formation of RAFT oligomers in the aqueous phase, and their inability to enter particles may contribute to phase separation/coagulation.<sup>149</sup>

Prescott et al.<sup>310</sup> carried out emulsion polymerizations of styrene using a PS seed (KPS/SDS/60 °C) and RAFT agent with very low water solubility, PPPDTA. Prior to seeded polymerization, the RAFT agent and acetone were added to the seed emulsion to aid in transporting the RAFT agent to the particles; subsequently, acetone/water was removed by evaporation, followed by addition of water to yield the final seed emulsion. Seeded emulsion polymerizations (intervals II and III) were carried out without significant coagulation or phase separation, with good control/livingness, but with more severe induction periods and retardation than in bulk.

Seeded emulsion polymerization of styrene has also been performed successfully by Georges and co-workers<sup>352</sup> using a seed prepared via a precipitation technique, whereby an acetone solution of the polymeric RAFT agent based on PPPDTA was added to an aqueous solution of PVA, resulting in precipitation and formation of seed particles (acetone was removed prior to seeded polymerization). This approach

### Scheme 17. Iodine Transfer Polymerization (ITP)



resulted in good control/livingness as well as colloidal stability ( $d \approx 150$  nm) and has also been applied to NMP<sup>327</sup> and ATRP.<sup>342</sup>

Seeded emulsion polymerizations have also been performed using xanthates.<sup>146–149,355</sup>

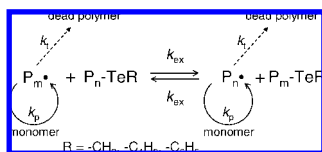
## 2.5. Miscellaneous Miniemulsion and Emulsion CLRP

### 2.5.1. Iodine Transfer Polymerization (ITP)

ITP is based on an exchange process whereby propagating radicals are deactivated reversibly via degenerative transfer (Scheme 17).<sup>33–36</sup> ITP has to date been implemented in miniemulsion for styrene<sup>377–380</sup> and *n*BA.<sup>381</sup> Charleux and co-workers<sup>378</sup> carried out ITP of styrene in miniemulsion at 70 °C with the transfer agent perfluorohexyl iodide ( $C_6F_{13}I$ ) using both AIBN and the water-soluble V-501 with SDS. It was assumed that the transfer agent also fulfilled the role of hydrophobe to suppress Ostwald ripening, and hexadecane was not added. Stable dispersions without coagulation were obtained with  $d \approx 100$  nm. The efficiency of the transfer agent was 100% and the livingness was good, but the MWDs were relatively broad as a result of the low transfer constant of  $C_6F_{13}I$  ( $C_{ex} = k_{ex}/k_p = 1.4$ ), which is an intrinsic feature of ITP. This problem is worse for *n*BA with  $C_{ex} < 0.1$  but can be partially overcome by use of (i) monomer starved-feed conditions, whereby the low monomer concentration results in an increase in the rate of transfer relative to propagation,<sup>381</sup> (ii) copolymerization with styrene, which has a higher  $C_{ex}$ ,<sup>381</sup> and (iii) low temperature (the activation energy of propagation is greater than that of transfer).<sup>35</sup> Charleux and co-workers<sup>381</sup> synthesized styrene/*n*BA block copolymers with broad MWDs ( $M_w/M_n \approx 2$ ) but good livingness in miniemulsion using ITP, exploiting techniques (i) and (ii). ITP has also been employed for preparation of PS-*b*-PDMS-*b*-PS in miniemulsion using  $\alpha,\omega$ -diiodo PDMS.<sup>379</sup>

Reverse iodine transfer polymerization (RITP) was recently developed by Lacroix-Desmazes and co-workers.<sup>36,382,383</sup> The polymerization starts with  $I_2$  and a conventional radical initiator, leading to *in situ* generation of transfer agent R-I or P-I (where R is the primary radical from initiator and P is polymer), which is not sufficiently stable for long-term storage. When RITP was applied in aqueous miniemulsion with styrene at 60 °C,<sup>380</sup>  $I_2$  was however consumed by hydrolysis in the aqueous phase. This problem was solved by the addition of hydrogen peroxide as oxidant,<sup>380</sup> whereby  $I^-$  generated by  $I_2$  hydrolysis undergoes oxidation to regenerate  $I_2$ .

ITP has also been implemented in *ab initio* emulsion by Charleux and co-workers<sup>378</sup> for styrene/ $C_6F_{13}I$ /V-501/SDS/70 °C with good colloidal stability but poor control ( $M_w/M_n = 1.73–2.03$  and  $M_n > M_{n,th}$ ). The high hydrophobicity of  $C_6F_{13}I$  leads to slow transport from monomer droplets to the particles, and consequently a lower rate of transfer and fewer

**Scheme 18. Organotellurium-Mediated Radical Polymerization (TERP)**

chains than expected based on the overall stoichiometry. RITP has been successfully implemented in *ab initio* emulsion by Lacroix-Desmazes and co-workers.<sup>384,385</sup> RITP of *n*BA was performed in *ab initio* emulsion (V-501/SDS/85 °C).<sup>384</sup> After an induction period due to the high concentration of I<sub>2</sub>, polymerization proceeded to high conversion (*d* = 106 nm). The MWDs were broad, but *M<sub>n</sub>* increased linearly with conversion and the MWDs shifted to higher MW. However, *M<sub>n</sub>* > *M<sub>n,th</sub>* due to the low efficiency of I<sub>2</sub> due to hydrolytic disproportionation of I<sub>2</sub> in the aqueous phase. The problem of hydrolytic disproportionation was overcome by making use of KPS as both initiator and oxidant;<sup>380</sup> that is, KPS fulfilled the role of oxidant that hydrogen peroxide played in the miniemulsion work described above.<sup>385</sup> RITP of *n*BA was carried out at 85 °C with [KPS]<sub>0</sub>/[I<sub>2</sub>]<sub>0</sub> = 4.5, with conversion reaching almost 100% in 5 h (*d* = 83 nm) and *M<sub>n</sub>* ≈ *M<sub>n,th</sub>*, although the MWD was relatively broad.

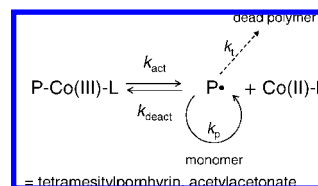
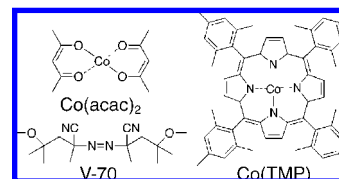
**2.5.2. Organotellurium-Mediated Radical Polymerization (TERP)**

Yamago and co-workers recently developed TERP and clarified various mechanistic/kinetic features in bulk/solution.<sup>42–46</sup> TERP comprises two activation processes: thermal dissociation (TD) and degenerative transfer (DT).<sup>42,43,46</sup> TD is only significant at high temperature—at the normally employed polymerization temperatures for TERP (<80 °C), the main mechanism is DT (Scheme 18), and TD can be neglected.<sup>43</sup>

Okubo and co-workers<sup>386</sup> performed TERP of MMA, styrene, and *n*BA in miniemulsion using a hydrophobic TERP agent (AIBN/hexadecane/SDS/60 °C) with good colloidal stability (*d<sub>n</sub>* ≈ 100 nm) and satisfactory livingness to high conversion. The MWDs were relatively broad for MMA and styrene but narrow for *n*BA. For MMA, significant retardation was observed compared to the corresponding conventional miniemulsion polymerization (without TERP agent). Unlike RAFT, TERP does not proceed via a relatively long-lived intermediate, and TERP in bulk/solution is normally not accompanied by retardation.<sup>43</sup> It is therefore likely that retardation is caused by the heterogeneous nature of the system, possibly related to exit of small radicals. AIBN radicals and the propagating radicals may add to the initial TERP agent, generating a small radical which may exit. Successful synthesis of various block copolymers using two-step TERP in aqueous media was also demonstrated. Moreover, the merit of TERP that the order of monomer addition is of little importance was shown to hold also in aqueous dispersed systems.

**2.5.3. Cobalt-Mediated Radical Polymerization (CMRP)**

The presence of a very small amount of certain low-spin Co(II) complexes such as {bis{μ-[(2,3-butanedione dioximate)(2-)-O, O']}]tetrafluorodiborate(2-)-N,N',N'',N'''}cobalt (COBF) during methacrylate polymerization results in formation of polymer with 2-carbalkoxy-2-propenyl end groups (macromonomer) via catalytic chain

**Scheme 19. Cobalt-Mediated Radical Polymerization (CMRP)****Scheme 20**

transfer.<sup>387–389</sup> The mechanism involves hydrogen abstraction from the α-methyl group of the propagating radical by Co(II), generating macromonomer and Co(III). Co(III) subsequently undergoes hydrogen transfer with monomer, generating Co(II) and a monomer radical, which reinitiates polymerization. This reaction is predominant for methacrylates, whereas in the case of styrene polymerization, Co(III)–C bonds are competitively generated. Co(III)–C bonds are weak, and the cleavage of Co(III)–C occurs readily, generating Co(II) and a carbon-center radical. In the case of acrylates, reversible formation of Co(III)–C bonds is the main reaction, resulting in the formation of a CLRP equilibrium (Scheme 19).<sup>49–51,390–394</sup> Wayland et al.<sup>51</sup> reported CMRP of MA at 60 °C using cobalt tetramesitylporphyrin (TMP) as a control agent (Scheme 20), obtaining good control/livingness.

CMRP of VAc has been implemented in aqueous suspension<sup>392</sup> and miniemulsion<sup>393</sup> by Jerome and co-workers. CMRP of VAc in suspension using cobalt acetylacetonate (Co(II)(acac)<sub>2</sub>; Scheme 20) as a control agent and V-70 as initiator was carried out.<sup>392</sup> CLRP of VAc is in general difficult due to the high reactivity of the nonconjugated propagating radical as well as the high fraction of head-to-tail addition,<sup>43</sup> but has been achieved with CMRP<sup>390</sup> as well as with ITP,<sup>395,396</sup> RAFT (MADIX),<sup>121,301,397,398</sup> and TERP (*M<sub>n</sub>* < 5000).<sup>43,46</sup> CMRP of VAc in suspension at 30 °C with PVA-co-PVAc as stabilizer resulted in *M<sub>n</sub>* > *M<sub>n,th</sub>* and somewhat broad MWDs.<sup>392</sup> Quantification of the partitioning of the deactivator Co(II)(acac)<sub>2</sub> between the organic and aqueous phases revealed that excessive partitioning to the aqueous phase was occurring. Low initiator efficiency of V-70 (11–48%) caused *M<sub>n</sub>* > *M<sub>n,th</sub>*. In order to avoid partitioning of Co(II)(acac)<sub>2</sub>, CMRP was carried out in bulk to low conversion, and this monomer solution was subsequently dispersed in water. This technique prevented exit of Co(II)(acac)<sub>2</sub> during the initial stage of the polymerization, yielding higher initiator efficiency (67–73%) and good control/livingness (*M<sub>n</sub>* = 60500, *M<sub>w</sub>*/*M<sub>n</sub>* = 1.35 at 95% conversion for 4 h). PVAc of higher MW (*M<sub>n</sub>* = 100000, *M<sub>w</sub>*/*M<sub>n</sub>* = 1.40 at 75% for 70 min) was also achieved using this approach.

Jerome and co-workers<sup>393</sup> also reported CMRP of VAc in miniemulsion at low temperature (0–30 °C) using PVAc macroinitiators end-capped by a Co(acac)<sub>2</sub> complex and SDS. *R<sub>p</sub>* was unusually high (94% conversion in 60 min), accompanied by good control/livingness generating submicron-size PVAc particles (*d<sub>n</sub>* ≈ 100 nm). The values of *R<sub>p</sub>* in this



study and in the corresponding suspension work<sup>392</sup> are much higher than those in bulk/solution CLRP of VAc.

## 2.6. Microemulsion Polymerization

### 2.6.1. General Considerations

A microemulsion is a thermodynamically stable, macroscopically homogeneous mixture of two immiscible liquids and a surfactant, which forms spontaneously without external shear forces (unlike a miniemulsion). Before polymerization, a microemulsion consists of monomer-swollen micelles ( $d = 5\text{--}10\text{ nm}$ ), and during the course of the polymerization, some of these micelles are converted to polymer particles.<sup>112,114</sup>

A microemulsion polymerization is similar to a miniemulsion polymerization in the sense that, in an ideal case where each monomer-swollen micelle is converted to a polymer particle, there is no need for transport of control agent through the aqueous phase. However, only a fraction of monomer-swollen micelles become nucleated, and the remaining monomer-swollen micelles act as monomer reservoirs, supplying monomer to the particles similar to the case in an emulsion polymerization.<sup>112,114,319</sup> In a conventional microemulsion polymerization, the number of monomer-swollen micelles greatly exceeds that of polymer particles (typically by a factor of  $10^3$ ).<sup>319</sup> This monomer diffusion process, as well as some degree of coalescence, usually results in polymer particles with  $d = 20\text{--}60\text{ nm}$ .<sup>112,114</sup> Depending on the nucleation rate and the relative rates of diffusion and partitioning of control agents and monomer, control/livingness can be adversely affected. Other factors that may affect microemulsion CLRP include compartmentalization<sup>156,157,160,161,164</sup> (the confined space effect and the segregation effect) as well as effects related to differing numbers of reactants in different particles. The latter is only a factor for very small particles when there are very few control agents per particle, and thus it is normally not important in other dispersed systems such as emulsion and miniemulsion polymerization.

Microemulsion CLRP has been performed using NMP,<sup>187,326</sup> ATRP,<sup>197,198,344,399,400</sup> RAFT,<sup>319</sup> and ITP.<sup>401,402</sup>

### 2.6.2. Microemulsion NMP

Microemulsion NMP of styrene has been carried out at  $125\text{ }^\circ\text{C}$  using the cationic surfactant TTAB by Okubo and co-workers.<sup>187</sup> TEMPO-mediated polymerizations were very slow, consistent with the confined space effect<sup>156</sup> (compartmentalization) reducing the rate of deactivation and the efficiency of thermal initiation (section 2.2). The MWDs were relatively broad, and the particles were fairly large for a microemulsion ( $d_n = 39\text{--}129\text{ nm}$ ). The broad MWDs probably originated in alkoxyamine decomposition as well as differing diffusion rates of monomer and low MW alkoxyamines (and nitroxide) between monomer-swollen micelles and polymer particles, causing the [monomer]/[alkoxyamine] ratio to vary between particles. The poor results with TEMPO were thus indirectly related to the low  $R_p$ . Polymerizations with SG1, which has a higher equilibrium constant than TEMPO,<sup>11</sup> proceeded much faster, resulting in  $d_n = 21\text{--}37\text{ nm}$  and considerably lower  $M_w/M_n$  than that for TEMPO.

NMP of *n*BA employing the water-soluble SG1-based alkoxyamine A-Na under microemulsion-like conditions has been reported by Charleux and co-workers.<sup>326</sup> A very dilute

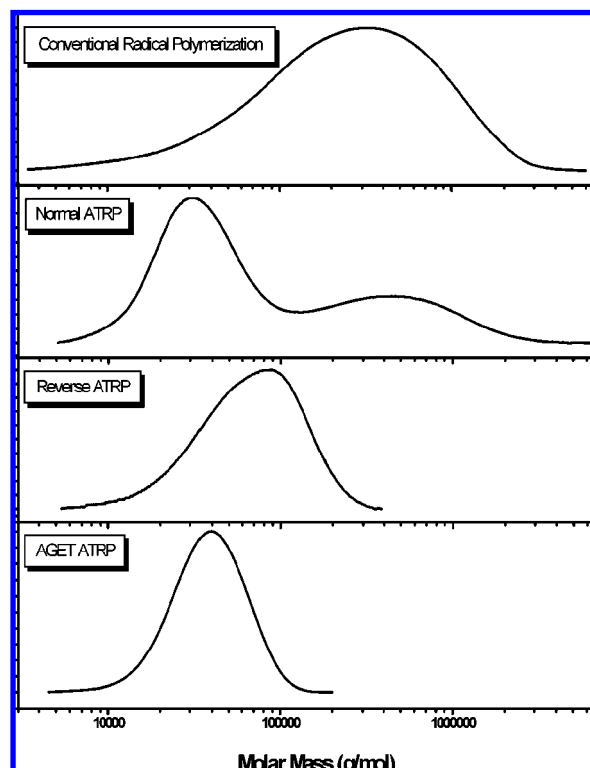


**Figure 9.** MWDs of PMMA obtained in microemulsion by conventional radical polymerization and different variants of ATRP at  $65\text{ }^\circ\text{C}$ . Reprinted with permission from ref 197. Copyright 2005 American Chemical Society.

aqueous *n*BA emulsion with a high Dowfax 8390 concentration was used, whereby most monomer was located in monomer-swollen micelles. Polymerization to approximately 60% conversion yielded  $M_n \approx 1000$  and  $M_w/M_n = 1.14$ , which was followed by introduction of monomer in one shot to swell the seed particles for further polymerization.

### 2.6.3. Microemulsion ATRP

Min and Matyjaszewski<sup>197</sup> reported microemulsion ATRP of MMA (limited data for styrene) using direct ATRP (EBiB/CuBr), reverse ATRP (V-50/CuBr<sub>2</sub>), as well as AGET ATRP (EBiB/CuBr<sub>2</sub>/ascorbic acid) employing Brij 98 and the hydrophobic ligand BPMODA at  $65\text{ }^\circ\text{C}$ . Direct ATRP resulted in bimodal MWDs (Figure 9), attributed to exit of Cu(II) from monomer-swollen micelles containing a single propagating radical and a single Cu(II) species, resulting in uncontrolled polymerization occurring in parallel with CLRP. This would be a consequence of the small number of Cu-complexes per monomer-swollen micelle ( $\approx 15$ ). Reverse ATRP led to monomodal MWDs but high  $M_w/M_n (=1.61)$  due to slow initiator decomposition. The particle size was large ( $d_h = 70\text{ nm}$ ) due to the slow initiation, although the monomer-swollen micelle size was  $10\text{ nm}$  before polymerization. A similar increase in particle size was also observed in microemulsion NMP,<sup>187</sup> which is a result of monomer transfer from non-nucleated monomer-swollen micelles to particles when initiation is slow. The best results were obtained using AGET ATRP, which resulted in good control/livingness ( $M_w/M_n = 1.28$ ) and a narrow particle size distribution with  $d_h = 43\text{ nm}$ . Ascorbic acid reacts rapidly with Cu(II) in the aqueous phase or at the interface, generating Cu(I), which takes part in activation with EBiB after entry into monomer-swollen micelles. The same AGET

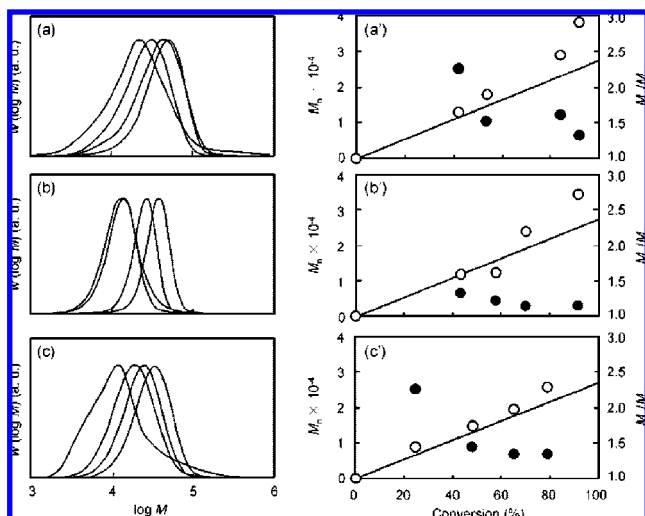


**Figure 10.** MWDs (a–c),  $M_n$  (a'–c'); straight lines are  $M_{n,theoretical}$ , and  $M_w/M_n$  (a'–c') obtained in microemulsion ATRP of *i*BMA at 40 °C using emulsifier systems TTAB (a, a'), TTAB/E911 (b, b'), and TTAB/E931 (c, c'). Reprinted with permission from ref 198. Copyright 2007 Wiley-VCH Verlag GmbH & Co.

ATRP microemulsion procedure has also been applied successfully to *n*BA.<sup>344</sup>

Direct ATRP of *i*BMA in microemulsion was carried out by Okubo et al.<sup>198</sup> employing EB*i*B/dNBpy2 and the cationic emulsifier TTAB at 40 °C, resulting in a monomodal and relatively narrow MWD ( $M_w/M_n = 1.32$ ; Figure 10a) and a transparent emulsion with  $d_n = 13$  nm. This is in contrast to the bimodal MWDs obtained by Min and Matyjaszewski<sup>197</sup> in direct ATRP. The source of this apparent discrepancy is likely to have its origin in the way of addition of EB*i*B. Min and Matyjaszewski carried out emulsification at 60 °C, whereas this was done at room temperature by Okubo et al. Thus, once the polymerization temperature was reached, essentially all EB*i*B would have entered the monomer-swollen micelles. In the work of Matyjaszewski and co-workers, it is likely that activation would occur in monomer-swollen micelles prior to all alkyl halide having entered micelles. The presence of a small amount of the nonionic emulsifier Emulgen 911 in the *i*BMA/TTAB microemulsion surprisingly resulted in very narrow MWD ( $M_w/M_n = 1.14$ ) even at high conversion (>90%;  $d_n = 12$  nm; Figure 10b). Emulgen 911 did not influence the corresponding bulk ATRP. The improved control by E911 may be caused by complex formation between CuBr<sub>2</sub> and E911 within the particles,<sup>403,404</sup> reducing exit of Cu(II) to the aqueous phase. The presence of the less hydrophobic Emulgen 931, which would not suppress Cu(II) exit, did not improve the MWD (Figure 10c).

Yi and co-workers reported reverse ATRP in microemulsion of styrene<sup>399</sup> and MMA<sup>400</sup> using AIBN/CuCl<sub>2</sub>/bpy/SDS/*n*-hexanol. In the case of styrene, the viscosity-average MWs increased linearly with conversion in the presence of 1 wt % NaCl (based on water) (no MWDs reported;  $d = 10$ –100 nm). The MWD was broad for MMA ( $M_w/M_n = 1.58$ ). The relatively poor levels of control were most likely caused by excessive exit of Cu-complexes resulting from the insufficient hydrophobicity of the ligand bpy.

#### 2.6.4. Microemulsion RAFT Polymerization

There is to date only one report on RAFT in microemulsion.<sup>319</sup> Kaler and co-workers investigated the RAFT po-

lymerization of HMA at 75 °C employing the RAFT agent CPDB, the water-soluble initiator V-50, and the cationic surfactant DTAB. The level of retardation on addition of the RAFT agent was much stronger than that in bulk. The particles ( $d = 18$ –30 nm) were somewhat smaller than those from the corresponding microemulsion polymerization without RAFT agent and also had a somewhat narrower particle size distribution. The [RAFT agent]/[V-50] ratio is crucial in obtaining good control. At [RAFT agent]/[V-50] > 1.5,  $M_n \approx M_{n,theoretical}$  and  $M_w/M_n < 1.5$ , whereas [RAFT agent]/[V-50] < 1.5 led to poor control ( $M_w/M_n > 1.8$ ). Kinetic modeling and simulations<sup>318</sup> indicated that the poor level of control/livingness at low [RAFT agent]/[V-50] originates in monomer-swollen micelles that are nucleated late in the polymerization not containing a sufficient amount of RAFT agent. This is a consequence of the rate of transport of the RAFT agent from monomer-swollen micelles to polymer particles (nucleated monomer-swollen micelles) being faster than that of monomer.

#### 2.6.5. ITP in Microemulsion

Iodide-mediated copolymerization has been carried out under microemulsion-like conditions for vinylidene fluoride/hexafluoropropylene using the bifunctional iodine chain transfer agent C<sub>6</sub>F<sub>12</sub>I<sub>2</sub> at 80 °C.<sup>401</sup> The polymerization exhibited controlled/living characteristics, but chain transfer to polymer and copolymerization involving polymer chains with terminal unsaturations (generated by termination by disproportionation) resulted in  $M_w/M_n \approx 2$ .

### 2.7. Dispersion and Precipitation Polymerizations

#### 2.7.1. General Considerations

In a precipitation<sup>405</sup> or dispersion polymerization,<sup>115,116,406,407</sup> the system is initially homogeneous. Particle formation occurs as a result of polymer chains propagating to a critical chain length ( $J_{crit}$ ) at which they are no longer soluble. The growing chains subsequently phase separate from the continuous medium, and particle formation occurs. The fundamental difference between a precipitation and a dispersion polymerization is that a colloidal stabilizer is present in the latter. Dispersion polymerization is a useful method for synthesis of micron- and submicron-sized polymer particles with narrow particle size distribution. The most commonly used solvents are hydrocarbons such as the alkanes as well as more polar media such as alcohol/water mixtures. Supercritical carbon dioxide (scCO<sub>2</sub>) has recently received attention as a more environmentally benign alternative.<sup>108,408–413</sup>

In a conventional (nonliving) precipitation/dispersion polymerization,  $J_{crit}$  of an individual chain is reached in  $\ll 1$  s. In CLRP, the DP increases linearly with conversion, and the conversion at which  $J_{crit}$  is reached is therefore much higher than in a conventional precipitation/dispersion polymerization. In other words, the value of  $M_{n,theoretical}$  is expected to strongly influence the polymerization.

Emulsion polymerization generally results in submicron-sized particles with narrow particle size distribution, and the particle size distribution in miniemulsion polymerization is inevitably broad. However, addition of CLRP reagents as well as cross-linkers to a dispersion polymerization leads to significant broadening of the particle size distributions. The length (conversion range) of the nucleation stage is a key factor—a short nucleation stage is required for a narrow

particle size distribution. However, the nucleation stage is prolonged in dispersion CLRP because high MW polymer is not formed instantaneously as it is in a nonliving system, resulting in broad particle size distributions. This problem has recently been overcome with the “two-stage” approach<sup>414–417</sup> of Song and Winnik, whereby the RAFT agent or the cross-linker<sup>416</sup> is added after the nucleation stage (<a few percent conversion<sup>418</sup>).

Partitioning of deactivator (nitroxide (NMP) or transition-metal complex (ATRP)) and monomer between the continuous phase and the particle phase as well as compartmentalization of propagating radicals and deactivator (if the particles are sufficiently small) may significantly influence the course of precipitation/dispersion polymerizations. However, such effects are more difficult to elucidate in dispersion/precipitation polymerizations than in emulsion/miniemulsion polymerizations, because, in the former, both the continuous and the particle phases often constitute significant polymerization loci (unlike in the latter).

Dispersion/precipitation polymerizations have been carried out for NMP,<sup>108,109,408,409,411–413,419–422</sup> ATRP,<sup>410,413,414,423</sup> RAFT,<sup>408,412,417,424–428</sup> and ITP.<sup>417</sup>

## 2.7.2. NMP

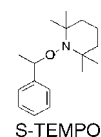
**2.7.2.1. Precipitation NMP.** Precipitation NMP has been carried out for styrene in ethylene glycol/water<sup>420</sup> and scCO<sub>2</sub>.<sup>109,419,422</sup> Armes and co-workers performed precipitation NMP of styrene using BPO/TEMPO (112–130 °C), with  $M_n = 2800$  and  $M_w/M_n = 1.15$  at 20% conversion (only one polymerization reported).<sup>420</sup>

ScCO<sub>2</sub> has attracted attention as a benign, inexpensive, nonflammable, and widely available medium as an alternative to volatile organic compounds (VOC).<sup>429</sup> Most polymers exhibit very low solubility in scCO<sub>2</sub>, and it is therefore a useful solvent for precipitation/dispersion polymerizations. Odell and Hamer<sup>419</sup> carried out NMP of styrene using TEMPO in scCO<sub>2</sub> at 125 °C. At reactor loadings of 30 and 50 vol % styrene, the polymerizations proceeded with good control/livingness. However, with 10 vol % styrene, the polymerization stopped at low conversion.

Okubo and co-workers<sup>109</sup> reported TEMPO-based precipitation NMP of styrene in scCO<sub>2</sub> at 110 °C to high conversion, with the product recovered as a powder after venting of the CO<sub>2</sub>. A relatively high monomer loading (40% w/v) and a large excess of SG1 were required to obtain both a controlled/living polymerization and high conversion. The polymerization proceeded at a rate similar to that of the corresponding solution polymerization, and kinetic analysis indicated that the polymer phase was the predominant locus of polymerization after the onset of heterogeneity.<sup>108</sup> High conversions were achieved, which is in sharp contrast with previous work on conventional (nonliving) radical precipitation polymerization of styrene in scCO<sub>2</sub>.<sup>430,431</sup> This is most likely a consequence of the high temperatures employed rather than the controlled/living nature. Recent work has revealed that styrene precipitation NMP in scCO<sub>2</sub> at 110 °C with 70% w/v monomer can proceed with better control over the MWDs than the corresponding solution polymerizations for both SG1 and TIPNO,<sup>422</sup> illustrating how benign scCO<sub>2</sub> may provide new avenues for improved control of radical polymerization.

**2.7.2.2. Dispersion NMP.** Dispersion NMP of styrene has been reported in decane,<sup>421</sup> in alcoholic<sup>420,432</sup> and aqueous

## Scheme 21



S-TEMPO

alcoholic media<sup>420</sup> using TEMPO, and in scCO<sub>2</sub> employing SG1.<sup>108,409,411</sup>

Dispersion NMP of styrene employing BPO/TEMPO has been carried out in decane with a PS-*b*-(polyethylene-*alt*-propene) (Kraton G1701) stabilizer at 135 °C.<sup>421</sup> Very significant polymerization occurred in the continuous phase, especially for the polymerization with the lowest  $M_{n,th}$ . From the conversion at the onset of heterogeneity (based on  $M_{n,th}$  vs conversion),  $J_{crit} \approx 58$  ( $M_n \approx 6000$ ). The control/livingness was reasonable ( $M_w/M_n \leq 1.52$ ), although markedly inferior to bulk due to polymerization occurring in both phases. The longer polymerization times in the dispersion system are also likely to have impacted control/livingness negatively due to termination and alkoxyamine decomposition.<sup>169,230</sup> In addition to prolonged nucleation (section 2.7.1), particle formation on cooling may have played a role in causing a very wide particle size distribution of  $d = 50$  nm to 10  $\mu$ m.

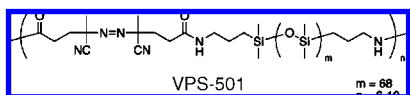
Armes and co-workers<sup>420</sup> used alcoholic and aqueous alcoholic media instead of decane to carry out TEMPO-mediated dispersion NMP of styrene (using BPO, KPS, or 1-phenyl-1-(2,2,6,6-tetramethyl-1-piperidinyloxy)ethane; Scheme 21), thereby reducing the solubility of PS chains in the continuous medium (PVP as stabilizer). Attempted dispersion polymerizations using various alcohols at 120 °C resulted in particle formation only on cooling. Dispersion polymerizations were carried out successfully using ethylene glycol and ethylene glycol/water mixtures at 112–130 °C, with  $M_w/M_n \leq 1.31$ , although  $M_n > M_{n,th}$ . However, results were only reported for systems with unusually low MWs ( $M_{n,th} = 4100$  at 100% conversion), and the final conversions were low. The particle size distributions were broad ( $d = 0.73$ –3.64  $\mu$ m).

Choe and co-workers<sup>433</sup> carried out TEMPO-mediated dispersion polymerization of styrene at 125 °C using PVP in various glycols, resulting in  $d = 0.32$ –10  $\mu$ m. The particle size decreased with increasing [TEMPO]/[AIBN] and decreasing solubility of styrene in the glycol. The MWs increased with conversion but deviated significantly from  $M_{n,th}$ , partly caused by grafting of PVP. The  $M_w/M_n$  values were reasonable, decreasing with increasing solubility of styrene in the glycol ( $M_w/M_n = 1.25$  at 55% conversion for tripropylene glycol), suggesting that particle formation and the resulting two-phase system results in some loss of control, possibly due to significant polymerization occurring in both the continuous and the particle phase. Addition of appropriate amounts of CSA (using tripropylene glycol) resulted in an increase in  $R_p$  while maintaining reasonable control/livingness,<sup>432</sup> consistent with results in bulk.<sup>226–229</sup>

Charleux and co-workers<sup>434</sup> reported aqueous dispersion polymerization of *N,N*-diethylacrylamide at 112 °C (pH = 10) using a poly(sodium acrylate)-SG1 macroinitiator ( $M_n = 2000$ ) as a route to temperature-responsive particles with a pH-sensitive hairy layer in an approach similar to their previous work on *ab initio* emulsion polymerization.<sup>323,324</sup> The lower critical solution temperature (LCST) of the homopolymer is 32 °C, and particle formation was proposed to occur by self-assembly of the amphiphilic block copolymer formed *in situ*. Cross-linked particles were also synthesized



Scheme 22



using this approach with the cross-linker *N,N'*-methylene bisacrylamide ( $d = 49\text{--}188\text{ nm}$  at  $15\text{ }^\circ\text{C}$ ).

SG1-mediated dispersion polymerizations of styrene (20% (w/v)) in  $\text{scCO}_2$  at  $110\text{ }^\circ\text{C}$  were carried out by Okubo and co-workers using a PDMS based azo initiator as inistab (Scheme 22),<sup>411</sup> which is a species that fulfills both roles of initiator and stabilizer. In the presence of sufficient amounts of inistab, the polymerizations proceeded to high conversion to yield the polymeric product as a powder. Although the MWDs were broad in many cases,  $M_n$  increasing close to linearly with conversion with  $M_n \approx M_{n,\text{th}}$ , as well as successful chain extensions, indicated high livingness. The broad MWDs were most likely caused by initiating species growing from one or both ends (the azo initiator contained approximately eight azo moieties per molecule). The particles ( $d = 2\text{--}10\text{ }\mu\text{m}$ ) were highly nonspherical, possibly indicating imperfect stabilization and significant coagulation. The fact that a significant number of chains would grow from both ends leads to polymer where both ends would be anchored to the particle, while the middle part of the chain extends into the  $\text{scCO}_2$ . This may lead to a reduced thickness of the colloidal protective layer and less effective stabilization. The morphology may also be affected by  $\text{CO}_2$  removal, because the particles swell to a highly plasticized state in  $\text{scCO}_2$ . Moreover, the high temperature and the relatively low MWs may result in particle formation on cooling, causing broad particle size distributions.<sup>419,421</sup>

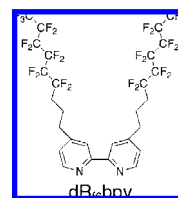
SG1-mediated dispersion polymerizations of styrene (20% (w/v)) in  $\text{scCO}_2$  at  $110\text{ }^\circ\text{C}$  were also conducted using an alkoxyamine inistab (PDMS-*b*-PS-SG1) as initiator and stabilizer in the presence of 100% excess free SG1,<sup>409</sup> giving good control/livingness ( $M_w/M_n = 1.36$ ) and  $d_n \approx 132\text{ nm}$  at 60% conversion. The inistab approach is attractive because it alleviates the need for expensive stabilizers, and the stabilizer is covalently linked to the particle, leading to robust stabilization.

SG1-mediated dispersion polymerization of styrene in  $\text{scCO}_2$  has also been performed successfully to high conversion using a PDMS-*b*-PMMA stabilizer and AIBN at  $110\text{ }^\circ\text{C}$ ,<sup>108</sup> resulting in  $M_w/M_n = 1.12\text{--}1.43$  and  $M_n \approx M_{n,\text{th}}$ . The polymer was recovered as a powder at 85% conversion ( $d_n = 147\text{ nm}$ ). A large excess of free SG1 was required to obtain satisfactory control, as in the corresponding precipitation polymerization.<sup>109</sup>  $J_{\text{crit}}$  at 40% styrene loading (w/v) was determined as 28 (corresponding to 8% conversion). Polymerizations conducted in toluene under otherwise the same conditions proceeded at a similar rate (approximately 20% faster) to those in  $\text{scCO}_2$ . The number of chains increased with conversion in both the dispersion and solution polymerizations, with a somewhat greater increase in dispersion, tentatively ascribed to chain transfer to monomer (or the Diels–Alder dimer).<sup>79,108</sup>

### 2.7.3. ATRP

**2.7.3.1. Precipitation ATRP.** DeSimone and co-workers<sup>413</sup> carried out precipitation ATRP of MMA in  $\text{scCO}_2$  at  $85\text{ }^\circ\text{C}$  using methyl 2-bromopropionate/CuCl/Cu(0) and the ligand dR<sub>6</sub>bpy (Scheme 23), specifically chosen for its high

Scheme 23



solubility in  $\text{CO}_2$ . Cu(0) was added to increase  $R_p$  (Cu(0) reduces Cu(II) to Cu(I)<sup>431</sup>). However, the conversion did not increase beyond 55%. Similar difficulties in reaching high conversion have been encountered in conventional (nonliving) precipitation polymerization of styrene in  $\text{scCO}_2$  at  $65\text{ }^\circ\text{C}$ .<sup>430,431</sup>

**2.7.3.2. Dispersion ATRP.** DeSimone and co-workers<sup>413</sup> carried out dispersion ATRP of MMA in  $\text{scCO}_2$  at  $85\text{ }^\circ\text{C}$  with methyl 2-bromopropionate/CuCl/Cu(0)/dR<sub>6</sub>bpy, employing poly(1,1-dihydroperfluorooctyl acrylate) as stabilizer. High conversion was reached, and the polymer was collected as a free flowing powder after venting of the  $\text{CO}_2$ . Reasonable control/livingness was obtained with  $M_n \approx M_{n,\text{th}}$  and  $M_w/M_n = 1.41$ .

Okubo and co-workers<sup>410</sup> used a bromo-terminated PDMS macroinitiator ( $M_n = 6200$ ;  $M_w/M_n = 1.06$ ) as inistab in dispersion ATRP of MMA in  $\text{scCO}_2$  at  $65\text{ }^\circ\text{C}$ . Polymer was recovered as a powder at high conversion (>90%) with good control/livingness ( $d = 300$  and  $558\text{ nm}$  for 10 and 5 wt % inistab relative to MMA, respectively). In contrast to the conventional dispersion polymerization of MMA in  $\text{scCO}_2$  using a PDMS macroazoinitiator<sup>435</sup> (as well as in conventional dispersion polymerization of vinyl monomers in organic solvents in the absence of cross-linker,<sup>115,116</sup> and various dispersion CLRP<sub>s</sub><sup>412,417,420,421,426,432,433,436</sup>), the particles were nonspherical. Similar nonspherical, but larger ( $d = 2\text{--}10\text{ }\mu\text{m}$ ), particles were obtained in the dispersion NMP of styrene in  $\text{scCO}_2$  employing a PDMS-based azoinitiator.<sup>411</sup> Such an irregular particle shape may be related to poor stabilization and subsequent coagulation, and may also be affected by the venting of  $\text{CO}_2$  (the particles would be swollen by  $\text{CO}_2$ ). As anticipated based on the PDMS-*b*-PMMA structure and the solubility of the PDMS segment in  $\text{CO}_2$ , the particles had core-shell morphology, with a PDMS shell and a PMMA core. The interior of the particles exhibited a sea-island morphology with PDMS domains imbedded in a PMMA matrix, most likely resulting from coagulation of small polymer particles at the early stage of the polymerization.

Wan and Pan<sup>423</sup> carried out dispersion ATRP of 4-vinylpyridine in ethanol/water using [poly(ethylene glycol) methyl ether] 2-bromoisobutyrate as inistab (CuBr/PMDETA/ $60\text{ }^\circ\text{C}$ ) with very good control/livingness, yielding particles with  $d \approx 30\text{ nm}$  and relatively narrow particle size distribution. Nucleation was proposed to proceed via formation of micelles involving the *in situ* formed diblock copolymer. The limiting conversion appeared to be as low as <60%, possibly related to unfavorable monomer partitioning between the particles and the continuous phase. Cross-linked particles were also prepared with the cross-linker *N,N'*-methylene bisacrylamide.

Min and Matyjaszewski<sup>414</sup> performed dispersion ATRP (ligand TPMA) of styrene in ethanol at  $70\text{ }^\circ\text{C}$  with PVP and Triton X-305, focusing on achieving a narrow particle size distribution. Direct ATRP (EBiB) and reverse ATRP (AIBN) both resulted in broad particle size distributions. However,

the “two-stage” approach<sup>415–417</sup> using reverse ATRP, whereby  $\text{CuBr}_2/\text{TPMA}$  was added at 3% conversion, resulted in narrow particle size distributions. The MWDs indicated livingness but were relatively broad with  $M_w/M_n = 1.6$  at approximately 90% conversion. This two-stage technique was also applied to a cross-linking system by adding both DVB and  $\text{CuBr}_2/\text{TPMA}$ .

## 2.7.4. RAFT

**2.7.4.1. RAFT Dispersion Polymerization.** RAFT dispersion polymerization has been reported using ethanol/water,<sup>417</sup> ethanol,<sup>426,427</sup> cyclohexane,<sup>428</sup> isodecane,<sup>425</sup> and  $\text{scCO}_2$ .<sup>408,412</sup>

Song and Winnik<sup>417</sup> carried out RAFT dispersion polymerization of styrene in ethanol/water (95/5) at 70 °C using PVP and Triton X-305 (octylphenol ethoxylate), the RAFT agent CMPDB, and the azoinitiator V-59 according to the two-stage method.<sup>415,417</sup> Addition of the RAFT agent at the beginning of the polymerization causes a significant decrease in MW, and the polymer chains thus remain in solution to much higher conversion than without the RAFT agent, delaying the nucleation process, which leads to broader particle size distributions. Moreover, particle formation may occur on cooling, as a significant fraction of chains remain in solution due to the low MWs. Stable particles of very narrow size distribution were obtained, and  $M_n$  increased linearly with conversion with  $M_w/M_n < 1.5$ . However, the polymerizations were only taken to approximately 40% conversion.

RAFT dispersion polymerization of styrene has also been carried out by Choe and co-workers<sup>426,427</sup> using AIBN/*t*-BDB/ethanol/PVP at 50–70 °C. Addition of all ingredients at time zero resulted in poor colloidal stability, whereas the two-stage strategy resulted in stable particles ( $d \approx 2 \mu\text{m}$ ) and narrow particle size distribution. Good control/livingness could however only be obtained when relatively low MWs were targeted ( $M_n \approx 6000$  at 50% conversion). RAFT dispersion photopolymerization of styrene in ethanol using PVP has also been carried out, but the level of control was poor and the particle size distributions were broad.<sup>436</sup>

Howdle and co-workers<sup>408,412</sup> carried out RAFT dispersion polymerization of MMA in  $\text{scCO}_2$  at 65 °C with various low MW RAFT agents, AIBN, and a PDMS stabilizer, without employing the two-stage strategy. High MW, good control/livingness, and colloidal stability ( $d \approx 1\text{--}2 \mu\text{m}$ ) were achieved, but the particle size distributions were relatively broad. Block copolymer synthesis was demonstrated by subsequent addition of styrene and AIBN to the reactor.

A number of RAFT dispersion polymerizations have been reported to proceed via self-assembly of diblock copolymers formed *in situ*. Zheng and Pan<sup>428</sup> reported RAFT dispersion polymerization of 4-vinylpyridine in cyclohexane using a PS-RAFT agent. Save and Charleux and co-workers<sup>425</sup> performed dispersion polymerization of MA in isodecane at 80 °C using a poly(2-ethylhexyl acrylate) RAFT agent based on DTB and TTC. Good control/livingness was obtained with

Scheme 24

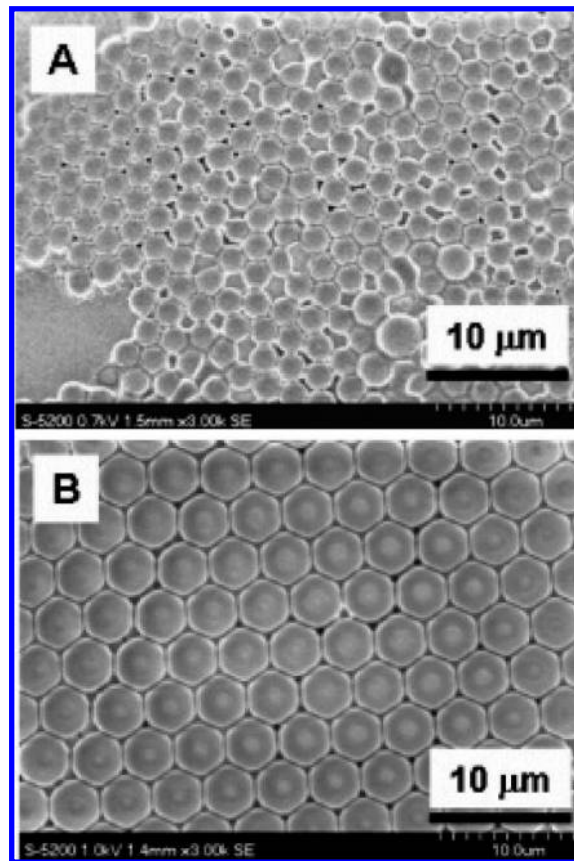
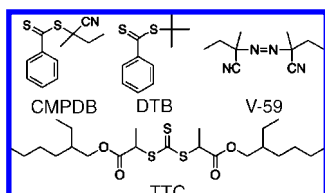


**Figure 11.** SEM images of PS particles prepared by dispersion ITP (2 wt %  $\text{C}_6\text{F}_{13}\text{I}$  based on total styrene) in ethanol at 70 °C by the two-stage method at different reaction times: (A) 3 and (B) 24 h. Reprinted with permission from ref 417. Copyright 2006 American Chemical Society.

TTC ( $d = 30\text{--}50 \text{ nm}$ ) but not with DTB (despite the latter performing well in bulk), which is speculated to be related to the partitioning characteristics of the propagating radicals. Bathfield et al.<sup>424</sup> carried out dispersion polymerizations of *n*BA in ethanol/water at 70 °C with hydrophilic poly(*N*-acryloylmorpholine) RAFT agents as stabilizers, including use of an end-functionalized (carbohydrate derivative) polymeric RAFT agent, with the ultimate goal being synthesis of particles with a functionalized surface. Approximately half of the chains were estimated to be block copolymer, resulting in hairy particles of  $d \approx 100\text{--}300 \text{ nm}$ .

## 2.7.5. Dispersion ITP

Song and Winnik<sup>417</sup> performed dispersion ITP of styrene in ethanol and ethanol/water at 70 °C using PVP and Triton X-305 and 2,2'-azobis(2-methylbutyronitrile), employing both a one stage process and the two-stage method. Using a one stage process in ethanol, the particle size increased on addition of the chain transfer agent  $\text{C}_6\text{F}_{13}\text{I}$ , and the particle size distribution became broader, similar to earlier work using  $\text{CBr}_4$  as transfer agent.<sup>437</sup> The nucleation stage was prolonged on addition of  $\text{C}_6\text{F}_{13}\text{I}$ . The two-stage process led to a narrower particle size distribution, but still broader than that in the absence of  $\text{C}_6\text{F}_{13}\text{I}$  (Figure 11). The control/livingness was relatively poor in these polymerizations. Polymerizations were subsequently carried out in ethanol/water (95/5) according to the two-stage method, resulting in monodisperse particles.  $J_{\text{crit}}$  is lower in the more polar ethanol/water than in ethanol, and the reduction in the length of the nucleation

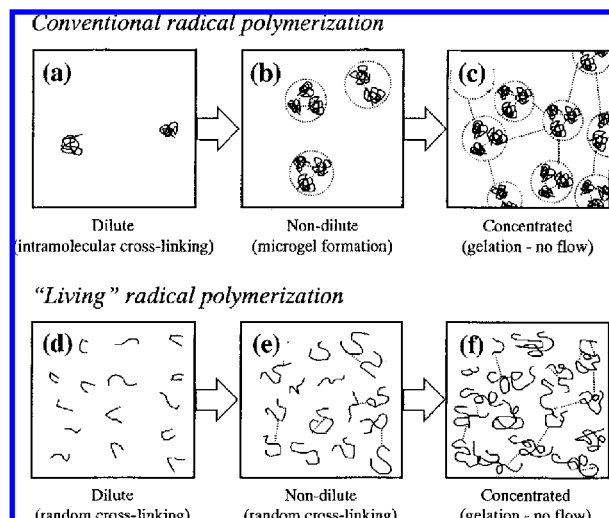


**Figure 12.** Schematic representation of cross-linking processes in conventional (a–c) and controlled/living (d–f) radical polymerizations in bulk/solution. Reprinted with permission from ref 439. Copyright 1999 American Chemical Society.

stage favors formation of monodisperse particles.  $M_n$  increased close to linearly with conversion to 80% conversion and  $M_w/M_n \approx 2$  (the relatively high  $M_w/M_n$  is intrinsic to ITP<sup>11</sup>).

### 3. Cross-linking CLRP in Dispersed Systems

#### 3.1. General Considerations

The pioneering work in cross-linking CLRP was done by Ide and Fukuda,<sup>438,439</sup> who demonstrated that cross-linking CLRP proceeds fundamentally differently from its linear counterpart (Figure 12). Their studies of the TEMPO-mediated radical cross-linking copolymerization of styrene and 4,4'-divinylbiphenyl in bulk revealed that the apparent pendant reactivity (i.e., the apparent reactivity of the second unsaturation of 4,4'-divinylbiphenyl as incorporated into the polymer) is considerably lower than that in the corresponding nonliving system. The origin lies in the different primary chain lengths (a primary chain is the imaginary linear chain resulting from breaking all cross-links connected to it). The primary chain length in CLRP is typically much lower than that in a nonliving system. As a consequence, the local concentration of pendant unsaturations around the radical center is lower in CLRP, and thus the apparent reaction rate of pendant unsaturations is lower. In a typical nonliving system, intramolecular cross-linking dominates at low conversion.<sup>440,441</sup> This local concentration effect is much weaker in CLRP, resulting in more homogeneous networks without microgels, higher swelling, and different mechanical properties.<sup>439,442</sup> Similar results have been observed for ATRP<sup>443,444</sup> and RAFT<sup>445</sup> of various cross-linking systems.

The primary chains grow over the entire polymerization in cross-linking CLRP. On the other hand, in a nonliving cross-linking radical polymerization, primary chains are initiated throughout the polymerization and usually reach their final length (i.e., terminate) within a few seconds. In cross-linking CLRP, the primary chains can often be identified as a narrow peak located in the low MW region, with the cross-linked/branched polymer chains appearing as a high MW shoulder,<sup>446,447</sup> as illustrated in Figure 13 for the

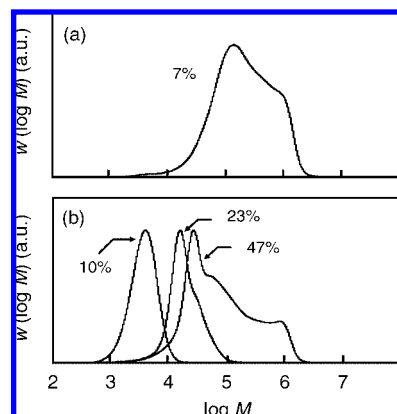


**Figure 13.** MWDs of aqueous microemulsion copolymerizations of styrene (99 mol %) and DVB (1 mol %): (a) Conventional radical polymerization at 70 °C with  $[BPO]_0 = 0.013$  M; (b) NMP at 125 °C with  $[BPO]_0 = 0.013$  M and  $[TEMPO]_0 = 0.022$  M. Conversions as indicated. Reprinted with permission from ref 442. Copyright 2007 Elsevier Ltd.

TEMPO-mediated copolymerization of styrene/DVB in microemulsion and the corresponding nonliving copolymerization.<sup>442</sup>

Nonliving radical cross-linking polymerization in dispersed systems has been studied fairly extensively,<sup>448–452</sup> but there are few examples of direct comparisons with bulk/solution in terms of pendant reactivities and gel formation. Experimental and theoretical work by Tobita et al.<sup>453–457</sup> on conventional radical copolymerization of mono- and divinyl compounds has clarified that the network development is entirely different in emulsion polymerization compared to bulk. At low and intermediate conversions (interval II), the cross-link density is higher in emulsion than in bulk as a result of the polymer concentration in the polymer particles being higher than that in bulk at the same conversion. In addition, the “limited space effect” restricts the maximum MW to that of all polymer in one particle and significantly influences the cross-linking process as manifested in  $M_w$  increasing linearly with conversion in some cases.<sup>453,456,457</sup>

Cross-linking CLRP in dispersed systems has been reported for NMP,<sup>221–223,434,442</sup> ATRP,<sup>262,269,270,414,423,458–460</sup> RAFT,<sup>428,461</sup> and ITP.<sup>402</sup>

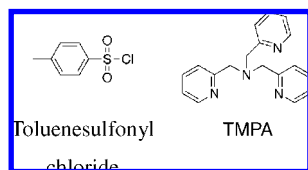
#### 3.2. Cross-linking NMP

Cross-linking NMP of styrene (99 mol %) and DVB (1 mol %) using a PS-TEMPO macroinitiator in aqueous miniemulsion at 125 °C with SDBS proceeds very differently compared to the corresponding bulk system.<sup>221,222</sup> In the monomer conversion range 0–60% (all polymer soluble in THF), the pendant conversions were lower in miniemulsion than in bulk. Moreover, a marked dependence on particle size was revealed; an increase in  $d$  from 50 to 600 nm resulted in a significant decrease in pendant conversion. Remarkably, for  $d = 600$  nm, the pendant conversion was zero at as high as 30% monomer conversion.

The interface between the aqueous and the organic phases is believed to influence the miniemulsion polymerization process.<sup>222</sup> Concentration gradients within the particles affect the [monomer]/[pendant unsaturation] ratio and therefore also the MWD, because it would change the rate of monomer addition relative to the rate of reaction of pendant unsaturations. Moreover, the mobility of polymeric species located



Scheme 25



near the interface<sup>462</sup> or adsorbed at the interface may be reduced, thus affecting pendant reactivity. PDVB migrates to the interface of toluene droplets in an aqueous emulsion, with the driving force being lowering of the interfacial tension. This migration is accelerated by the presence of a hydrophobic nonsolvent such as linear PS or hexadecane. This would cause the [monomer]/[pendant unsaturation] ratio to decrease near the interface, resulting in an increase in the relative rate of reaction of pendant unsaturations. This migration to the interface forms the basis of the SaPSeP method for preparation of hollow polymer particles,<sup>463–465</sup> as well as other similar methods.<sup>466,467</sup> Consistent with the above, miniemulsion polymerizations in the presence of 30 wt % of tetradecane resulted in an increase in pendant conversions, reflected in the appearance of a pronounced high MW peak ( $MW = 10^5$ – $10^6$ ).<sup>222</sup> The rate of gel formation relative to monomer conversion was the same in miniemulsion and solution when the organic phase contained 6 vol % tetradecane and 48 vol % toluene. However, at 54 vol % tetradecane and no toluene, the conversion at the gel-point was lower in miniemulsion than in solution, consistent with enhanced apparent pendant reactivity in miniemulsion in the presence of tetradecane.<sup>223</sup>

Okubo and co-workers<sup>442</sup> reported the compressive strengths as functions of conversion of micron-sized, cross-linked P(S-DVB) particles prepared by conventional radical copolymerization and TEMPO-mediated radical copolymerization in aqueous microsuspension, which indicated that network formation is more homogeneous in the NMP system than in the conventional system.

Charleux and co-workers<sup>434</sup> reported aqueous dispersion cross-linking polymerization of *N,N*-diethylacrylamide/*N,N'*-methylene bisacrylamide at 112 °C (pH = 10) employing a poly(sodium acrylate)-SG1 macroinitiator ( $M_n = 2000$ ) to prepare hairy, surfactant-free microgel particles. In a first approach, all cross-linker was added at the initial stage, but macrogelation occurred for cross-linker contents above 3 mol %. This problem was overcome by use of the two-stage approach, whereby the cross-linker was added after the nucleation step, resulting in polymer particles with  $d \approx 100$  nm. The particle nucleation step was proposed to proceed via self-assembly of the amphiphilic block copolymer formed *in situ*.

### 3.3. Cross-linking ATRP

Ali and Stover carried out cross-linking suspension ATRP of MMA/poly(ethylene glycol monomethyl ether) methacrylate/diethylene glycol dimethacrylate (toluenesulfonyl chloride (Scheme 25)/CuBr/dNbpy2/70 °C) with the objective of preparing microcapsules containing polar oil (section 4.3).<sup>458,459</sup> Hollow particles were indeed obtained, despite the corresponding conventional polymerization yielding matrix particles. Gelation is delayed in cross-linking CLRP compared to in a conventional system, thus allowing time for phase separation to occur, which is a requirement for formation of such hollow particles. The same technique was

also successfully applied to MMA/poly(ethylene glycol) monomethacrylate/diethylene glycol dimethacrylate.

Wan and Pen<sup>423</sup> reported cross-linking dispersion ATRP of 4-vinylpyridine/*N,N'*-methylenebisacrylamide in ethanol/water using [poly(ethylene glycol) methyl ether] 2-bromoisobutyrate as inistab (CuBr/PMDETA/60 °C). The polymerization was proposed to proceed via *in situ* block copolymer formation and subsequent self-assembly into micelles, which were eventually cross-linked to yield  $d \approx 30$  nm.

Min and Matyjaszewski<sup>414</sup> prepared cross-linked styrene/DVB particles by reverse ATRP in a dispersion using ethanol as the continuous phase (CuBr<sub>2</sub>/AIBN/TPMA/PVP/Triton X-305), focusing on achieving a narrow particle size distribution. To this end, the two-stage approach<sup>415–417</sup> was employed, whereby both CuBr<sub>2</sub>/TPMA and DVB were added after completion of the nucleation stage, resulting in spherical, monodisperse cross-linked particles.

Matyjaszewski and co-workers<sup>262</sup> prepared cross-linked hydrophilic polymer particles using inverse miniemulsion AGET ATRP (CuBr<sub>2</sub>/TPMA/ascorbic acid/Span 80/30 °C) of oligo(ethylene glycol) monomethyl ether methacrylate in the presence of a cross-linking agent based on a disulfide-functionalized dimethacrylate, employing a water-soluble poly(ethylene glycol) functionalized bromoisobutyrate as initiator with cyclohexane as the continuous phase. The cross-linking agent was chosen for its ability to decompose in a reducing environment, thus making the particles promising candidates for drug delivery scaffolds. The obtained particles were insoluble with  $d = 260$  nm and a fairly broad particle size distribution. The swelling ratios in organic solvents were significantly greater than those for the corresponding particles prepared by conventional radical polymerization, demonstrating the increased network homogeneity obtained by CLRP.<sup>438,439,443</sup> Matyjaszewski and co-workers<sup>269,270</sup> have further investigated similar cross-linked hydrophilic polymer particles for drug delivery applications.

### 3.4. Cross-Linking RAFT Polymerization

Only limited work exists on cross-linking polymerization via RAFT in dispersed systems. Chan et al.<sup>461</sup> prepared cross-linked PnBA particles for drug delivery applications by dispersion polymerization in ethanol/triethyl amine at 65 °C using CDB, the cross-linker ethylene glycol dimethacrylate, and an acid-cleavable bisacrylate acetal cross-linker. A bimodal particle size distribution was obtained, with >90% of the particles with  $d \approx 150$ –500 nm, with the remainder being micron-sized particles. Zheng and Pan<sup>428</sup> reported RAFT dispersion polymerization of 4-vinylpyridine/DVB in cyclohexane using a PS-RAFT agent. Similar to the work of Wan and Pen,<sup>423</sup> the data were consistent with self-assembly of the *in situ* formed diblock copolymers, resulting in the formation of a PS shell and poly(4-vinylpyridine-*co*-DVB) core microphase separated particles with  $d < 50$  nm.

### 3.5. Cross-Linking ITP

Iodide-mediated copolymerization of vinylidene fluoride and the diene  $CH_2=CH-(CF_2)_6-CH=CH_2$  has been carried out in microemulsion using Galden ammonium carboxylate as emulsifier, and bifunctional iodine chain transfer agents of the type  $I-(CF_2)_n-I$  ( $n = 4$ –8).<sup>402</sup> The resulting MWDs

clearly revealed the presence of linear primary chains as well as branched/cross-linked high MW polymer.

## 4. Particle Morphology

### 4.1. General Considerations

Particle morphology is an important particle characteristic which can exert strong influence on physical properties and is therefore of great importance with regard to applications.<sup>468–473</sup> Various techniques are available for synthesis of polymer particles with domains of differing composition as well as a range of particle shapes.<sup>468–470,474–477</sup> In general, the particle morphology in composite polymer particles comprising a mixture of homopolymers, copolymer, or terpolymer develops as a result of macro- or microphase separation. The morphology is dictated by a number of factors such as thermodynamics, polymerization kinetics, as well as diffusion rates of both monomer and polymer. The morphology can be classified as thermodynamically<sup>478–482</sup> or kinetically<sup>483–486</sup> controlled. Thermodynamic factors favor the morphology with the lowest free energy, whereas the kinetically controlled morphology is that obtained when the kinetics of the system prevent the equilibrium morphology from being attained (e.g., high viscosity leading to low diffusion rates). With respect to morphology, two important differences between CLRP and conventional radical polymerization are that the MWs are generally much lower in CLRP and the time taken for a chain to reach its final MW is much longer in CLRP. In general terms, this favors thermodynamically stable morphologies vs kinetically controlled morphologies for CLRP.

The main attraction of CLRP has to date been the ability to prepare polymer of controlled MWs, narrow MWDs, block copolymers, as well as more complex architectures previously not accessible via radical polymerization. However, the use of CLRP also opens up new ways of controlling particle morphology, making novel particle morphologies accessible, e.g. core–shell particles comprising block copolymer where the core and the shell are covalently linked. One of the key aspects is the effect of block copolymers on particle morphology as compatibilizers. The presence of block copolymer can reduce the interfacial free energy between different polymer domains, thereby significantly changing the thermodynamically stable morphology and also altering the morphology development under kinetic control. Very recently, control of particle morphology by use of CLRP has led to new means of preparing novel core–shell particles,<sup>147,311,331,332,357,376,410,434,487,488</sup> microcapsules/hollow particles,<sup>458,460,489–493</sup> as well as multilayered particles,<sup>250,494,495</sup> in many cases directly related to block copolymer formation by CLRP. In addition to the areas described below, CLRP also finds extensive use in synthesis of hairy particles by surface-initiated polymerization using seed particles (beyond the scope of the present review).

### 4.2. Core–Shell Particles

In conventional radical polymerization, core–shell particles are traditionally prepared by seeded polymerizations, where the seed particles form the core and the second stage monomer forms the shell under conditions of kinetic control. The core and the shell are not covalently linked but are composed of different polymer chains. CLRP enables preparation of core–shell particles where the core and the shell are covalently linked, which may lead to improved

control over the core–shell morphology and possibly access to novel morphologies. The fact that the polymer constituting the shell is covalently linked to the polymer of the core may make it possible to prepare novel core–shell particles, for example where the shell comprises very hydrophilic polymer such as PAA.

Such morphology control by CLRP can be achieved based on *in situ* generation of amphiphilic diblock copolymers which subsequently partake in nucleation via self-assembly (*ab initio* emulsion polymerization)<sup>311,331,332</sup> or homogeneous nucleation (dispersion<sup>410,434</sup> and emulsion<sup>376</sup> polymerization). Core–shell particles of PAA-*b*-PnBA-*b*-PS ( $d \approx 50$  nm) were prepared by Gilbert and co-workers utilizing RAFT *ab initio* emulsion polymerization via self-assembly using consecutive feeds of *n*BA and styrene;<sup>311,331,332</sup> that is, the second monomer forms the core, unlike in a conventional seeded emulsion polymerization (under kinetic morphology control). Most polymer chains stretched from the aqueous phase through the shell and to the core of the particle, although some hydrophilic chain ends were buried within the particle (i.e., the particles were larger than predicted based on all chains being anchored at the oil–water interface).<sup>311</sup> Such core–shell particles would also be accessible via NMP using the technique developed by Charleux and co-workers,<sup>323,324</sup> which relies on self-assembly of SG1-terminated poly(sodium acrylate)-based amphiphilic diblock copolymer. The idea of utilizing CLRP to control particle morphology by use of living chains containing a hydrophilic moiety at the  $\alpha$ -end, whereby chains would grow from the particle interface toward the core, was also discussed by Charleux and co-workers with regard to miniemulsion systems.<sup>143</sup> Okubo and co-workers<sup>410</sup> prepared PDMS-*b*-PMMA core–shell particles consisting of a PDMS-shell and a PMMA core by use of dispersion ATRP in supercritical CO<sub>2</sub>.

Core–shell particles where the core is covalently bonded to the shell can also be prepared by seeded emulsion polymerization<sup>147,355</sup> where the second stage monomer forms the shell as part of a diblock copolymer. For example, RAFT emulsion polymerization of styrene and subsequent seeded emulsion RAFT copolymerization of *n*BA and AAEMA utilizing starved feed monomer addition resulted in the formation of PS-*b*-P(*n*BA-*co*-AAEMA) particles exhibiting a core–shell structure (core-PS/shell-P(*n*BA-*co*-AAEMA)).<sup>147</sup> In further work,<sup>355</sup> PS-*b*-PnBA-*b*-PAAEMA and PS-*b*-PAAEMA-*b*-PnBA particles were prepared utilizing the same technique. During film formation using the thus obtained particles, AAEMA units react with an added diamine, leading to cross-links. The mechanical properties of the films were superior to those of the corresponding films based on polymer blends. Moreover, the mechanical properties could to some extent be controlled by the location of AAEMA (i.e., via the nature of the block copolymer), providing a means to control of the film properties for a specific application.

### 4.3. Hollow Particles

Hollow polymer particles (nanocapsules) find various applications such as in microencapsulation and drug delivery, and as opacifiers and impact modifiers. A variety of methods based on conventional radical polymerization are available for their synthesis, e.g. osmotic swelling based methods (stepwise alkali/acid method,<sup>496–498</sup> alkali/cooling method<sup>499–501</sup>), phase separation between liquid-core and polymer-shell (e.g., SaPSeP method<sup>463–465</sup>),<sup>466,467</sup> treatment after formation of

core-shell particles (extraction or calcination of core material), and interfacial polymerization.<sup>470</sup>

RAFT miniemulsion polymerization using KPS and the RAFT agent CDB (which does not induce retardation) to prepare PS nanocapsules with liquid cores (isooctane;  $d < 100$  nm) was reported by Klumperman and co-workers.<sup>493</sup> Polymerization mainly occurs at the interphase due to anchoring of negatively charged KPS-derived end groups, resulting in the formation of a polymer shell. Solid particles were however also formed, presumably due to secondary nucleation. The use of AIBN does not lead to hollow particles, because the generated oligomer radicals do not exhibit surface activity. The choice of RAFT agent is also important—the use of a RAFT agent that causes retardation (PPDPA) and KPS resulted in formation of solid particles. This was postulated to be related to a slower increase in viscosity, thus allowing diffusion of radicals having undergone chain transfer (and thus not containing a KPS-derived end group) toward the core of the particle.

Luo and co-workers<sup>489–492</sup> further developed the above approach into interfacially confined CLRP in miniemulsion, which involves the use of a surface active RAFT agent that operates as control agent and surfactant. Colloidally stable, submicron-sized hollow particles containing nonadecane as core material were prepared by miniemulsion RAFT polymerization of styrene using KPS and ammonolyzed P(S-MAn)-*b*-PS oligomer in the absence of additional surfactant.<sup>491,492</sup> Addition of entering radicals to the initial RAFT agent at the oil/water interface would generate amphiphilic P(S-MAn)-*b*-PS oligomer radicals that are anchored at the interface, confining polymerization to the interfacial region generating a shell. The final emulsion included approximately 8 wt % solid particles.<sup>491</sup> If the extent of ammonolysis is too high (i.e., too hydrophilic RAFT agent), solid particles are formed due to homogeneous nucleation in the aqueous phase. Fine-tuning of the hydrophilicity via the extent of ammonolysis as well as using SDS as cosurfactant resulted in improvements in both the yield and morphology (more well-defined) of the hollow particles.<sup>492</sup> Further improvements in terms of a more narrow particle size distribution and uniform shell thickness ( $d \approx 112$  nm; shell thickness  $\approx 20$  nm) were reported by use of miniemulsion RAFT polymerization of styrene with hexadecane as core material with PAA-*b*-PS oligomer as surfactant and RAFT agent and SDS as cosurfactant (Figure 14).<sup>490</sup> Interfacially confined RAFT miniemulsion polymerization is an attractive technique for synthesis of hollow particles, as it offers flexibility with regard to design (shell thickness, functionalization of the surface), is highly efficient, proceeds in one single step, and is environmentally friendly.

One of the most well-known techniques for preparation of hollow particles involves phase separation between cross-linked polymer and hydrophobic core liquid during polymerization.<sup>463–467</sup> Phase separation has to occur at relatively low conversion for formation of the hollow structure, because otherwise the polymer will not have sufficient mobility to diffuse to and adsorb at the interface. Ali and Stöver developed an ATRP-based methodology for synthesis of hollow particles containing a relative polar solvent, not readily accessible using conventional radical polymerization.<sup>458,460</sup> Solution ATRP of MMA and poly(ethylene glycol monomethyl ether) methacrylate was carried out in diphenyl ether (toluenesulfonyl chloride/CuBr/dNbpy2/70 °C) to  $M_n \approx 2500$ , diethylene glycol dimethacrylate was added, and

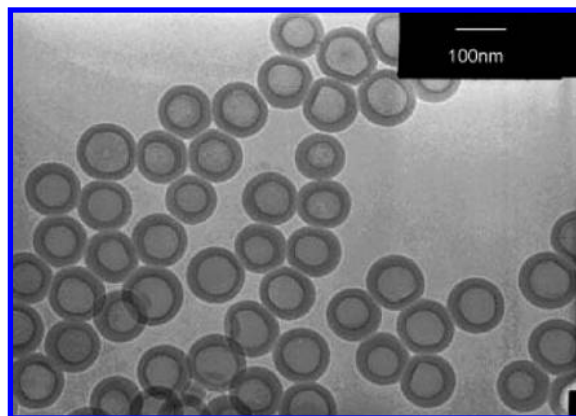


**Figure 14.** TEM image of hollow PS particles containing hexadecane (after centrifugal removal of solid particles) prepared by interfacially confined RAFT polymerization in miniemulsion using PAA-*b*-PS oligomer as surfactant and RAFT agent employing SDS as cosurfactant at 68 °C. Reprinted with permission from ref 490. Copyright 2007 Wiley-VCH Verlag GmbH & Co.

the solution was mixed with water to yield a suspension. Subsequent suspension ATRP resulted in multihollow and hollow particles, whereas matrix particles were formed in the corresponding conventional radical polymerization. In this case, core-shell particles form if thermodynamically favored, provided there is sufficient time for thermodynamic equilibrium to be attained. If cross-linking is too fast, the cross-linked polymer is trapped inside the particle and unable to migrate to the interface. The apparent pendant reactivity in cross-linking CLRP is lower than that in a conventional system (section 3.1), and the resulting delay in gelation allows time for thermodynamic equilibrium to be reached. The same ATRP approach was also applied to MMA/poly(ethylene glycol) monomethacrylate/diethylene glycol dimethacrylate, where the distinct difference compared to the above work lies in the preferential partitioning of poly(ethylene glycol) monomethacrylate to the aqueous phase, resulting in some interfacial nature of the polymerization.<sup>460</sup> Less poly(ethylene glycol) monomethacrylate (the polar component which imparts interfacial activity on the polymer) was required for formation of hollow particles than in conventional radical polymerization, consistent with earlier work.<sup>458,459</sup>

#### 4.4. Multilayered Particles

The presence of block copolymer can have a large impact on particle morphology as a result of the block copolymer acting as a compatibilizer, which increases the interfacial area between different polymer domains at thermodynamic equilibrium; that is, a phase separated morphology is formed more easily. Asua and Leiza<sup>502,503</sup> prepared PS/PMMA composite particles (1/1, w/w) by two-stage polymerization (miniemulsion and seeded emulsion) with and without SG1 as control agent (NMP) at 90 °C to investigate the effect of block copolymer formed *in situ* during the second stage polymerization of MMA. Hemispherical morphology was obtained in the absence of SG1, whereas the addition of a small amount of SG1 (i.e., a small amount of block copolymer) resulted in a slight change in the morphology within the hemispherical particles. On increasing the SG1 content, the morphology changed from hemispherical to core-shell as a result of formation of block copolymer which acts as compatibilizer, thus causing a decrease in the polymer-polymer interfacial tension, resulting in a greater



polymer–polymer interfacial area at thermodynamic equilibrium (which may or may not be reached depending on the particle viscosity).

Block copolymer particles prepared by CLRP in dispersed systems display very unique multilayered “onion”-like morphology under certain conditions.<sup>250,495</sup> In nonliving systems, block or graft polymer may be generated during seeded polymerizations of styrene with PMMA seed particles, and if the fraction of such polymer is sufficiently high, multilayered particles may form.<sup>504–506</sup> The particle morphology in systems comprising A-B block copolymers generally depends on the extent of microphase separation, which is governed by: (i) overall DP, (ii) the Flory–Huggins interaction parameter ( $\chi$ ), and (iii) the volume fraction of polymer A.<sup>506,507</sup> Under appropriate conditions (i.e., a certain block copolymer, certain volume fractions of both segments of the block copolymer, and sufficient time for phase separation), multilayered particles may be obtained by post-treatment of polymer particles prepared by seeded dispersion polymerization<sup>504–506</sup> or by evaporation of toluene from toluene droplets containing block copolymer or a mixture of block copolymer/homopolymer.<sup>481,507</sup> The formation mechanism of such a morphology is believed to be based on alternative lamination of polymers from the particle/water interface toward the center of the particle.<sup>481,506</sup> Interestingly, recent research has revealed that such particles can be prepared directly by ATRP<sup>250,494</sup> or NMP<sup>495</sup> in dispersed systems.

Seeded ATRP of styrene using PiBMA seed particles prepared by miniemulsion polymerization resulted in multilayered particles with a layer thickness of approximately 20 nm (Figure 15).<sup>250</sup> In the case of a recipe where the block copolymer at 100% conversion consists of two blocks of equal length, a sea–island morphology is obtained at low conversion where the sea is the first block (macroinitiator) and the islands are the second block, and multilayered particles are formed as the length of the second block approaches that of the first block.<sup>494</sup> In this work,<sup>250</sup> the conversion during synthesis of the first block (PiBMA) was close to 100%, and it is thus likely that a significant fraction of dead polymer was present, resulting in  $M_n > M_{n,th}$  of the block copolymer in the second step. Multilayered particles were nonetheless obtained, indicating that the block copolymer also fulfills the role of compatibilizer between the PS segments of the block copolymer and the PiBMA homopolymer (dead macroinitiator).

Charleux and co-workers<sup>495</sup> reported multilayered particles comprising diblock and triblock copolymers of various monomers prepared by miniemulsion and *ab initio* emulsion SG1-based NMP. The formation of multilayered particles was investigated considering the segregation strength during microphase separation. The degree of microphase separation depends on the segregation strength between segment A and segment B. In the case that polyA is prepared first and there is residual monomer A present during polymerization of B with polyA macroinitiator, the molar fraction of A in the resulting polyB segment affects the segregation strength. When preparing PnBA-*b*-PS particles by *ab initio* emulsion NMP (first block: PnBA), the addition of styrene at 81% nBA conversion resulted in strong microphase separation, i.e. formation of multilayered particles. However, addition of styrene at intermediate nBA conversion (55%) led to lower segregation strength and, consequently, sea–island microphase separation.

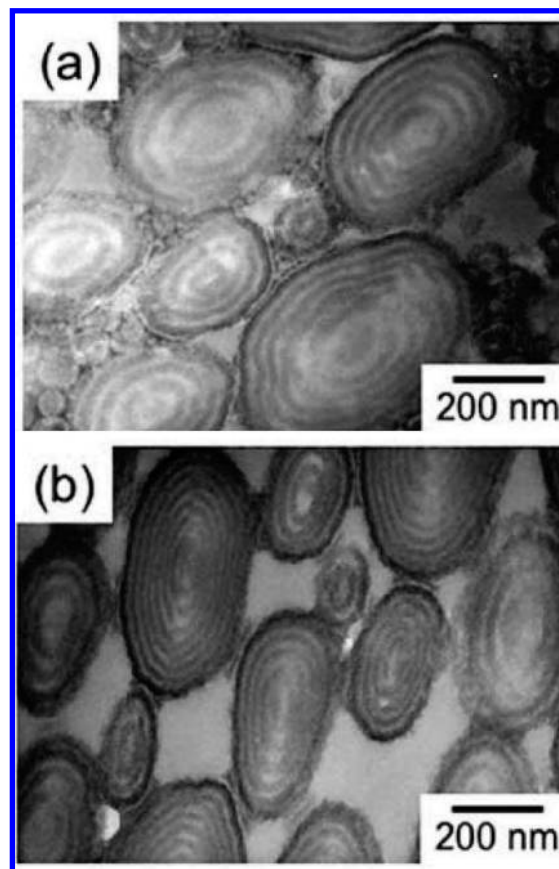


**Figure 15.** TEM images of ultrathin cross sections of PiBMA-*b*-PS particles prepared by seeded ATRP at 70 °C using PiBMA-Br particles as seeds, which were in turn prepared by miniemulsion ATRP (70 °C) with Tween 80 concentrations of 3 (a) and 6 (b) wt %. Reprinted with permission from ref 250 Copyright 2005 Elsevier Ltd.

## 5. Conclusions and Outlook

Impressive progress in CLRP in bulk/solution has been made over the past 15 years following its inception. In more recent years, great advances have also been accomplished in the field of CLRP in dispersed systems. Implementation of CLRP in the industrially important (aqueous) dispersed systems, which results in formation of polymeric nanoparticles ( $d = 20$  nm to  $10\text{ }\mu\text{m}$ ) with a wide range of applications, is crucial for future commercial success of CLRP. Moreover, in recent years, environmental concerns and legislation have given rise to “green chemistry” and created a demand for environmentally and chemically benign solvents such as water and supercritical carbon dioxide. It is now possible to perform CLRP in emulsion and miniemulsion etc. for a wide variety of systems, including the three most common techniques of NMP, ATRP, and RAFT. Significant problems have had to be overcome, however, mainly related to colloidal instability and reactant partitioning between phases. Remaining challenges with regard to implementation of CLRP in dispersed systems mainly include development of more robust *ab initio* emulsion polymerization systems. Methods based on macroinitiator self-assembly are elegant but require separate synthesis of a macroinitiator and monomer feed techniques (for ATRP and RAFT; not a requirement for NMP). Successful *ab initio* emulsion ATRP has to date only been achieved using reverse ATRP, which is associated with a number of disadvantages.

The use of CLRP for synthesis of composite polymer particles has been shown to provide a variety of new avenues for control of particle morphology and synthesis of novel particle morphologies. In the latter category, perhaps the most striking example is the synthesis of core-shell particles consisting of block copolymer such that the core and the shell are chemically linked.<sup>147,311,331,332,357,376,410,434,487,488</sup>

Other recent developments include synthesis of hollow particles<sup>458,460,489–493</sup> as well as particles with complex multilayered structures<sup>250,494,495</sup> by use of CLRP-based approaches.

Research in CLRP in dispersed systems is now beginning to shift from mere implementation of CLRP in dispersed systems to instead striving to exploit intrinsic features of dispersed systems to improve the performance of CLRP compared to that of the corresponding bulk/solution systems, as well as to prepare polymer not accessible via bulk/solution CLRP. In recent years, a number of examples have been reported where CLRP in dispersed systems behaves distinctly differently from that in bulk/solution. Examples include control/livingness to very high MW (not accessible in bulk/solution) for aqueous miniemulsion ATRP,<sup>199,255</sup> improved MWD control in precipitation NMP in supercritical carbon dioxide compared to in solution,<sup>422</sup> as well as increased polymerization rate while maintaining satisfactory control/livingness in aqueous miniemulsion NMP.<sup>185,188</sup> One of the major differences between bulk/solution and dispersed systems is that, in the latter, the polymerization proceeds in tiny confined spaces. It has been shown theoretically that such compartmentalization can lead to improved control/livingness under appropriate conditions (the confined space effect and the segregation effect<sup>156</sup>), consistent with recent experimental results.<sup>176</sup> Another example where compartmentalization is exploited is in the preparation of molecular brushes by ATRP in miniemulsion, whereby the yield can be significantly improved relative to bulk.<sup>268</sup> Future research will undoubtedly lead to numerous such discoveries with respect to polymer microstructure and morphology, which in turn is likely to enable preparation of novel polymers, nanoscale polymer particles, and nanomaterials, and in this sense the field of CLRP in dispersed systems remains in its infancy with great potential for the future.

## 6. List of Abbreviations

AA	acrylic acid
AAEMA	acetoacetoxyethyl methacrylate
Aerosol MA-80	sodium dihexyl sulfosuccinate
AGET	activators generated by electron transfer
AIBN	2,2'-azobis(isobutyronitrile)
ATRP	atom transfer radical polymerization
<i>n</i> BA	<i>n</i> -butyl acrylate
BDA	benzyl dithioacetate
BDB	benzyl dithiobenzoate
bde	bis( <i>N,N'</i> -dimethylaminoethyl) ether
BDIB	benzyl dithioisobutyrate
BDMBA	4-((benzodithioyl)methyl)benzoic acid
<i>i</i> BMA	isobutyl methacrylate
<i>n</i> BMA	<i>n</i> -butyl methacrylate
BPMODA	bis(2-pyridylmethyl)octadecylamine
BPO	benzoyl peroxide
bpy	2,2'-bipyridine
BSCTSPA	2-[[[(butylsulfanyl)carbonothioyl]sulfanyl]propanoic acid
CDB	cumyl dithiobenzoate
CLRP	controlled/living radical polymerization
CMPDB	1-cyano-1-methylpropyl dithiobenzoate

CMRP	cobalt-mediated radical polymerization
CPDB	2-cyanoprop-2-yl dithiobenzoate
CSA	camphorsulfonic acid
CTAB	cetyltrimethylammonium bromide
cmc	critical micelle concentration
<i>d</i>	particle diameter
<i>d<sub>h</sub></i>	hydrodynamic particle diameter
<i>d<sub>n</sub></i>	number-average particle diameter
<i>d<sub>w</sub></i>	weight-average particle diameter
DBTC	dibenzyltrithiocarbonate
dNbpy1	4,4'-di(5-nonyl)-2,2'-bipyridine
dNbpy2	4,4'-dinonyl-2,2'-bipyridine
Dowfax 8390	disulfonated alkyldiphenyloxide sodium salt
DP	degree of polymerization
dR <sub>16</sub> bpy	4,4'-di(tridecafluoro-1,1,2,2,3,3-hexahydroxynonyl)-2,2'-bipyridine
DT	degenerative transfer
DTAB	dodecyltrimethylammonium bromide
DTB	<i>tert</i> -butyl dithiobenzoate
EBiB	2-ethylbromoisobutyrate
ECPDB	2-(ethoxycarbonyl)propyl-2-yl dithiobenzoate
EHA <sub>6</sub> TREN	tris(2-bis(3-(2-ethylhexoxy)-3-oxopropyl)aminoethyl)amine
EHMA	2-ethylhexyl methacrylate
EEXP	ethyl-2-(ethylxanthyl)propionate
ETFEXP	ethyl-2-( <i>O</i> -trifluoroethylxanthyl)propionate
EXEB	1-( <i>O</i> -ethylxanthyl)ethylbenzene
Γ	partitioning coefficient
HD	hexadecane
HLB	hydrophilic-lipophilic balance
inistab	initiator + stabilizer
ITP	iodine transfer polymerization
<i>J<sub>crit</sub></i>	critical chain length
<i>K</i>	activation-deactivation equilibrium constant (M)
<i>k<sub>deact</sub></i>	deactivation rate coefficient (M <sup>-1</sup> s <sup>-1</sup> )
<i>k<sub>act</sub></i>	activation rate coefficient (s <sup>-1</sup> )
<i>k<sub>ex</sub></i>	degenerative chain transfer rate coefficient (M <sup>-1</sup> s <sup>-1</sup> )
<i>k<sub>i,th</sub></i>	thermal initiation rate coefficient for styrene (M <sup>-2</sup> s <sup>-1</sup> )
<i>k<sub>p</sub></i>	propagation rate coefficient (M <sup>-1</sup> s <sup>-1</sup> )
<i>k<sub>t</sub></i>	termination rate coefficient (M <sup>-1</sup> s <sup>-1</sup> )
<i>k<sub>t</sub>'</i>	cross-termination rate coefficient (M <sup>-1</sup> s <sup>-1</sup> )
KPS	potassium persulfate
<i>M<sub>n</sub></i>	number-average molecular weight (g/mol)
<i>M<sub>n,th</sub></i>	theoretical molecular weight (g/mol)
<i>M<sub>w</sub></i>	weight-average molecular weight (g/mol)
MA	methyl acrylate
MADIX	macromolecular design via the interchange of xanthates
MA <sub>n</sub>	maleic anhydride
Me <sub>6</sub> TREN	tris(2-(dimethylamino)ethyl)amine
MMA	methyl methacrylate
MONAMS	SG1-based alkoxyamine
MW	molecular weight
MWD	molecular weight distribution
<i>N<sub>A</sub></i>	Avogadro's number
<i>N<sub>cycles</sub></i>	number of activation-deactivation cycles
NMP	nitroxide-mediated radical polymerization
OEOMA	oligo(ethylene glycol) monomethyl ether methacrylate
OH-EBiB	2-hydroxyethyl 2-bromoisobutyrate
P <sup>•</sup>	propagation radical
PAA	poly(acrylic acid)
PAAEMA	poly(acetoacetoxyethyl methacrylate)
P <sub>n</sub> BA	poly( <i>n</i> -butyl acrylate)
P <sub>i</sub> BMA	poly(isobutyl methacrylate)
P <sub>n</sub> BMA	poly( <i>n</i> -butyl methacrylate)
PDMS	poly(dimethylsiloxane)
PDVB	polydivinylbenzene

PEHMA	poly(2-ethylhexyl methacrylate)
PEO	poly(ethylene oxide)
PEPDTA	1-phenylethyl phenyldithioacetate
PhEDB	1-phenyl ethyl dithiobenzoate
PHEMA	poly(2-hydroxyethyl methacrylate)
PMDETA	<i>N,N,N',N',N'</i> -pentamethyldiethylenetriamine
PMMA	poly(methyl methacrylate)
PPPDTA	2-phenylprop-2-yl phenyldithioacetate
PRE	persistent radical effect
PS	polystyrene
PT	alkoxyamine
PVA	poly(vinyl alcohol)
PVAc	poly(vinyl acetate)
PVP	poly( <i>N</i> -vinyl pyrrolidone)
RAFT	reversible addition–fragmentation chain transfer
$R_{i,th}$	rate of thermal (spontaneous) initiation ( $M s^{-1}$ )
$R_p$	polymerization rate ( $M s^{-1}$ )
RI	refractive index
RITP	reverse iodine transfer polymerization
$\rho$	entry rate coefficient ( $s^{-1}$ )
SaPSeP	self-assembling of phase-separated polymer
scCO <sub>2</sub>	supercritical carbon dioxide
SDBS	sodium dodecyl benzene sulfonate
SDS	sodium dodecyl sulfate
SEM	scanning electron microscopy
SG1	<i>N-tert</i> -butyl- <i>N</i> -[1-diethylphosphono-(2,2-dimethylpropyl)] nitroxide
SR&N1	simultaneous reverse and normal initiation
T <sup>•</sup>	nitroxide
TBSMSB	4-thiobenzoyl sulfanylmethylsodium benzoate
TD	thermal dissociation
TEM	transmission electron microscopy
TEMPO	2,2,6,6-tetramethylpiperidine- <i>N</i> -oxyl
TERP	organotellurium-mediated radical polymerization
TIPNO	2,2,5-trimethyl-4-phenyl-3-azahexane-3-nitroxide
tNtpy	4,4',4''-tris(5-nonyl)-2,2':6',2''-terpyridine
TPMA	tris[(2-pyridyl)methyl]amine
TTAB	tetradecyltrimethylammonium bromide
TTC	<i>S,S'</i> -bis[1-(2-ethylhexyloxycarbonyl)ethyl] trithio-carbonate
UV	ultraviolet
V-50	2,2'-azobis(2-amidinopropane) dihydrochloride
V-59	2,2'-azobis(2-methylbutyronitrile)
V-501	4,4'-azobis(4-cyanopentanoic acid) (ACPA)
VA-044	2,2'-azobis[2-(2-imidazolin-2-yl)propane]dihydrochloride
VA-060	2,2'-azobis[2-[1-(2-hydroxyethyl)-2-imidazolin-2-yl]propane] dihydrochloride
$v_p$	particle volume

## 7. Acknowledgments

This work was supported by a Grant-in-Aid for Scientific Research (Grant 17750109), a Grants-in-Aid program grant (19550125), and a Research Fellowship for Young Scientists (Y. K.) from the Japan Society for the Promotion of Science (JSPS), as well as a Kobe University Takuetsu-shita Research Project Grant.

## 8. References

- Cunningham, M. F. *Prog. Polym. Sci.* **2002**, 27, 1039.
- Cunningham, M. F. *Prog. Polym. Sci.* **2008**, 33, 365.
- Qiu, J.; Charleux, B.; Matyjaszewski, K. *Prog. Polym. Sci.* **2001**, 26, 2083.
- Save, M.; Guillaenuef, Y.; Gilbert, R. G. *Aust. J. Chem.* **2006**, 59, 693.
- Monteiro, M. J.; Charleux, B. In *Chemistry and Technology of Emulsion Polymerization*; van Herk, A. M., Ed.; Blackwell Publishing Ltd.: Oxford, 2005; p 111.
- Cunningham, M. F. C. R. *Chimie* **2003**, 6, 1351.
- McLeary, J. B.; Klumperman, B. *Soft Matter* **2006**, 2, 45.
- Asua, J. M. *Prog. Polym. Sci.* **2002**, 27, 1283.
- Schork, F. J.; Luo, Y. W.; Smulders, W.; Russum, J. P.; Butte, A.; Fontenot, K. *Adv. Polym. Sci.* **2005**, 175, 129.
- Braunecker, W. A.; Matyjaszewski, K. *Prog. Polym. Sci.* **2007**, 32, 93.
- Goto, A.; Fukuda, T. *Prog. Polym. Sci.* **2004**, 29, 329.
- Matyjaszewski, K. *Controlled Radical Polymerization*; Matyjaszewski, K., Ed.; ACS Symposium Series 685; American Chemical Society: Washington, DC, 1998.
- Matyjaszewski, K. *Controlled/Living Radical Polymerization: Progress in ATRP, NMP and RAFT*; Matyjaszewski, K., Ed.; ACS Symposium Series 768; American Chemical Society: Washington, DC, 2000.
- Matyjaszewski, K. *Advances in Controlled/Living Radical Polymerization*; Matyjaszewski, K., Ed.; ACS Symposium Series 854; American Chemical Society: Washington, DC, 2003.
- Matyjaszewski, K. *Controlled/Living Radical Polymerization: From Synthesis to Materials*; Matyjaszewski, K., Ed.; ACS Symposium Series 944; American Chemical Society: Washington, DC, 2006.
- Hawker, C. J.; Bosman, A. W.; Harth, E. *Chem. Rev.* **2001**, 101, 3661.
- Kamigaito, M.; Ando, T.; Sawamoto, M. *Chem. Rev.* **2001**, 101, 3689.
- Matyjaszewski, K.; Xia, J. *Chem. Rev.* **2001**, 101, 2921.
- Moad, G.; Rizzardo, E.; Thang, S. H. *Aust. J. Chem.* **2005**, 58, 379.
- Perrier, S.; Takolpuckdee, P. *J. Polym. Sci., Part A: Polym. Chem.* **2005**, 43, 5347.
- Moad, G.; Rizzardo, E.; Thang, S. H. *Aust. J. Chem.* **2006**, 59, 669.
- Barner-Kowollik, C.; Buback, M.; Charleux, B.; Coote, M. L.; Drache, M.; Fukuda, T.; Goto, A.; Klumperman, B.; Lowe, A. B.; McLeary, J. B.; Moad, G.; Monteiro, M. J.; Sanderson, R. D.; Tonge, M. P.; Vana, P. *J. Polym. Sci., Part A: Polym. Chem.* **2006**, 44, 5809.
- Matyjaszewski, K. In *Advances in Controlled/Living Radical Polymerization*; Matyjaszewski, K., Ed.; ACS Symposium Series 854; American Chemical Society: Washington, DC, 2003; p 2.
- Szwarc, M.; Levy, M.; Milkovich, R. *J. Am. Chem. Soc.* **1956**, 78, 2656.
- Otsu, T. *J. Polym. Sci., Part A: Polym. Chem.* **2000**, 38, 2121.
- Otsu, T.; Yoshida, M. *Makromol. Chem., Rapid. Commun.* **1982**, 3, 127.
- Georges, M. K.; Veregin, R. P. N.; Kazmaier, P. M.; Hamer, G. K. *Macromolecules* **1993**, 26, 2987.
- Solomon, D. H.; Rizzardo, E.; Cacioli, P. U. S. Patent 4, 1986.
- Kato, M.; Kamigaito, M.; Sawamoto, M.; Higashimura, T. *Macromolecules* **1995**, 28, 1721.
- Wang, J. S.; Matyjaszewski, K. *J. Am. Chem. Soc.* **1995**, 117, 5614.
- Chiefari, J.; Chong, Y. K.; Ercole, F.; Krstina, J.; Jeffery, J.; Le, T. P. T.; Mayadunne, R. T. A.; Meijs, G. F.; Moad, C. L.; Moad, G.; Rizzardo, E.; Thang, S. H. *Macromolecules* **1998**, 31, 5559.
- Destarac, M.; Brochon, C.; Catala, J. M.; Wilczewska, A. *Macromol. Chem. Phys.* **2002**, 203, 2281.
- Gaynor, S. G.; Wang, J. S.; Matyjaszewski, K. *Macromolecules* **1995**, 28, 8051.
- Matyjaszewski, K.; Gaynor, S. G.; Wang, J. S. *Macromolecules* **1995**, 28, 2093.
- Goto, A.; Ohno, K.; Fukuda, T. *Macromolecules* **1998**, 31, 2809.
- David, G.; Boyer, C.; Tonnar, J.; Ameduri, B.; Lacroix-Desmazes, P.; Boutevin, B. *Chem. Rev.* **2006**, 106, 3936.
- Percec, V.; Popov, A. V.; Ramirez-Castillo, E.; Coelho, J. F. J. *J. Polym. Sci., Part A: Polym. Chem.* **2005**, 43, 773.
- Percec, V.; Popov, A. V.; Ramirez-Castillo, E.; Monteiro, M.; Barboiu, B.; Weichold, O.; Asandei, A. D.; Mitchell, C. M. *J. Am. Chem. Soc.* **2002**, 124, 4940.
- Monteiro, M. J.; Guliashvili, T.; Percec, V. *J. Polym. Sci., Part A: Polym. Chem.* **2006**, 45, 1835.
- Percec, V.; Guliashvili, T.; Ladislav, J. S.; Wistrand, A.; Stjern Dahl, A.; Sienkowska, M. J.; Monteiro, M. J.; Sahoo, S. *J. Am. Chem. Soc.* **2006**, 128, 14156.
- Matyjaszewski, K.; Tsarevsky, N. V.; Braunecker, W. A.; Dong, H.; Huang, J.; Jakubowski, W.; Kwak, Y.; Nicolay, R.; Tang, W.; Yoon, J. A. *Macromolecules* **2007**, 40, 7795.
- Goto, A.; Kwak, Y.; Fukuda, T.; Yamago, S.; Iida, K.; Nakajima, M.; Yoshida, J. *J. Am. Chem. Soc.* **2003**, 125, 8720.
- Kwak, Y.; Goto, A.; Fukuda, T.; Kobayashi, Y.; Yamago, S. *Macromolecules* **2006**, 39, 4671.
- Kwak, Y.; Tezuka, M.; Goto, A.; Fukuda, T.; Yamago, S. *Macromolecules* **2007**, 40, 1881.
- Yamago, S.; Iida, K.; Yoshida, J. *J. Am. Chem. Soc.* **2002**, 124, 2874.
- Yamago, S. *J. Polym. Sci., Part A: Polym. Chem.* **2006**, 44, 1.
- Ray, B.; Kotani, M.; Yamago, S. *Macromolecules* **2006**, 39, 5259.
- Yamago, S.; Ray, B.; Iida, K.; Yoshida, J.; Tada, T.; Yoshizawa, K.; Kwak, Y.; Goto, A.; Fukuda, T. *J. Am. Chem. Soc.* **2004**, 126, 13908.
- Wayland, B. B.; Basickes, L.; Mukerjee, S.; Wei, M.; Fryd, M. *Macromolecules* **1997**, 30, 8109.



- (50) Wayland, B. B.; Peng, C. H.; Fu, X.; Lu, Z.; Fryd, M. *Macromolecules* **2006**, *39*, 8219.
- (51) Wayland, B. B.; Poszmik, G.; Mukerjee, S.; Fryd, M. *J. Am. Chem. Soc.* **1994**, *116*, 7943.
- (52) Goto, A.; Zushi, H.; Hirai, N.; Wakada, T.; Tsujii, Y.; Fukuda, T. *J. Am. Chem. Soc.* **2007**, *129*, 13347.
- (53) Caille, J. R.; Debuigne, A.; Jerome, R. *Macromolecules* **2005**, *38*, 27.
- (54) Debuigne, A.; Caille, J. R.; Jerome, R. *Macromolecules* **2005**, *38*, 6310.
- (55) Kos, T.; Strissel, C.; Yagci, Y.; Nugay, T.; Nuyken, O. *Eur. Polym. J.* **2005**, *41*, 1265.
- (56) Raether, B.; Nuyken, O.; Wieland, P.; Bremser, W. *Macromol. Symp.* **2002**, *177*, 25.
- (57) Junkers, T.; Stenzel, M. H.; Davis, T. P.; Barner-Kowollik, C. *Macromol. Rapid Commun.* **2007**, *28*, 746.
- (58) Toy, A. A.; Chaffey-Millar, H.; Davis, T. P.; Stenzel, M. H.; Izgorodina, E. I.; Coote, M. L.; Barner-Kowollik, C. *Chem. Commun.* **2006**, 835.
- (59) Chung, T. C.; Hong, H. In *Advances in Controlled/Living Radical Polymerization*; Matyjaszewski, K., Ed.; ACS Symposium Series 854; American Chemical Society: Washington, DC, 2003; p 481.
- (60) Krstina, J.; Moad, C. L.; Moad, G.; Rizzardo, E.; Berge, C. T. *Macromol. Symp.* **1996**, *111*, 13.
- (61) Krstina, J.; Moad, G.; Rizzardo, E.; Winzor, C. L.; Berge, C. T.; Fryd, M. *Macromolecules* **1995**, *28*, 5381.
- (62) Chen, E. K. Y.; Teertstra, S. J.; Chan-Seng, D.; Otieno, P. O.; Hicks, R. G.; Georges, M. K. *Macromolecules* **2007**, *40*, 8609.
- (63) Fischer, H. In *Advances in Controlled/Living Radical Polymerization*; Matyjaszewski, K., Ed.; ACS Symposium Series 854; American Chemical Society: Washington, DC, 2003; p 10.
- (64) Barner-Kowollik, C.; Quinn, J. F.; Nguyen, T. L. U.; Heuts, J. P. A.; Davis, T. A. *Macromolecules* **2001**, *34*, 7849.
- (65) Fukuda, T.; Terauchi, T.; Goto, A.; Ohno, K.; Tsujii, Y.; Miyamoto, T.; Kobatake, S.; Yamada, B. *Macromolecules* **1996**, *29*, 6393.
- (66) Muller, A. H. E.; Yan, D.; Litvinenko, G.; Zhuang, R.; Dong, H. *Macromolecules* **1995**, *28*, 7335.
- (67) Muller, A. H. E.; Zhuang, R.; Yan, D.; Litvinenko, G. *Macromolecules* **1995**, *28*, 4326.
- (68) Fischer, H. *J. Polym. Sci., Part A: Polym. Chem.* **1999**, *37*, 1885.
- (69) Fischer, H. *Chem. Rev.* **2001**, *101*, 3581.
- (70) Fischer, H.; Souaille, M. *Macromol. Symp.* **2001**, *174*, 231.
- (71) Goto, A.; Fukuda, T. *Macromolecules* **1997**, *30*, 4272.
- (72) Souaille, M.; Fischer, H. *Macromolecules* **2000**, *33*, 7378.
- (73) Souaille, M.; Fischer, H. *Macromolecules* **2002**, *35*, 248.
- (74) Cunningham, M. F.; Ng, D. C. T.; Milton, S. G.; Keoshkerian, B. J. *Polym. Sci., Part A: Polym. Chem.* **2006**, *44*, 232.
- (75) Tang, W.; Fukuda, T.; Matyjaszewski, K. *Macromolecules* **2006**, *39*, 4332.
- (76) Russell, G. T. *Aust. J. Chem.* **2002**, *55*, 399.
- (77) Gilbert, R. G. *Trends Polym. Sci.* **1995**, *3*, 222.
- (78) Gilbert, R. G. *Emulsion Polymerization: A Mechanistic Approach*; Academic Press: London, 1995.
- (79) Zetterlund, P. B.; Saka, Y.; McHale, R.; Nakamura, T.; Aldabbagh, F.; Okubo, M. *Polymer* **2006**, *47*, 7900.
- (80) Benoit, D.; Chaplinski, V.; Braslau, R.; Hawker, C. J. *J. Am. Chem. Soc.* **1999**, *121*, 3904.
- (81) Hawker, C. J. In *Handbook of Radical Polymerization*; Matyjaszewski, K., Davis, T. P., Eds.; Wiley-Interscience: New York, 2002; p 463.
- (82) Matyjaszewski, K.; Shipp, D. A.; Wang, J. L.; Grimaud, T.; Patten, T. E. *Macromolecules* **1998**, *31*, 6836.
- (83) Matyjaszewski, K.; Xia, J. In *Handbook of Radical Polymerization*; Matyjaszewski, K., Davis, T. P., Eds.; Wiley-Interscience: New York, 2002; p 523.
- (84) Shipp, D. A.; Wang, J. L.; Matyjaszewski, K. *Macromolecules* **1998**, *31*, 8005.
- (85) Chong, Y. K.; Le, T. P. T.; Moad, G.; Rizzardo, E.; Thang, S. H. *Macromolecules* **1999**, *32*, 2071.
- (86) Kazmaier, P. M.; Daimon, K.; Georges, M. K.; Hamer, G. K.; Veregin, R. P. N. *Macromolecules* **1997**, *30*, 2228.
- (87) Rodlert, M.; Harth, E.; Hawker, C. J. *J. Polym. Sci., Part A: Polym. Chem.* **2000**, *38*, 4749.
- (88) Scott, M. E.; Parent, J. S.; Hennigar, S. L.; Whitney, R. A.; Cunningham, M. F. *Macromolecules* **2002**, *35*, 7628.
- (89) Bertin, D.; Chauvin, F.; Marque, S.; Tordo, P. *Macromolecules* **2002**, *35*, 3790.
- (90) Nicolas, J.; Dire, C.; Mueller, L.; Belleney, J.; Charleux, B.; Marque, S. R. A.; Bertin, D.; Magnet, S.; Couvreur, L. *Macromolecules* **2006**, *39*, 8274.
- (91) Bon, S. F.; Chambard, G.; German, A. L. *Macromolecules* **1999**, *32*, 8269.
- (92) Davis, K. A.; Matyjaszewski, K. *Adv. Polym. Sci.* **2002**, 159.
- (93) Matyjaszewski, K. *Prog. Polym. Sci.* **2005**, *30*, 858.
- (94) Moad, G.; Solomon, H. *The Chemistry of Radical Polymerization*; Elsevier: Oxford, 2006.
- (95) Baumert, M.; Müllhaupt, R. *Macromol. Rapid Commun.* **1997**, *18*, 787.
- (96) Cuervo-Rodriguez, R.; Bordege, V.; Fernández-Monreal, M. C.; Fernández-García, M.; Madruga, E. L. *J. Polym. Sci., Part A: Polym. Chem.* **2004**, *42*, 4168.
- (97) Fukuda, T.; Terauchi, T.; Goto, A.; Tsujii, Y.; Miyamoto, T.; Shimizu, Y. *Macromolecules* **1996**, *29*, 3050.
- (98) Arehart, S. V.; Matyjaszewski, K. *Macromolecules* **1999**, *32*, 2221.
- (99) Haddleton, D. M.; Crossman, M. C.; Hunt, K. H.; Topping, C.; Waterson, C.; Suddaby, K. G. *Macromolecules* **1997**, *30*, 3992.
- (100) Matyjaszewski, K. *Macromol. Symp.* **2002**, *183*, 71.
- (101) Roos, S. G.; Mueller, A. H. E.; Matyjaszewski, K. *Macromolecules* **1999**, *32*, 8331.
- (102) Ziegler, M. J.; Matyjaszewski, K. *Macromolecules* **2001**, *34*, 415.
- (103) Feldermann, A.; Toy, A. A.; Phan, H.; Stenzel, M. H.; Davis, T. P.; Barner-Kowollik, C. *Polymer* **2004**, *45*, 3997.
- (104) Barner-Kowollik, C.; Buback, M.; Egorov, M.; Fukuda, T.; Goto, A.; Olaj, O. F.; Russell, G. T.; Vana, P.; Yamada, B.; Zetterlund, P. B. *Prog. Polym. Sci.* **2005**, *30*, 605.
- (105) Buback, M.; Junkers, T.; Vana, P. *Macromol. Rapid Commun.* **2005**, *26*, 796.
- (106) Johnston-Hall, G.; Stenzel, M. H.; Davis, T. P.; Barner-Kowollik, C.; Monteiro, M. J. *Macromolecules* **2007**, *40*, 2730.
- (107) Vana, P.; Davis, T. P.; Barner-Kowollik, C. *Macromol. Rapid Commun.* **2002**, *23*, 952.
- (108) McHale, R.; Aldabbagh, F.; Zetterlund, P. B.; Minami, H.; Okubo, M. *Macromolecules* **2006**, *39*, 6853.
- (109) McHale, R.; Aldabbagh, F.; Zetterlund, P. B.; Okubo, M. *Macromol. Chem. Phys.* **2007**, *208*, 1813.
- (110) van Herk, A. M., *Chemistry and Technology of Emulsion Polymerization*; Blackwell Publishing Ltd.: Oxford, 2005.
- (111) Landfester, K. *Macromol. Rapid Commun.* **2001**, *22*, 896.
- (112) Candau, F. In *Polymeric Dispersions: Principles and Applications*; Asua, J. M., Ed.; Kluwer Academic Publishers: 1997; p 127.
- (113) Paul, B. K.; Moulik, S. P. *Curr. Sci.* **2001**, *80*, 990.
- (114) Chow, P. Y.; Gan, L. M. *Adv. Polym. Sci.* **2005**, *175*, 257.
- (115) Barrett, K. E. J. *Dispersion Polymerization in Organic Media*; Wiley: London, 1975.
- (116) Cawse, J. L. In *Emulsion Polymerization and Emulsion Polymers*; Lovell, P. A., El-Aasser, M. S.; Eds.; John Wiley & Sons Ltd: West Sussex, 1997; p 743.
- (117) Taylor, P. *Adv. Colloid Interface Sci.* **1998**, *75*, 107.
- (118) Higuchi, W. I.; Misra, J. *J. Pharm. Sci.* **1962**, *51*, 459.
- (119) Kabalnov, A. S.; Pertzov, A. V.; Shchukin, E. D. *Colloids Surf.* **1987**, *24*, 19.
- (120) Reimers, J. L.; Schork, F. J. *J. Appl. Polym. Sci.* **1996**, *60*, 251.
- (121) Russum, J. P.; Barbre, N. D.; Jones, C. W.; Schork, F. J. *J. Polym. Sci., Part A: Polym. Chem.* **2005**, *43*, 2188.
- (122) Russum, J. P.; Jones, C. W.; Schork, F. J. *Macromol. Rapid Commun.* **2004**, *25*, 1064.
- (123) Russum, J. P.; Jones, C. W.; Schork, F. J. *Ind. Eng. Chem. Res.* **2005**, *44*, 2484.
- (124) Smulders, W. W.; Jones, C. C.; Schork, F. J. *Macromolecules* **2004**, *37*, 9345.
- (125) Qi, G.; Schork, F. J. *Langmuir* **2006**, *22*, 9075.
- (126) Luo, Y.; Tsavalas, J.; Schork, F. J. *Macromolecules* **2001**, *34*, 5501.
- (127) Ugelstad, J.; Mork, P. C.; Kaggerud, K. H.; Ellingsen, T.; Berge, A. *Adv. Colloid Interface Sci.* **1980**, *13*, 101.
- (128) Ugelstad, J.; Kaggerud, K. H.; Hansen, F. K.; Berge, A. *Makromol. Chem.* **1979**, *180*, 737.
- (129) Monteiro, M. J.; Hodgson, M.; De-Brouwer, H. *J. Polym. Sci., Part A: Polym. Chem.* **2000**, *38*, 3864.
- (130) Uzulina, I.; Kanagasabapathy, S.; Claverie, J. *Macromol. Symp.* **2000**, *150*, 33.
- (131) Tsavalas, J. G.; Schork, F. J.; de-Brouwer, H.; Monteiro, M. J. *Macromolecules* **2001**, *34*, 3938.
- (132) Huang, X.; Sudol, E. D.; Dimonie, V. L.; Anderson, C. D.; El-Aasser, M. S. *Macromolecules* **2006**, *39*, 6944.
- (133) Miller, C. M.; Sudol, E. D.; Silebi, C. A.; El-Aasser, M. S. *Macromolecules* **1995**, *28*, 2765.
- (134) Miller, C. M.; Sudol, E. D.; Silebi, C. A.; El-Aasser, M. S. *Macromolecules* **1995**, *28*, 2754.
- (135) Blythe, P. J.; Klein, A.; Sudol, E. D.; El-Aasser, M. S. *Macromolecules* **1999**, *32*, 6952.
- (136) Blythe, P. J.; Morrison, B. R.; Mathauer, K. A.; Sudol, E. D.; El-Aasser, M. S. *Macromolecules* **1999**, *32*, 6944.
- (137) Blythe, P. J.; Morrison, B. R.; Mathauer, K. A.; Sudol, E. D.; El-Aasser, M. S. *Langmuir* **2000**, *16*, 898.
- (138) Farcet, C.; Lansalot, M.; Charleux, B.; Pirri, R.; Vairon, J. P. *Macromolecules* **2000**, *33*, 8559.

- (139) Lansalot, M.; Farcet, C.; Charleux, B.; Vairon, J. P.; Pirri, R.; Tordo, P. In *Controlled/Living Radical Polymerization: Progress in ATRP, NMP and RAFT*; Matyjaszewski, K., Ed.; ACS Symposium Series 768; American Chemical Society: Washington, DC, 2000; p 138.
- (140) Farcet, C.; Charleux, B.; Pirri, R. *Macromolecules* **2001**, *34*, 3823.
- (141) Farcet, C.; Charleux, B. *Macromol. Symp.* **2002**, *182*, 249.
- (142) Farcet, C.; Nicolas, J.; Charleux, B. *J. Polym. Sci., Part A: Polym. Chem.* **2002**, *40*, 4410.
- (143) Nicolas, J.; Charleux, B.; Guerret, O.; Magnet, S. *Macromolecules* **2004**, *37*, 4453.
- (144) Yang, L.; Luo, Y. W.; Li, B. G. *J. Polym. Sci., Part A: Polym. Chem.* **2006**, *44*, 2293.
- (145) Charmot, D.; Corpart, P.; Adam, H.; Zard, S. Z.; Biadatti, T.; Bouhadir, G. *Macromol. Symp.* **2000**, *150*, 23.
- (146) Monteiro, M. J.; Sjöberg, M.; van der Vlist, J.; Göttgens, C. M. J. *Polym. Sci., Part A: Polym. Chem.* **2000**, *38*, 4206.
- (147) Monteiro, M. J.; de Barbeyrac, J. *Macromolecules* **2001**, *34*, 4416.
- (148) Smulders, W.; Gilbert, R. G.; Monteiro, M. J. *Macromolecules* **2003**, *36*, 4309.
- (149) Smulders, W.; Monteiro, M. J. *Macromolecules* **2004**, *37*, 4474.
- (150) Monteiro, M. J.; Adamy, M. M.; Leeuwen, B. J.; van Herk, A. M.; Destarac, M. *Macromolecules* **2005**, *38*, 1538.
- (151) Adamy, M.; van Herk, A. M.; Destarac, M.; Monteiro, M. J. *Macromolecules* **2003**, *36*, 2293.
- (152) Luo, Y. W. *Chem. J. Chin. Univ.* **2003**, *24*, 1926.
- (153) Peklak, A. D.; Butte, A. J. *Polym. Sci., Part A: Polym. Chem.* **2006**, *44*, 6114.
- (154) Prescott, S. W.; Ballard, M. J.; Rizzardo, E.; Gilbert, R. G. *Macromol. Theory Simul.* **2006**, *15*, 70.
- (155) Luo, Y.; Liu, B.; Wang, Z.; Gao, J.; Li, B. J. *Polym. Sci., Part A: Polym. Chem.* **2007**, *45*, 2304.
- (156) Zetterlund, P. B.; Okubo, M. *Macromolecules* **2006**, *39*, 8959.
- (157) Tobita, H.; Yanase, F. *Macromol. Theory Simul.* **2007**, *16*, 476.
- (158) Charleux, B. *Macromolecules* **2000**, *33*, 5358.
- (159) Hui, A. W.; Hamielec, A. E. *J. Appl. Polym. Sci.* **1972**, *16*, 749.
- (160) Zetterlund, P. B.; Okubo, M. *Macromol. Theory Simul.* **2007**, *16*, 221.
- (161) Kagawa, Y.; Zetterlund, P. B.; Minami, H.; Okubo, M. *Macromol. Theory Simul.* **2006**, *15*, 608.
- (162) Butte, A.; Storti, G.; Morbidelli, M. *DEHEMA Monographs* **1998**, *134*, 497.
- (163) Zetterlund, P. B.; Kagawa, Y.; Okubo, M. To be published.
- (164) Tobita, H. *Macromol. Theory Simul.* **2007**, *16*, 810.
- (165) Tobita, H. *Macromol. Symp.* **2008**, *261*, 36.
- (166) Ma, J. W.; Cunningham, M. F.; McAuley, K. B.; Keoshkerian, B.; Georges, M. K. *Macromol. Theory Simul.* **2002**, *11*, 953.
- (167) Ma, J. W.; Cunningham, M. F.; McAuley, K. B.; Keoshkerian, B.; Georges, M. K. *Chem. Eng. Sci.* **2003**, *58*, 1163.
- (168) Ma, J. W.; Cunningham, M. F.; McAuley, K. B.; Keoshkerian, B.; Georges, M. K. *J. Polym. Sci., Part A: Polym. Chem.* **2001**, *39*, 1081.
- (169) Goto, A.; Kwak, Y.; Yoshikawa, C.; Tsujii, Y.; Sugiura, Y.; Fukuda, T. *Macromolecules* **2002**, *35*, 3520.
- (170) Zetterlund, P. B.; Okubo, M. *Macromol. Theory Simul.* **2005**, *14*, 415.
- (171) Kagawa, Y.; Zetterlund, P. B.; Minami, H.; Okubo, M. *Macromolecules* **2007**, *40*, 3062.
- (172) Cunningham, M. F.; Tortosa, K.; Lin, M.; Keoshkerian, B.; Georges, M. K. *J. Polym. Sci., Part A: Polym. Chem.* **2002**, *40*, 2828.
- (173) Tortosa, K.; Smith, J. A.; Cunningham, M. F. *Macromol. Rapid Commun.* **2001**, *22*, 957.
- (174) Ma, J. W.; Cunningham, M. F.; McAuley, K. B.; Keoshkerian, B.; Georges, M. *Chem. Eng. Sci.* **2003**, *58*, 1177.
- (175) Ma, J. W.; Cunningham, M. F.; McAuley, K. B.; Keoshkerian, B.; Georges, M. K. *Macromol. Theory Simul.* **2003**, *12*, 72.
- (176) Maehata, H.; Buragina, C.; Cunningham, M.; Keoshkerian, B. *Macromolecules* **2007**, *40*, 7126.
- (177) Prodpran, T.; Dimonie, V. L.; Sudol, E. D.; El-Aasser, M. S. *Macromol. Symp.* **2000**, *155*, 1.
- (178) Pan, G.; Sudol, E. D.; Dimonie, V. L.; El-Aasser, M. S. *Macromolecules* **2001**, *34*, 481.
- (179) Keoshkerian, B.; MacLeod, P. J.; Georges, M. K. *Macromolecules* **2001**, *34*, 3594.
- (180) Pan, G.; Sudol, E. D.; Dimonie, V. L.; El-Aasser, M. S. *Macromolecules* **2002**, *35*, 6915.
- (181) Cunningham, M. F.; Tortosa, K.; Ma, J. W.; McAuley, K. B. *Macromol. Symp.* **2002**, *182*, 273.
- (182) Cunningham, M. F.; Xie, M.; McAuley, K. B.; Keoshkerian, B.; Georges, M. K. *Macromolecules* **2002**, *35*, 59.
- (183) Cunningham, M.; Lin, M.; Buragina, C.; Milton, S.; Ng, D.; Hsu, C. C.; Keoshkerian, B. *Polymer* **2005**, *46*, 1025.
- (184) Cunningham, M. F.; Lin, M.; Keoshkerian, B. *JCT Res.* **2004**, *1*, 33.
- (185) Nakamura, T.; Zetterlund, P. B.; Okubo, M. *Macromol. Rapid Commun.* **2006**, *27*, 2014.
- (186) Lin, M.; Hsu, J. C. C.; Cunningham, M. F. *J. Polym. Sci., Part A: Polym. Chem.* **2006**, *44*, 5974.
- (187) Wakamatsu, J.; Kawasaki, M.; Zetterlund, P. B.; Okubo, M. *Macromol. Rapid Commun.* **2007**, *28*, 2346.
- (188) Zetterlund, P. B.; Nakamura, T.; Okubo, M. *Macromolecules* **2007**, *40*, 8663.
- (189) Alam, Md. N.; Zetterlund, P. B.; Okubo, M. *J. Polym. Sci., Part A: Polym. Chem.* **2007**, *45*, 4995.
- (190) Alam, Md. N.; Zetterlund, P. B.; Okubo, M. *Polymer* **2008**, *49*, 3428.
- (191) Alam, Md. N.; Zetterlund, P. B.; Okubo, M. *Polymer* **2008**, *49*, 883.
- (192) Zetterlund, P. B.; Okubo, M. *Macromol. Theory Simul.* **2006**, *15*, 40.
- (193) Nicolas, J.; Charleux, B.; Guerret, O.; Magnet, S. *Macromolecules* **2005**, *38*, 9963.
- (194) Delaittre, G.; Charleux, B. *Macromolecules* **2008**, *41*, 2361.
- (195) Matyjaszewski, K.; Qiu, J.; Tsarevsky, N. V.; Charleux, B. *J. Polym. Sci., Part A: Polym. Chem.* **2000**, *38*, 4724.
- (196) Li, M.; Matyjaszewski, K. *Macromolecules* **2004**, *37*, 2106.
- (197) Min, K.; Matyjaszewski, K. *Macromolecules* **2005**, *38*, 8131.
- (198) Kagawa, Y.; Kawasaki, M.; Zetterlund, P. B.; Okubo, M. *Macromol. Rapid Commun.* **2007**, *28*, 2354.
- (199) Simms, R. W.; Cunningham, M. F. *Macromolecules* **2007**, *40*, 860.
- (200) Simms, R. W.; Cunningham, M. F. *Macromolecules* **2008**, *41*, 5148.
- (201) Wang, A. R.; Zhu, S.; Kwak, Y.; Goto, A.; Fukuda, T.; Monteiro, M. J. *J. Polym. Sci., Part A: Polym. Chem.* **2003**, *41*, 2833.
- (202) Barner-Kowollik, C.; Coote, M. L.; Davis, T. P.; Radom, L.; Vana, P. *J. Polym. Sci., Part A: Polym. Chem.* **2003**, *41*, 2828.
- (203) Lansalot, M.; Davis, T. P.; Heuts, J. P. A. *Macromolecules* **2002**, *35*, 7582.
- (204) Luo, Y.; Wang, R.; Yang, L.; Li, B.; Zhu, S. *Macromolecules* **2006**, *39*, 1328.
- (205) Kwak, Y.; Goto, A.; Tsujii, Y.; Murata, Y.; Komatsu, K.; Fukuda, T. *Macromolecules* **2002**, *35*, 3026.
- (206) Prescott, S. W.; Ballard, M. J.; Rizzardo, E.; Gilbert, R. G. *Macromolecules* **2005**, *38*, 4901.
- (207) Butte, A.; Storti, G.; Morbidelli, M. *Macromol. Theory Simul.* **2002**, *11*, 37.
- (208) Smith, W. V.; Ewart, R. H. *J. Chem. Phys.* **1948**, *16*, 592.
- (209) Licht, G.; Gilbert, R. G.; Napper, D. H. *J. Polym. Sci., Polym. Chem. Ed.* **1980**, *18*, 1292.
- (210) Prescott, S. W. *Macromolecules* **2003**, *36*, 9608.
- (211) Buback, M.; Egorov, M.; Gilbert, R. G.; Kaminsky, V.; Olaj, O. F.; Russell, G. T.; Vana, P.; Zifferer, G. *Macromol. Chem. Phys.* **2002**, *203*, 2570.
- (212) Barner-Kowollik, C.; Davis, T. P.; Heuts, J. P. A.; Stenzel, M. H.; Vana, P.; Whittaker, M. J. *Polym. Sci., Part A: Polym. Chem.* **2003**, *41*, 365.
- (213) Buback, M.; Vana, P. *Macromol. Rapid Commun.* **2006**, *27*, 1299.
- (214) Yang, L.; Luo, Y.; Li, B. *Polymer* **2006**, *47*, 751.
- (215) MacLeod, P. J.; Barber, R.; Odell, P. G.; Keoshkerian, B.; Georges, M. K. *Macromol. Symp.* **2000**, *155*, 31.
- (216) Charleux, B. In *Advances in Controlled/Living Radical Polymerization*; Matyjaszewski, K., Ed.; ACS Symposium Series 854; American Chemical Society: Washington, DC, 2003; p 438.
- (217) Lin, M.; Cunningham, M. F.; Keoshkerian, B. *Macromol. Symp.* **2004**, *206*, 263.
- (218) Farcet, C.; Belleney, J.; Charleux, B.; Pirri, R. *Macromolecules* **2002**, *35*, 4912.
- (219) Pan, G.; Sudol, E. D.; Dimonie, V. L.; El-Aasser, M. S. *J. Polym. Sci., Part A: Polym. Chem.* **2004**, *42*, 4921.
- (220) Cunningham, M. F.; Ng, D. C. T.; Milton, S. G.; Keoshkerian, B. *J. Polym. Sci., Part A: Polym. Chem.* **2005**, *44*, 232.
- (221) Zetterlund, P. B.; Alam, Md. N.; Minami, H.; Okubo, M. *Macromol. Rapid Commun.* **2005**, *26*, 955.
- (222) Alam, Md. N.; Zetterlund, P. B.; Okubo, M. *Macromol. Chem. Phys.* **2006**, *207*, 1732.
- (223) Saka, Y.; Zetterlund, P. B.; Okubo, M. *Polymer* **2007**, *48*, 1229.
- (224) Marestin, C.; Noel, C.; Guyot, A.; Claverie, J. *Macromolecules* **1998**, *31*, 4041.
- (225) Schmidt-Naake, G.; Drache, M.; Taube, C. *Makromol. Chem.* **1999**, *265*, 62.
- (226) Georges, M. K.; Veregin, R. P. N.; Kazmaier, P. M.; Hamer, G. K.; Saban, M. *Macromolecules* **1994**, *27*, 7228.
- (227) Odell, P. G.; Veregin, R. P. N.; Michalak, L. M.; Brousmiche, D.; Georges, M. K. *Macromolecules* **1995**, *28*, 8453.
- (228) Veregin, R. P. N.; Odell, P. G.; Michalak, L. M.; Georges, M. K. *Macromolecules* **1996**, *29*, 4161.
- (229) Malmstrom, E.; Miller, R. D.; Hawker, C. J. *Tetrahedron* **1997**, *53*, 15225.
- (230) Ohno, K.; Tsujii, Y.; Fukuda, T. *Macromolecules* **1997**, *30*, 2503.
- (231) Greszta, D.; Matyjaszewski, K. *J. Polym. Sci., Part A: Polym. Chem.* **1997**, *35*, 1857.



- (232) Li, J.; Zhu, X.; Zhu, J.; Cheng, Z. *Radiat. Phys. Chem.* **2007**, *76*, 23.
- (233) Keoshkerian, B.; Georges, M. K.; Quinlan, M.; Veregin, R.; Goodbrand, B. *Macromolecules* **1998**, *31*, 7559.
- (234) Debuigne, A.; Radhakrishnan, T.; Georges, M. K. *Macromolecules* **2006**, *39*, 5359.
- (235) Georges, M. K.; Lukkarila, J. L.; Szkurhan, A. R. *Macromolecules* **2004**, *37*, 1297.
- (236) Keoshkerian, B.; Szkurhan, A. R.; Georges, M. K. *Macromolecules* **2001**, *34*, 6531.
- (237) Charleux, B.; Nicolas, J. *Polymer* **2007**, *48*, 5813.
- (238) Benoit, D.; Grimaldi, S.; Robin, S.; Finet, J.-P.; Tordo, P.; Gnanou, Y. *J. Am. Chem. Soc.* **2000**, *122*, 5929.
- (239) Tsarevsky, N.; Matyjaszewski, K. *Chem. Rev.* **2007**, *107*, 2270.
- (240) Nanda, A. K.; Matyjaszewski, K. *Macromolecules* **2003**, *36*, 1487.
- (241) Nanda, A. K.; Matyjaszewski, K. *Macromolecules* **2003**, *36*, 599.
- (242) Tang, W.; Nanda, A. K.; Matyjaszewski, K. *Macromol. Chem. Phys.* **2005**, *206*, 1171.
- (243) Tsarevsky, N. V.; Pintauer, T.; Matyjaszewski, K. *Macromolecules* **2004**, *37*, 9768.
- (244) Jewrajka, S. K.; Mandal, B. M. *J. Polym. Sci., Part A: Polym. Chem.* **2004**, *42*, 2483.
- (245) Lee, S. B.; Russell, A. J.; Matyjaszewski, K. *Biomacromolecules* **2003**, *4*, 1386.
- (246) Oh, J. K.; Min, K.; Matyjaszewski, K. *Macromolecules* **2006**, *39*, 3161.
- (247) Perrier, S.; Armes, S. P.; Wang, X.-S.; Malet, F.; Haddleton, D. M. *J. Polym. Sci., Part A: Polym. Chem.* **2001**, *39*, 1696.
- (248) Perrier, S.; Haddleton, D. M. *Macromol. Symp.* **2002**, *182*, 261.
- (249) Okubo, M.; Minami, H.; Zhou, J. *Colloid Polym. Sci.* **2004**, *282*, 747.
- (250) Kagawa, Y.; Minami, H.; Okubo, M.; Zhou, J. *Polymer* **2005**, *46*, 1045.
- (251) Landfester, K.; Bechthold, N.; Tiarks, F.; Antonietti, M. *Macromolecules* **1999**, *32*, 5222.
- (252) Li, M.; Matyjaszewski, K. *Macromolecules* **2003**, *36*, 6028.
- (253) Qiu, J.; Pintauer, T.; Gaynor, S. G.; Matyjaszewski, K.; Charleux, B.; Vairon, J.-P. *Macromolecules* **2000**, *33*, 7310.
- (254) Simms, R. W.; Cunningham, M. F. *J. Polym. Sci., Part A: Polym. Chem.* **2006**, *44*, 1628.
- (255) Simms, R. W.; Cunningham, M. F. *Macromol. Symp.* **2008**, *261*, 32.
- (256) Li, M.; Jahed, N. M.; Min, K.; Matyjaszewski, K. *Macromolecules* **2004**, *37*, 2434.
- (257) Min, K.; Li, M.; Matyjaszewski, K. *J. Polym. Sci., Part A: Polym. Chem.* **2005**, *43*, 3616.
- (258) Bombalski, L.; Min, K.; Dong, H.; Tang, C.; Matyjaszewski, K. *Macromolecules* **2007**, *40*, 7429.
- (259) Min, K.; Gao, H.; Matyjaszewski, K. *J. Am. Chem. Soc.* **2005**, *127*, 3825.
- (260) Min, K.; Jakubowski, W.; Matyjaszewski, K. *Macromol. Rapid Commun.* **2006**, *27*, 594.
- (261) Oh, J. K.; Perineau, F.; Matyjaszewski, K. *Macromolecules* **2006**, *39*, 8003.
- (262) Oh, J. K.; Tang, C.; Gao, H.; Tsarevsky, N. V.; Matyjaszewski, K. *J. Am. Chem. Soc.* **2006**, *128*, 5578.
- (263) Stoffelbach, F.; Belardi, B.; Santos, J. M. R. C. A.; Tessier, L.; Matyjaszewski, K.; Charleux, B. *Macromolecules* **2007**, *40*, 8813.
- (264) Gaynor, S. G.; Qiu, J.; Matyjaszewski, K. *Macromolecules* **1998**, *31*, 5951.
- (265) Matyjaszewski, K.; Qiu, J.; Shipp, D. A.; Gaynor, S. G. *Macromol. Symp.* **2000**, *155*, 15.
- (266) Min, K.; Oh, J. K.; Matyjaszewski, K. *J. Polym. Sci., Part A: Polym. Chem.* **2007**, *45*, 1413.
- (267) Gao, H.; Min, K.; Matyjaszewski, K. *Macromol. Chem. Phys.* **2006**, *207*, 1709.
- (268) Min, K.; Yu, S.; Lee, H.; Mueller, L.; Sheiko, S. S.; Matyjaszewski, K. *Macromolecules* **2007**, *40*, 6557.
- (269) Oh, J. K.; Siegwart, D. J.; Lee, H.; Sherwood, G.; Peteanu, L.; Hollinger, J. O.; Kataoka, K.; Matyjaszewski, K. *J. Am. Chem. Soc.* **2007**, *129*, 5939.
- (270) Oh, J. K.; Siegwart, D. J.; Matyjaszewski, K. *Biomacromolecules* **2007**, *8*, 3326.
- (271) Oh, J. K.; Dong, H.; Zhang, R.; Matyjaszewski, K.; Schlaad, H. *J. Polym. Sci., Part A: Polym. Chem.* **2007**, *45*, 4764.
- (272) Xia, J.; Matyjaszewski, K. *Macromolecules* **1997**, *30*, 7692.
- (273) Xia, J.; Matyjaszewski, K. *Macromolecules* **1999**, *32*, 5199.
- (274) Gromada, J.; Matyjaszewski, K. *Macromolecules* **2001**, *34*, 7664.
- (275) Ikkaku, Y.; Togo, M.; Okubo, M.; Matsumoto, T. *J. Adhesion Soc. Jpn.* **1981**, *17*, 264.
- (276) Zhao, C. L.; Dobler, F.; Pitch, T.; Holl, Y.; Lambla, M. *J. Colloid Interface Sci.* **1989**, *128*, 437.
- (277) Peng, H.; Cheng, S.; Feng, L.; Fan, Z. *J. Appl. Polym. Sci.* **2003**, *89*, 3175.
- (278) Pintauer, T.; Matyjaszewski, K. *Coord. Chem. Rev.* **2005**, *249*, 1155.
- (279) Tsarevsky, N. V.; Matyjaszewski, K. *J. Polym. Sci., Part A: Polym. Chem.* **2006**, *44*, 5098.
- (280) Butte, A.; Storti, G.; Morbidelli, M. *Macromolecules* **2001**, *34*, 5885.
- (281) de-Brouwer, H.; Monteiro, M. J.; Tsavalas, J. G.; Schork, F. J. *Macromolecules* **2000**, *33*, 9239.
- (282) Lee, H.; Lee, J. M.; Shim, S. E.; Lee, B. H.; Choe, S. *Polymer* **2005**, *46*, 3661.
- (283) McLeary, J. B.; Tonge, M. P.; de Wet Roos, D.; Sanderson, R. D.; Klumperman, B. *J. Polym. Sci., Part A: Polym. Chem.* **2004**, *42*, 960.
- (284) Moad, G.; Chiefari, J.; Chong, Y. K.; Krstina, J.; Mayadunne, R. T. A.; Postma, A.; Rizzardo, E.; Thang, S. H. *Polym. Int.* **2000**, *49*, 993.
- (285) Russum, J. P.; Jones, C. W.; Schork, F. J. *AIChE J.* **2006**, *52*, 1566.
- (286) Tonge, M. P.; McLeary, J. B.; Vosloo, J. J.; Sanderson, R. D. *Macromol. Symp.* **2003**, *193*, 289.
- (287) Uzulina, I.; Gaillard, N.; Guyot, A.; Claverie, J. C. R. *Chimie* **2003**, *6*, 1375.
- (288) Vosloo, J. J.; De-Wet-Roos, D.; Tonge, M. P.; Sanderson, R. D. *Macromolecules* **2002**, *35*, 4894.
- (289) Yang, L.; Luo, Y.; Li, B. *J. Polym. Sci., Part A: Polym. Chem.* **2005**, *43*, 4972.
- (290) Bowes, A.; McLeary, J. B.; Sanderson, R. D. *J. Polym. Sci., Part A: Polym. Chem.* **2007**, *45*, 588.
- (291) Matahwa, H.; McLeary, J. B.; Sanderson, R. D. *J. Polym. Sci., Part A: Polym. Chem.* **2006**, *44*, 427.
- (292) Qi, G. G.; Jones, C. W.; Schork, J. F. *Ind. Eng. Chem. Res.* **2006**, *45*, 7084.
- (293) Yu, Z. Q.; Ji, X. L.; Ni, P. H. *Colloid Polym. Sci.* **2006**, *285*, 211.
- (294) Kanagasabapathy, S.; Sudalai, A.; Benicewicz, B. C. *Macromol. Rapid Commun.* **2001**, *22*, 1076.
- (295) Al-Bagoury, M.; Buchholz, K.; Yaacoub, E. J. *Polym. Adv. Technol.* **2007**, *18*, 313.
- (296) Shim, S. E.; Lee, H.; Choe, S. *Macromolecules* **2004**, *37*, 5565.
- (297) Qinghua, Z.; Xiaoli, Z.; Fengqiu, C.; Ying, S.; Qiongyan, W. *J. Polym. Sci., Part A: Polym. Chem.* **2007**, *45*, 1585.
- (298) Zhang, F.; Ni, P.; Xiong, Q.; Yu, Z. *J. Polym. Sci., Part A: Polym. Chem.* **2005**, *43*, 2931.
- (299) Zhou, X. D.; Ni, P. H.; Yu, Z. Q.; Zhang, F. *J. Polym. Sci., Part A: Polym. Chem.* **2007**, *45*, 471.
- (300) Bussels, R.; Bergman-Gottgens, C.; Meuldijk, J.; Koning, C. *Polymer* **2005**, *46*, 8546.
- (301) Simms, R. W.; Davis, T. P.; Cunningham, M. F. *Macromol. Rapid Commun.* **2005**, *26*, 592.
- (302) Qi, G.; Jones, C. W.; Schork, F. J. *Macromol. Rapid Commun.* **2007**, *28*, 1010.
- (303) Luo, Y.; Liu, X. J. *J. Polym. Sci., Part A: Polym. Chem.* **2004**, *42*, 6248.
- (304) Guo, T. Y.; Tang, D.; Song, M.; Zhang, B. *J. Polym. Sci., Part A: Polym. Chem.* **2007**, *45*, 5067.
- (305) Smulders, W. W.; Jones, C. W.; Schork, F. J. *AIChE J.* **2005**, *51*, 1009.
- (306) Biasutti, J. D.; Davis, T. P.; Lucien, F. P.; Heuts, J. P. A. *J. Polym. Sci., Part A: Polym. Chem.* **2005**, *43*, 2001.
- (307) Baussard, J. F.; Habib-Jiwan, J. L.; Laschewsky, A.; Mertoglu, M.; Storsberg, J. *Polymer* **2004**, *45*, 3615.
- (308) Loiseau, J.; Doerr, N.; Suau, J. M.; Egraz, J. B.; Ilauro, M. F.; Ladaviere, C.; Claverie, J. *Macromolecules* **2003**, *36*, 3066.
- (309) McCormick, C. L.; Lowe, A. B. *Acc. Chem. Res.* **2004**, *37*, 312.
- (310) Prescott, S. W.; Ballard, M. J.; Rizzardo, E.; Gilbert, R. G. *Macromolecules* **2002**, *35*, 5417.
- (311) Ferguson, C. J.; Hughes, R. J.; Nguyen, D.; Pham, B. T. T.; Gilbert, R. G.; Serelis, A. K.; Such, C. H.; Hawke, B. S. *Macromolecules* **2005**, *38*, 2191.
- (312) Matsumoto, T.; Okubo, M.; Onoe, S. *Kobunshi Ronbunshu* **1975**, *32*, 522.
- (313) Okubo, M.; Kanada, K.; Matsumoto, T. *J. Appl. Polym. Sci.* **1987**, *33*, 1511.
- (314) McLeary, J. B.; Calitz, F. M.; McKenzie, J. M.; Tonge, M. P.; Sanderson, R. D.; Klumperman, B. *Macromolecules* **2005**, *38*, 3151.
- (315) Perrier, S.; Barner-Kowollik, C.; Quinn, J. F.; Vana, P.; Davis, T. P. *Macromolecules* **2002**, *35*, 8300.
- (316) Vana, P.; Davis, T. P.; Barner-Kowollik, C. *Macromol. Theory Simul.* **2002**, *11*, 823.
- (317) Luo, Y. W.; Yu, B. *Polym.-Plast. Technol. Eng.* **2004**, *43*, 1299.
- (318) Hermanson, K. D.; Liu, S. Y.; Kaler, E. W. *J. Polym. Sci., Part A: Polym. Chem.* **2006**, *44*, 6055.
- (319) Liu, S. Y.; Hermanson, K. D.; Kaler, E. W. *Macromolecules* **2006**, *39*, 4345.
- (320) Zhou, X.; Ni, P.; Yu, Z. *Polymer* **2007**, *48*, 6262.



- (321) Landfester, K.; Willert, M.; Antonietti, M. *Macromolecules* **2000**, *33*, 2370.
- (322) Thomas, D. B.; Convertine, A. J.; Hester, R. D.; Lowe, A. B.; McCormick, C. L. *Macromolecules* **2004**, *37*, 1735.
- (323) Delaittre, G.; Nicolas, J.; Lefay, C.; Save, M.; Charleux, B. *Chem. Commun.* **2005**, *5*, 614.
- (324) Delaittre, G.; Nicolas, J.; Lefay, C.; Save, M.; Charleux, B. *Soft Matter* **2006**, *2*, 223.
- (325) Maehata, H.; Liu, X.; Cunningham, M.; Keoshkerian, B. *Macromol. Rapid Commun.* **2008**, *29*, 479.
- (326) Nicolas, J.; Charleux, B.; Guerret, O.; Magnet, S. *Angew. Chem., Int. Ed.* **2004**, *43*, 6186.
- (327) Szkurhan, A. R.; Georges, M. K. *Macromolecules* **2004**, *37*, 4776.
- (328) Simms, R. W.; Hoidas, M. D.; Cunningham, M. F. *Macromolecules* **2008**, *41*, 1076.
- (329) Cao, J.; He, J.; Li, C.; Yang, Y. *Polym. J.* **2001**, *33*, 75.
- (330) Pohn, J.; Buragina, C.; Georges, M. K.; Keoshkerian, B.; Cunningham, M. F. *Macromol. Theory Simul.* **2008**, *17*, 73.
- (331) Ferguson, C. J.; Hughes, R. J.; Pham, B. T. T.; Hawket, B. S.; Gilbert, R. G.; Serelis, A. K.; Such, C. H. *Macromolecules* **2002**, *35*, 9243.
- (332) Sprong, E.; Leswin, J. S. K.; Lamb, D. J.; Ferguson, C. J.; Hawket, B. S.; Pham, B. T. T.; Nguyen, D.; Such, C. H.; Serelis, G. K.; Gilbert, R. G. *Macromol. Symp.* **2006**, *231*, 84.
- (333) Bon, S. A. F.; Bosveld, M.; Klumperman, B.; German, A. L. *Macromolecules* **1997**, *30*, 324.
- (334) Nicolas, J.; Charleux, B.; Magnet, S. *J. Polym. Sci., Part A: Polym. Chem.* **2006**, *44*, 4142.
- (335) Chambard, G.; de Man, P.; Klumperman, B. *Macromol. Symp.* **2000**, *150*, 45.
- (336) Eslami, H.; Zhu, S. *Polymer* **2005**, *46*, 5484.
- (337) Jousset, S.; Qiu, J.; Matyjaszewski, K.; Granel, C. *Macromolecules* **2001**, *34*, 6641.
- (338) Limer, A.; Haddleton, D. M. *Eur. Polym. J.* **2006**, *42*, 61.
- (339) Peng, H.; Cheng, S.; Feng, L. *J. Appl. Polym. Sci.* **2003**, *89*, 1542.
- (340) Peng, H.; Cheng, S.; Feng, L. *Polym. Int.* **2004**, *53*, 828.
- (341) Qiu, J.; Gaynor, S. G.; Matyjaszewski, K. *Macromolecules* **1999**, *32*, 2872.
- (342) Chan-Seng, D.; Georges, M. K. *J. Polym. Sci., Part A: Polym. Chem.* **2006**, *44*, 4027.
- (343) Eslami, H.; Zhu, S. *J. Polym. Sci., Part A: Polym. Chem.* **2006**, *44*, 1914.
- (344) Min, K.; Gao, H.; Matyjaszewski, K. *J. Am. Chem. Soc.* **2006**, *128*, 10521.
- (345) Peng, H.; Cheng, S.; Fan, Z. *Polym. Eng. Sci.* **2005**, *45*, 1508.
- (346) Matyjaszewski, K.; Shipp, D. A.; Qiu, J.; Gaynor, S. G. *Macromolecules* **2000**, *33*, 2296.
- (347) Yoo, S. H.; Lee, J. H.; Lee, J. C.; Jho, J. Y. *Macromolecules* **2002**, *35*, 1146.
- (348) Wan, X.; Ying, S. *J. Appl. Polym. Sci.* **2000**, *75*, 802.
- (349) Freiberg, M.; Meyerstein, D. *J. Chem. Soc., Faraday Trans.* **1980**, *76*, 1825.
- (350) Peng, H.; Cheng, S.; Fan, Z. *J. Appl. Polym. Sci.* **2005**, *98*, 2123.
- (351) Matyjaszewski, K.; Shipp, D. A.; McMurtry, G. P.; Gaynor, S. G.; Pakula, T. *J. Polym. Sci., Part A: Polym. Chem.* **2000**, *38*, 2023.
- (352) Szkurhan, A. R.; Kasahara, T.; Georges, M. K. *J. Polym. Sci., Part A: Polym. Chem.* **2006**, *44*, 5708.
- (353) Prescott, S. W.; Ballard, M. J.; Rizzardo, E.; Gilbert, R. G. *Aust. J. Chem.* **2002**, *55*, 415.
- (354) Luo, Y. W.; Cui, X. F. *J. Polym. Sci., Part A: Polym. Chem.* **2006**, *44*, 2837.
- (355) Monteiro, M. J.; de Barbeyrac, J. *Macromol. Rapid Commun.* **2002**, *23*, 370.
- (356) Okubo, M.; Sugihara, Y.; Kitayama, Y.; Kagawa, Y. To be submitted.
- (357) Monteiro, M. J.; de Barbeyrac, J. *Macromol. Rapid Commun.* **2002**, *23*, 370.
- (358) Nozari, S.; Tauer, K. *Polymer* **2005**, *46*, 1033.
- (359) Nozari, S.; Tauer, K.; Ali, M. I. *Macromolecules* **2005**, *38*, 10449.
- (360) Shim, S. E.; Shin, Y.; Jun, J. W.; Lee, K.; Jung, H.; Choe, S. *Macromolecules* **2003**, *36*, 7994.
- (361) Shim, S. E.; Shin, Y.; Lee, H.; Choe, S. *Polym. Bull.* **2003**, *51*, 209.
- (362) Shim, S. E.; Shin, Y.; Lee, H.; Jung, H. J.; Chang, Y. H.; Choe, S. *J. Ind. Eng. Chem.* **2003**, *9*, 619.
- (363) Whang, B. C. Y.; Lichti, G.; Gilbert, R. G.; Napper, D. H.; Sangster, D. F. *J. Polym. Sci., Polym. Lett. Ed.* **1980**, *18*, 711.
- (364) Lichti, G.; Sangster, D. F.; Whang, B. C. Y.; Napper, D. H.; Gilbert, R. G. *J. Chem. Soc., Faraday Trans. 1* **1982**, *78*, 2129.
- (365) Morrison, B. R.; Casey, B. S.; Lacik, I.; Leslie, G. L.; Sangster, D. F.; Gilbert, R. G.; Napper, D. H. *J. Polym. Sci., Part A: Polym. Chem.* **1994**, *32*, 631.
- (366) Barner-Kowollik, C.; Vana, P.; Davis, T. P. In *Handbook of Radical Polymerization*; Matyjaszewski, K., Davis, T. P., Eds.; Wiley-Interscience: New York, 2002; p 187.
- (367) Apostolovic, B.; Quattrini, F.; Butté, A.; Storti, G.; Morbidelli, M. *Helv. Chim. Acta* **2006**, *89*, 1641.
- (368) Urbani, C. N.; Nguyen, H. N.; Monteiro, M. J. *Aust. J. Chem.* **2006**, *59*, 728.
- (369) Delgado, J.; El-Aasser, M. S.; Sileb, C. A.; Vanderhoff, J. W.; Guillot, J. *J. Polym. Sci., Part B: Polym. Phys.* **1988**, *26*, 1495.
- (370) Freal-Saison, S.; Save, M.; Bui, C.; Charleux, B.; Magnet, S. *Macromolecules* **2006**, *39*, 8632.
- (371) Rimmer, S.; Tattersall, P. *Polymer* **1999**, *40*, 5729.
- (372) Jin, Y. Z.; Hahn, Y. B.; Nahm, K. S.; Lee, Y. S. *Polymer* **2005**, *46*, 11294.
- (373) Zhang, Z.; Zhu, X.; Zhu, J.; Cheng, Z. *Polym. Bull.* **2006**, *56*, 539.
- (374) Hartmann, J.; Urbani, C.; Whittaker, M. R.; Monteiro, M. J. *Macromolecules* **2006**, *39*, 904.
- (375) Gilbert, R. G. *Macromolecules* **2006**, *39*, 4256.
- (376) Ganeva, D. E.; Sprong, E.; de Bruyn, H.; Warr, G. G.; Such, C. H.; Hawket, B. S. *Macromolecules* **2007**, *40*, 6181.
- (377) Butte, A.; Storti, G.; Morbidelli, M. *Macromolecules* **2000**, *33*, 3485.
- (378) Lansalot, M.; Farcet, C.; Charleux, B.; Vairon, J. P.; Pirri, R. *Macromolecules* **1999**, *32*, 7354.
- (379) Pouget, E.; Tonnar, J.; Eloy, C.; Lacroix-Desmazes, P.; Boutevin, B. *Macromolecules* **2006**, *39*, 6009.
- (380) Tonnar, J.; Lacroix-Desmazes, P.; Boutevin, B. *Macromolecules* **2007**, *40*, 186.
- (381) Farcet, C.; Lansalot, M.; Pirri, R.; Vairon, J. P.; Charleux, B. *Macromol. Rapid Commun.* **2000**, *21*, 921.
- (382) Boyer, C.; Lacroix-Desmazes, P.; Robin, J. J.; Boutevin, B. *Macromolecules* **2006**, *39*, 4044.
- (383) Lacroix-Desmazes, P.; Severac, R.; Boutevin, B. *Macromolecules* **2005**, *38*, 6299.
- (384) Tonnar, J.; Lacroix-Desmazes, P.; Boutevin, B. *Macromol. Rapid Commun.* **2006**, *27*, 1733.
- (385) Tonnar, J.; Lacroix-Desmazes, P.; Boutevin, B. *Macromolecules* **2007**, *40*, 6076.
- (386) Sugihara, Y.; Kagawa, Y.; Okubo, M. *Macromolecules* **2007**, *40*, 9208.
- (387) Gridnev, A. A.; Ittel, S. D. *Chem. Rev.* **2001**, *101*, 3611.
- (388) Heuts, J. P. A.; Roberts, G. E.; Biasutti, J. D. *Aust. J. Chem.* **2002**, *55*, 381.
- (389) Yamada, B.; Zetterlund, P. B.; Sato, E. *Prog. Polym. Sci.* **2006**, *31*, 835.
- (390) Debuigne, A.; Caille, J. R.; Jerome, R. *Angew. Chem., Int. Ed.* **2005**, *44*, 1101.
- (391) Lu, Z.; Fryd, M.; Wayland, B. B. *Macromolecules* **2004**, *37*, 2686.
- (392) Debuigne, A.; Caille, J. R.; Detrembleur, C.; Jerome, R. *Angew. Chem., Int. Ed.* **2005**, *44*, 3439.
- (393) Detrembleur, C.; Debuigne, A.; Bryaskova, R.; Charleux, B.; Jerome, R. *Macromol. Rapid Commun.* **2006**, *27*, 37.
- (394) Debuigne, A.; Caille, J. R.; Jerome, R. *Macromolecules* **2005**, *38*, 5452.
- (395) Koumura, K.; Satoh, K.; Kamigaito, M.; Okamoto, Y. *Macromolecules* **2006**, *39*, 4054.
- (396) Wakioka, M.; Baek, K. Y.; Ando, T.; Kamigaito, M.; Sawamoto, M. *Macromolecules* **2002**, *35*, 330.
- (397) Stenzel, M. H.; Cummins, L.; Roberts, G. E.; Davis, T. P.; Vana, P. *Macromol. Chem. Phys.* **2003**, *204*, 1160.
- (398) Coote, M. L.; Radom, L. *Macromolecules* **2004**, *37*, 590.
- (399) Feng, H.; Dan, Y. *J. Appl. Polym. Sci.* **2006**, *99*, 1093.
- (400) Kai, P.; Yi, D. *J. Appl. Polym. Sci.* **2006**, *101*, 3670.
- (401) Apostolo, M.; Arcella, V.; Storti, G.; Morbidelli, M. *Macromolecules* **2002**, *35*, 6154.
- (402) Apostolo, M.; Biressi, G. *Macromol. Symp.* **2004**, *206*, 347.
- (403) Okubo, M.; Furukawa, Y.; Shiba, K.; Matoba, T. *Colloid Polym. Sci.* **2003**, *281*, 182.
- (404) Okubo, M.; Kobayashi, H.; Matoba, T.; Oshima, Y. *Langmuir* **2006**, *22*, 8727.
- (405) Guyot, A., In *Comprehensive Polymer Science*; Allen, G., Bevington, J. C., Eds.; Pergamon: Oxford, 1989; p 261.
- (406) Kawaguchi, S.; Ito, K. *Adv. Polym. Sci.* **2005**, *175*, 299.
- (407) Lok, K. P.; Ober, C. K. *Can. J. Chem.* **1985**, *63*, 209.
- (408) Gregory, A. M.; Thurecht, K. J.; Howdle, S. M. *Macromolecules* **2008**, *41*, 1215.
- (409) McHale, R.; Aldabbagh, F.; Zetterlund, P. B.; Okubo, M. *Macromol. Rapid Commun.* **2006**, *27*, 1465.
- (410) Minami, H.; Kagawa, Y.; Kuwahara, S.; Shigematsu, J.; Fujii, S.; Okubo, M. *Des. Monomers Polym.* **2004**, *7*, 553.
- (411) Ryan, J.; Aldabbagh, F.; Zetterlund, P. B.; Okubo, M. *Polymer* **2005**, *46*, 9769.
- (412) Thurecht, K. J.; Gregory, A. M.; Wang, W.; Howdle, S. M. *Macromolecules* **2007**, *40*, 2965.
- (413) Xia, J.; Johnson, T.; Gaynor, S. G.; Matyjaszewski, K.; DeSimone, J. M. *Macromolecules* **1999**, *32*, 4802.
- (414) Min, K.; Matyjaszewski, K. *Macromolecules* **2007**, *40*, 7217.

- (415) Song, J. S.; Tronc, F.; Winnik, M. A. *J. Am. Chem. Soc.* **2004**, *126*, 6562.
- (416) Song, J. S.; Winnik, M. A. *Macromolecules* **2005**, *38*, 8300.
- (417) Song, J. S.; Winnik, M. A. *Macromolecules* **2006**, *39*, 8318.
- (418) Yasuda, M.; Seki, H.; Yokoyama, H.; Ogino, H.; Ishimi, K.; Ishikawa, H. *Macromolecules* **2001**, *34*, 3261.
- (419) Odell, P. G.; Hamer, G. K. *Polym. Mater. Sci. Eng.* **1996**, *74*, 404.
- (420) Gabaston, L. I.; Jackson, R. A.; Armes, S. P. *Macromolecules* **1998**, *31*, 2883.
- (421) Holderle, M.; Baumert, M.; Mulhaupt, R. *Macromolecules* **1997**, *30*, 3420.
- (422) Aldabbagh, F.; Zetterlund, P. B.; Okubo, M. *Macromolecules* **2008**, *41*, 2732.
- (423) Wan, W. M.; Pan, C. Y. *Macromolecules* **2007**, *40*, 8897.
- (424) Bathfield, M.; D'Agosto, F.; Spitz, R.; Charreyre, M. T.; Pichot, C.; Delair, T. *Macromol. Rapid Commun.* **2007**, *28*, 1540.
- (425) Houillot, L.; Bui, C.; Save, M.; Charleux, B.; Farcet, C.; Moire, C.; Raust, J.-A.; Rodriguez, I. *Macromolecules* **2007**, *40*, 6500.
- (426) Saikia, P. J.; Lee, J. M.; Lee, B. H.; Choe, S. *J. Polym. Sci., Part A: Polym. Chem.* **2007**, *45*, 348.
- (427) Saikia, P. J.; Lee, J. M.; Lee, K.; Choe, S. *J. Polym. Sci., Part A: Polym. Chem.* **2008**, *46*, 872.
- (428) Zheng, G.; Pan, C. *Macromolecules* **2006**, *39*, 95.
- (429) Kendall, J. L.; Canelas, D. A.; Young, J. L.; DeSimone, J. M. *Chem. Rev.* **1999**, *99*, 543.
- (430) Canelas, D. A.; Betts, D. E.; DeSimone, J. M. *Macromolecules* **1996**, *29*, 2818.
- (431) Canelas, D. A.; DeSimone, J. M. *Macromolecules* **1997**, *30*, 5673.
- (432) Oh, S.; Kim, K.; Lee, B. H.; Shim, S. E.; Choe, S. *J. Polym. Sci., Part A: Polym. Chem.* **2005**, *44*, 62.
- (433) Shim, S. E.; Oh, S.; Chang, Y. H.; Jin, M. J.; Choe, S. *Polymer* **2004**, *45*, 4731.
- (434) Delaittre, G.; Save, M.; Charleux, B. *Macromol. Rapid Commun.* **2007**, *28*, 1528.
- (435) Okubo, M.; Fujii, S.; Maenaka, H.; Minami, H. *Colloid Polym. Sci.* **2002**, *280*, 183.
- (436) Shim, S. E.; Jung, H.; Lee, H.; Biswas, J.; Choe, S. *Polymer* **2003**, *44*, 5563.
- (437) Ahmad, H.; Tauer, K. *Colloid Polym. Sci.* **2003**, *281*, 686.
- (438) Ide, N.; Fukuda, T. *Macromolecules* **1997**, *30*, 4268.
- (439) Ide, N.; Fukuda, T. *Macromolecules* **1999**, *32*, 95.
- (440) Landin, D. T.; Macosko, C. W. *Macromolecules* **1988**, *21*, 846.
- (441) Matsumoto, A. *Adv. Polym. Sci.* **1995**, *123*, 41.
- (442) Tanaka, T.; Suzuki, T.; Saka, Y.; Zetterlund, P. B.; Okubo, M. *Polymer* **2007**, *48*, 3836.
- (443) Gao, H.; Min, K.; Matyjaszewski, K. *Macromolecules* **2007**, *40*, 7763.
- (444) Wang, A. R.; Zhu, S. *Polym. Eng. Sci.* **2005**, *45*, 720.
- (445) Norisuye, T.; Morinaga, T.; Tran-Cong-Miyata, Q.; Goto, A.; Fukuda, T.; Shibayama, M. *Polymer* **2005**, *46*, 1982.
- (446) Li, Y.; Armes, S. P. *Macromolecules* **2005**, *38*, 8155.
- (447) Wang, A. R.; Zhu, S. *J. Polym. Sci., Part A: Polym. Chem.* **2005**, *43*, 5710.
- (448) Bouvier-Fontes, L.; Pirri, R.; Magnet, S.; Asua, J. M.; Leiza, J. R. *Macromolecules* **2005**, *38*, 2722.
- (449) Ghazaly, H. M.; Daniels, E. S.; Dimonie, V. L.; Klein, A.; El-Aasser, M. S. *J. Appl. Polym. Sci.* **2001**, *81*, 1721.
- (450) Guo, H.; Hamielec, A. E.; Zhu, S. *J. Polym. Sci., Part A: Polym. Chem.* **1997**, *66*, 935.
- (451) Matsumoto, A.; Kodama, K.; Aota, H.; Capek, I. *Eur. Polym. J.* **1999**, *35*, 1509.
- (452) Matsumoto, A.; Kodama, K.; Mori, Y.; Aota, H. *J. M. S. Pure Appl. Chem.* **1998**, *A35*, 1459.
- (453) Nomura, M.; Tobita, H.; Suzuki, K. In *Polymer particles*; Okubo, M., Ed.; Springer: Berlin, 2005; Vol. 175.
- (454) Tobita, H. *Macromolecules* **1992**, *25*, 2671.
- (455) Tobita, H.; Kimura, K.; Fujita, K.; Nomura, M. *Polymer* **1993**, *34*, 2569.
- (456) Tobita, H.; Kumagai, M.; Aoyagi, N. *Polymer* **2000**, *41*, 481.
- (457) Tobita, H.; Yoshihara, Y. *J. Polym. Sci., Part B: Polym. Phys.* **1996**, *34*, 1415.
- (458) Ali, M. M.; Stover, H. D. H. *Macromolecules* **2003**, *36*, 1793.
- (459) Ali, M. M.; Stover, H. D. H. In *Advances in Controlled/Living Radical Polymerization*; Matyjaszewski, K., Ed.; ACS Symposium Series 854; American Chemical Society: Washington, DC, 2003; p 299.
- (460) Ali, M. M.; Stover, H. D. H. *J. Polym. Sci., Part A: Polym. Chem.* **2006**, *44*, 156.
- (461) Chan, Y.; Bulmus, V.; Zareie, M. H.; Byrne, F. L.; Barner, L.; Kavallaris, M. *J. Controlled Release* **2006**, *115*, 197.
- (462) Croxton, C. A.; Mills, M. F.; Gilbert, R. G.; Napper, D. H. *Macromolecules* **1993**, *26*, 3563.
- (463) Konishi, Y.; Okubo, M.; Minami, H. *Colloid Polym. Sci.* **2003**, *281*, 123.
- (464) Okubo, M.; Konishi, Y.; Minami, H. *Colloid Polym. Sci.* **2000**, *278*, 659.
- (465) Okubo, M.; Minami, H. *Colloid Polym. Sci.* **1997**, *275*, 992.
- (466) Dowding, P. J.; Atkin, R.; Vincent, B.; Bouillot, P. *Langmuir* **2004**, *20*, 11374.
- (467) Loxley, A.; Vincent, B. *J. Colloid Interface Sci.* **1998**, *208*, 49.
- (468) Dimonie, V. L.; Daniels, E. S.; Shaffer, O. L.; El-Aasser, M. S. In *Emulsion Polymerization and Emulsion Polymers*; Lovell, P. A., El-Aasser, M. S., Eds.; John Wiley & Sons Ltd.: West Sussex, 1997; p 293.
- (469) Karlsson, O. J.; Stubbs, J. M.; Carrier, R. H.; Sundberg, D. C. *Polym. React. Eng.* **2003**, *11*, 589.
- (470) McDonald, C. J.; Devon, M. *J. Adv. Colloid Interface Sci.* **2002**, *99*, 181.
- (471) Nakamura, Y.; Tabata, H.; Suzuki, H.; Iko, K.; Okubo, M.; Matsumoto, T. *J. Appl. Polym. Sci.* **1986**, *32*, 4865.
- (472) Okubo, M. *Makromol. Chem., Macromol. Symp.* **1990**, *35/36*, 307.
- (473) Okubo, M.; Seike, M.; Matsumoto, T. *J. Appl. Polym. Sci.* **1983**, *28*, 383.
- (474) Kobayashi, H.; Miyanaga, E.; Okubo, M. *Langmuir* **2007**, *23*, 8703.
- (475) Okubo, M.; Fujiwara, T.; Yamaguchi, A. *Colloid Polym. Sci.* **1998**, *276*, 186.
- (476) Okubo, M.; Katsuta, Y.; Matsumoto, T. *J. Polym. Sci., Polym. Lett. Ed.* **1982**, *20*, 45.
- (477) Saito, N.; Nakatsuru, R.; Kagari, Y.; Okubo, M. *Langmuir* **2007**, *23*, 11506.
- (478) Fujibayashi, T.; Okubo, M. *Langmuir* **2007**, *23*, 7958.
- (479) Okubo, M.; Takekoh, R.; Saito, N. *Prog. Colloid Polym. Sci.* **2003**, *124*, 73.
- (480) Saito, N.; Kagari, Y.; Okubo, M. *Langmuir* **2007**, *23*, 5914.
- (481) Saito, N.; Takekoh, R.; Nakatsuru, R.; Okubo, M. *Langmuir* **2007**, *23*, 5978.
- (482) Takekoh, R.; Okubo, M.; Araki, T.; Stöver, H. D. H.; Hitchcock, A. P. *Macromolecules* **2004**, *37*, 542.
- (483) Okubo, M.; Kanaida, K.; Matsumoto, T. *Colloid Polym. Sci.* **1987**, *265*, 876.
- (484) Okubo, M.; Miya, T.; Minami, H.; Takekoh, R. *J. Appl. Polym. Sci.* **2002**, *83*, 2013.
- (485) Stubbs, J.; Karlsson, O.; Jönsson, J. E.; Sundberg, E.; Durant, Y.; Sundberg, D. *Colloids Surf., A: Physicochem. Eng. Aspects* **1999**, *153*, 255.
- (486) Stubbs, J. M.; Sundberg, D. C. *J. Appl. Polym. Sci.* **2006**, *102*, 945.
- (487) Okubo, M.; Izumi, J.; Hosotani, T.; Yamashita, T. *Colloid Polym. Sci.* **1997**, *275*, 797.
- (488) Okubo, M.; Lu, Y. *Colloid Polym. Sci.* **1996**, *274*, 1020.
- (489) Klumperman, B. *Macromol. Chem. Phys.* **2006**, *207*, 861.
- (490) Lu, F.; Luo, Y.; Li, B. *Macromol. Rapid Commun.* **2007**, *28*, 868.
- (491) Luo, Y.; Gu, H. *Macromol. Rapid Commun.* **2006**, *27*, 21.
- (492) Luo, Y.; Gu, H. *Polymer* **2007**, *48*, 3262.
- (493) van Zyl, A. J. P.; Bosch, R. F. P.; McLeary, J. B.; Sanderson, R. D.; Klumperman, B. *Polymer* **2005**, *46*, 3607.
- (494) Kitayama, Y.; Kagawa, Y.; Okubo, M. To be submitted.
- (495) Nicolas, J.; Ruzette, A. V.; Farcet, C.; Gerard, P.; Magnet, S.; Charleux, B. *Polymer* **2007**, *48*, 7029.
- (496) Okubo, M.; Ichikawa, K.; Fujimura, M. *Colloid Polym. Sci.* **1991**, *269*, 1257.
- (497) Okubo, M.; Ichikawa, K.; Fujimura, M. In *Polymer Latexes*; Daniels, E. S., Sudol, E. D., El-Aasser, M. S., Eds.; ACS Symposium Series 492; American Chemical Society: Washington, DC, 1992; p 282.
- (498) Okubo, M.; Sakauchi, A.; Okada, M. *Colloid Polym. Sci.* **2002**, *280*, 303.
- (499) Okada, M.; Okubo, M.; Matoba, T. *Colloid Polym. Sci.* **2004**, *282*, 193.
- (500) Okubo, M.; Ito, A.; Kanenobu, T. *Colloid Polym. Sci.* **1996**, *274*, 801.
- (501) Okubo, M.; Ito, A.; Okada, M.; Suzuki, T. *Colloid Polym. Sci.* **2002**, *280*, 574.
- (502) Herrera, V.; Pirri, R.; Asua, J. M.; Leiza, J. R. *J. Polym. Sci., Part A: Polym. Chem.* **2007**, *45*, 2484.
- (503) Herrera, V.; Pirri, R.; Leiza, J. R.; Asua, J. M. *Macromolecules* **2006**, *39*, 6969.
- (504) Okubo, M.; Takekoh, R.; Izumi, J. *Colloid Polym. Sci.* **2001**, *279*, 513.
- (505) Okubo, M.; Takekoh, R.; Saito, N. *Colloid Polym. Sci.* **2003**, *281*, 945.
- (506) Okubo, M.; Takekoh, R.; Saito, N. *Colloid Polym. Sci.* **2004**, *282*, 1192.
- (507) Okubo, M.; Saito, N.; Takekoh, R.; Kobayashi, H. *Polymer* **2005**, *46*, 1151.